

Aus dem Institut für Immunologie
Institut der Ludwig-Maximilians-Universität München
Direktor: Prof. Dr. rer. nat. Thomas Brocker

Microbial-host interactions in the context of CD40-signaling in dendritic cells

Dissertation
zum Erwerb des Doktorgrades der Naturwissenschaften
an der Medizinischen Fakultät der
Ludwig-Maximilians-Universität zu München



vorgelegt von
Verena Friedrich
aus
München

2019

**Mit Genehmigung der Medizinischen Fakultät
der Universität München**

Betreuer: Prof. Dr. rer. nat. Thomas Brocker

Zweitgutachter: Prof. Dr. Dr. Michael von Bergwelt-Baildon

Dekan: Prof. Dr. med. dent. Reinhard Hickel

Tag der mündlichen Prüfung: 13.10.2020



LUDWIG-
MAXIMILIANS-
UNIVERSITÄT
MÜNCHEN

Promotionsbüro
Medizinische Fakultät



Eidesstattliche Versicherung

Friedrich, Verena

Name, Vorname

Ich erkläre hiermit an Eides statt,

dass ich die vorliegende Dissertation mit dem Titel

Microbial-host interactions in the context of CD40-signaling in dendritic cells

selbständig verfasst, mich außer der angegebenen keiner weiteren Hilfsmittel bedient und alle Erkenntnisse, die aus dem Schrifttum ganz oder annähernd übernommen sind, als solche kenntlich gemacht und nach ihrer Herkunft unter Bezeichnung der Fundstelle einzeln nachgewiesen habe.

Ich erkläre des Weiteren, dass die hier vorgelegte Dissertation nicht in gleicher oder in ähnlicher Form bei einer anderen Stelle zur Erlangung eines akademischen Grades eingereicht wurde.

München, 20.10.2020

Ort, Datum

Verena Friedrich

Unterschrift Doktorandin bzw. Doktorand

This work contains results presented in the following publications:

Friedrich, V., Barthels, C., Ogrinc Wagner, A., Garzetti, D., Ring, D., Stecher, B., Forne, I., Imhof, A., Brocker, T. "*Helicobacter hepaticus* as disease driver in a novel CD40-mediated model of colitis", manuscript in preparation

Ogrinc Wagner, A., Friedrich, V., Barthels, C., Marconi, P., Blutke, A., Brombacher, F., Brocker, T. "Strain specific maturation of Dendritic cells and production of IL-1 β controls CD40-driven colitis", *PLoS One* (2019)

*Barthels, C., *Ogrinc, A., Steyer, V., Meier, S, Simon, F., Wimmer, M., Blutke, A., Straub, T., Zimmer-Strobl, U., Lutgens, E., Marconi, P., Ohnmacht, C., Garzetti, D., Stecher, B., Brocker, T. "CD40-signalling abrogates induction of ROR γ t⁺ Treg cells by intestinal CD103⁺ DCs and causes fatal colitis", *Nature Communications* (2017), * = equal contribution

Abbreviations

ABX	mixture of antibiotics
AMP	antimicrobial peptide
APC	antigen presenting cell
BCR	B cell receptor
BSA	bovine serum albumin
CBL	cecal bacterial lysate
cDC	conventional DC
CD40L	CD40 ligand
cfu	colony-forming units
CX₃CR1	C-X3-C motif chemokine receptor 1
DC	dendritic cell
DNA	deoxyribonucleic acid
EDTA	ethylenediaminetetraacetic acid
ELISA	enzyme-linked immunosorbent assay
FACS	fluorescence-activated cell sorting
FCS	fetal calf serum
FoxP3	forkhead box protein P3
HBSS	Hank's balanced salt solution
Hh	<i>Helicobacter hepaticus</i>

HRP	horseradish peroxidase
Hsp	heat-shock protein
iBAQ	intensity-based absolute quantification
IBD	inflammatory bowel disease
IFN-γ	interferon- γ
Ig	immunoglobulin
IκB	inhibitor of κ B
IKK	inhibitor of κ B kinase
IL	interleukin
iTreg	induced regulatory T cell
LC-MS/MS	label-free liquid chromatography tandem mass spectrometry
LP	lamina propria
mAb	monoclonal antibody
MFI	mean fluorescence intensity
MHC	major histocompatibility complex
MHCI	MHC class I
MHCII	MHC class II
mLN	mesenteric lymph node
NEMO	NF- κ B essential modulator
NF-κB	nuclear factor- κ B

NIK	NF- κ B-inducing kinase
nTreg	natural regulatory T cell
OD	optical density
OTU	operational taxonomic unit
PBS	phosphate buffered saline
PCR	polymerase chain reaction
PP	peyer's patch
p.i.	post inoculation
PMA	phorbol-12-myristate-13-acetate
RA	retinoic acid
rRNA	ribosomal ribonucleic acid
RORγt	retinoic acid-related orphan receptor γ t
SDS-PAGE	sodium dodecyl sulfate-polyacrylamide gel electrophoresis
SEM	standard error of mean
SFB	segmented filamentous bacteria
SIgA	secretory IgA
SPF	specific-pathogen-free
STAT	signal transducer and activator of transcription
TCR	T cell receptor
TF	transcription factor

TGF-β	tumor growth factor β
Th	T helper
TLR	Toll-like receptor
TNFR	tumor necrosis factor receptor
Treg	regulatory T cell

Contents

Abbreviations	v
1 Summary	1
2 Zusammenfassung	2
3 Introduction	4
3.1 The immune system	4
3.1.1 Central and peripheral T cell tolerance	5
3.2 Dendritic cells	8
3.2.1 Conventional DCs	9
3.2.2 Intestinal DCs	9
3.2.3 CD40-signaling in DCs	11
3.3 Gut microbiota	14
3.3.1 Microbial-host interactions	14
3.3.2 Inflammatory Bowel Disease	21
3.3.3 <i>Helicobacter hepaticus</i>	22
3.4 The DC-LMP1/CD40 mouse model	25
3.5 Aim of the thesis	28
4 Material and Methods	29
4.1 Materials	29
4.1.1 Devices	29
4.1.2 Consumables	29
4.1.3 Chemicals	30
4.1.4 Buffer and media	31
4.1.5 Antibodies	33
4.1.6 Oligonucleotides	35

4.1.7	Mouse strains	37
4.2	Methods	38
4.2.1	Immunological and cell biology methods	38
4.2.2	Molecular biology methods	46
5	Results	49
5.1	Role of the non-canonical NF- κ B pathway in DC-LMP1/CD40 animals	49
5.1.1	Loss of colonic iTregs in DC-LMP1/CD40 animals depends on CD40-activated non-canonical NF- κ B signaling	51
5.2	Analysis of gut microbiota in DC-LMP1/CD40 mice	54
5.2.1	Dysbiosis in DC-LMP1/CD40 animals	55
5.3	Microbial-host interactions	58
5.3.1	Fecal bacteria in DC-LMP1/CD40 mice are highly IgA-coated	58
5.3.2	DC-LMP1/CD40 mice produce commensal-specific antibodies	59
5.3.3	Identification of bacterial antigens by serum antibody reactivity	61
5.4	<i>Helicobacter hepaticus</i> as disease driver	64
5.4.1	<i>Helicobacter hepaticus</i> -free DC-LMP1/CD40 mice are protected from early disease onset	65
5.4.2	DC-LMP1/CD40 mice rapidly develop strong intestinal inflammation upon reinfection with <i>Helicobacter hepaticus</i>	68
5.4.3	<i>Helicobacter hepaticus</i> affects colonic CD4 ⁺ T cell differentiation	70
6	Discussion	74
6.1	Role of the non-canonical NF- κ B pathway in DC-LMP1/CD40 animals	74
6.2	Dysbiosis in DC-LMP1/CD40 mice	76
6.3	Microbial-host interactions	77
6.3.1	Fecal bacteria in DC-LMP1/CD40 mice are highly IgA-coated	77
6.3.2	DC-LMP1/CD40 mice produce commensal-specific antibodies	78
6.3.3	Identification of bacterial antigens by serum antibody reactivity	80

6.4	<i>Helicobacter hepaticus</i> as disease driver	82
6.4.1	<i>Helicobacter hepaticus</i> -free DC-LMP1/CD40 mice are protected from early disease onset	83
6.4.2	DC-LMP1/CD40 mice rapidly develop strong intestinal inflammation upon reinfection with <i>Helicobacter hepaticus</i>	84
6.4.3	<i>Helicobacter hepaticus</i> affects colonic CD4 ⁺ T cell differentiation	84
	References	87
	Acknowledgements	115

1 Summary

Deciphering the role of gut microbiota in health and disease is an emerging field of research, addressing how the immune system regulates the microbiota and how this shapes host immunity. To study microbial-host interactions we used a CD40-mediated colitis model where CD11c⁺ dendritic cells (DCs) receive a constitutive CD40 signal.

We previously published that DC-LMP1/CD40 animals show a strong reduction in CD103⁺ DCs in mesenteric lymph nodes and colon which leads to an impaired generation of ROR γ t⁺Helios⁻ iTregs and an increase of inflammatory IL-17⁺IFN- γ ⁺ Th17/Th1 and IFN- γ ⁺ Th1 cells. This breakdown of intestinal tolerance leads to early onset of fatal colitis in DC-LMP1/CD40 mice. However, crossing these mice onto Rag1^{-/-} background or treatment with antibiotics could rescue them, indicating that colitis development in DC-LMP1/CD40 animals depends on T or B cells as well as on microbiota.

In the present work, we confirmed that CD40-signaling in DCs is activating the non-canonical NF- κ B pathway that is central for the pathogenesis in this colitis model. We further studied the impact of microbiota on disease development. We observed dysbiosis concomitant with "blooming" of *Enterobacteriaceae* in DC-LMP1/CD40 mice as a hallmark of colitis. Further, we could detect increased IgA-levels and bacteria highly coated with IgA in the feces as well as elevated IgA- and IgG-levels in sera from DC-LMP1/CD40 animals. Serum antibodies from transgenic animals are bacteria-specific and we identified a protein from *Helicobacter hepaticus* (*Hh*) as specific antigen. Finally, transgenic animals which were rendered *Hh*-free showed a strong delay in colitis onset, less morbidity and remarkably improved survival rates. In contrast, the reinfection of transgenic animals with *Hh* led to a rapid disease onset and the generation of inflammatory IL-17⁺IFN- γ ⁺ Th17/Th1 and IFN- γ ⁺ Th1 cells in the colon. Thus, the present work highlights the impact of gut microbiota on modulating the host immune response and its concomitant role on disease onset, progression and outcome in the CD40-mediated colitis model.

2 Zusammenfassung

Die Entschlüsselung der Rolle der Darmmikrobiota in Gesundheit und Krankheit ist ein aktuelles Forschungsfeld, das sich mit Wechselwirkungen zwischen Immunsystem und Mikrobiota auseinandersetzt. Für die Untersuchung der Mikrobiota-Wirt-Interaktionen wurde ein CD40-vermitteltes Colitis-Modell herangezogen, in dem CD11c⁺ Dendritische Zellen (DCs) ein konstitutives CD40 Signal erhalten.

Wir haben hierzu bereits veröffentlicht, dass DC-LMP1/CD40 Tiere eine starke Reduzierung der CD103⁺ DCs in mesenterischen Lymphknoten und im Colon zeigen, die zu einer reduzierten Produktion von ROR γ t⁺Helios⁻ iTregs und einer Vermehrung von inflammatorischen IL-17⁺IFN- γ ⁺ Th17/Th1 und IFN- γ ⁺ Th1 Zellen führt. Diese Beeinträchtigung der intestinalen Toleranz resultiert in einem frühen Ausbruch der Colitis in DC-LMP1/CD40 Tieren, die tödlich verläuft. Colitis trat nicht auf, wenn die Mäuse auf den Rag1^{-/-} Hintergrund gekreuzt oder mit Antibiotika behandelt wurden, was darauf schliessen lässt, dass die Entstehung von Colitis in DC-LMP1/CD40 Tieren von T oder B Zellen sowie von der Mikrobiota abhängt.

In der vorliegenden Arbeit konnten wir bestätigen, dass das CD40 Signal in DCs den nicht-kanonischen NF- κ B Signalweg aktiviert, der für die Pathogenese in unserem Colitis-Modell unerlässlich ist. Des Weiteren untersuchten wir den Einfluss der Mikrobiota auf die Krankheitsentwicklung in dem CD40-vermittelten Colitis-Modell. In DC-LMP1/CD40 Mäusen stellten wir eine für Colitis charakteristische Dysbiose mit einhergehendem "*Enterobacteriaceae* blooming" fest. Zusätzlich konnten wir erhöhte IgA-Level und hochgradig IgA-dekorierte Bakterien in den Exkrementen sowie erhöhte IgA- und IgG-Werte in Seren von DC-LMP1/CD40 Tieren detektieren. Zudem waren Serum-Antikörper von transgenen Tieren spezifisch für Bakterien und wir identifizierten ein Protein des *Helicobacter hepaticus* (*Hh*) als spezifisches Antigen. Schließlich zeigten transgene Tiere, die von *Hh* befreit wurden, einen stark verzögerten Colitis-Ausbruch, eine verringerte Morbidität sowie beachtlich verbesserte Überlebensraten. Im Gegensatz dazu führte die Infektion transgener Tiere mit *Hh* zu einem

schnellen Krankheitsausbruch und Generierung inflammatorischer IL-17⁺IFN- γ ⁺ Th17/Th1 und IFN- γ ⁺ Th1 Zellen im Colon.

Somit stellt die vorliegende Arbeit den Einfluss der Darmmikrobiota hinsichtlich der Modulierung der Wirtsimmunantwort und ihrer damit einhergehenden Rolle in Bezug auf den Krankheitsbeginn, -verlauf und -ausgang in unserem CD40-vermittelten Colitis-Modell heraus.

3 Introduction

3.1 The immune system

The immune system protects the body from invading pathogens like bacteria and viruses while self-proteins and beneficial bacteria have to be tolerated. To meet this challenge, the immune system has to discriminate between self and non-self. The immune system consists of two interlocking arms, the innate immunity as first line of defense followed by the adaptive immune response, providing immunological memory.

The innate immune system is activated immediately after infection when membrane bound pattern recognition receptors such as Toll-like receptors (TLRs) bind pathogen-associated molecular patterns expressed by invading microbes. These receptors show a rather small and less diverse repertoire that is germ-line encoded. Innate immunity further includes defensive barriers (skin, mucus), different cell types releasing pro-inflammatory cytokines (macrophages, natural killer cells) or acting as phagocytes (macrophages, neutrophils, monocytes), and various proteins (complement proteins, chemokines, defensins).

As second line of defense, adaptive immunity is acting antigen-dependent and antigen-specific to eliminate pathogens sufficiently. Antigen presenting cells (APCs) like dendritic cells (DCs) (but also B cells, macrophages, fibroblast and epithelial cells) are considered as interface between innate and adaptive immunity as they take up antigen from invading pathogens and present peptides on their surface via major histocompatibility complex (MHC) molecules recognized by the appropriate T cell receptor (TCR) on T cells. T cells representing the cell-mediated response are distinguished into cytotoxic T cells ($CD8^+$ T cells) or T helper (Th) cells ($CD4^+$ T cells). While $CD8^+$ T cells activated by peptide-MHC class I (MHCI) complex destroy infected cells by the production of perforin, granzyme or granulysin, Th cells activated by peptide-MHC class II (MHCII) secrete cytokines to attract other cells or activate B cells. In contrast to T cells, B cells bind native antigen directly on their B cell receptor (BCR) without the need of presentation on MHC molecules by APCs. Upon receiving signals from

Th cells, B cells will undergo differentiation into antibody-secreting plasma cells or memory B cells, representing the humoral response. On the one hand, secreted antibodies bind to pathogens for neutralization, complement activation or opsonization to finally eliminate the pathogen. On the other hand, memory B cells are generated to enable appropriate responses upon repeated contact with the same pathogen.

The opportunity to provide a huge repertoire of TCRs and BCRs with high specificity and affinity is achieved by V(D)J-recombination. In contrast to innate pattern recognition receptors with a fixed repertoire, the rearrangement of TCRs and BCRs from a constrained amount of gene segments enables the expression of a broad variety to recognize the whole spectrum of potential foreign antigens. However, as this process relies on a low frequency of precursor cells, the generation of appropriate cell numbers requires some time. Further, the random process of somatic recombination is also generating self-reactive receptors, which requires tolerance induction as further quality assurance to avoid autoimmunity.

3.1.1 Central and peripheral T cell tolerance

T cell development takes place in the thymus where they have to be trained to distinguish self- and nonself-antigens. As soon as the TCR is expressed on the surface of CD4⁺CD8⁺ double-positive thymocytes, cells are selected due to their strength of the interaction of the TCR with self-peptide-MHC complexes [1]. More than 90 % of double-positive thymocytes do not bind self-peptide-MHC at all and die by neglect [2]. In contrast, immature double-positive thymocytes expressing a TCR with intermediate affinity for self-peptide-MHC complexes are positively selected to differentiate into mature CD4 or CD8 single-positive thymocytes. Thymocytes bearing a high-affinity TCR for self-peptide-MHC complexes are eliminated (negative selection or clonal deletion), become Treg cells (clonal diversion) or a second round of TCR rearrangement (receptor editing) takes place [1].

Since about 25-40 % of self-reactive T cells might escape from clonal deletion [3] and the selection process is limited by the variety of antigens expressed in the thymus, tolerance has

to be induced in the periphery, too (peripheral tolerance). This concerns mainly food- and commensal-derived antigens which are first encountered outside the thymus but should be tolerated as well to prevent from allergic and inflammatory diseases [4].

To control self-reactive T cells in the periphery, DCs play a crucial role as professional APCs which effectively process antigen, express costimulatory molecules and secrete cytokines [5]. During both, steady state and inflammation, DCs are continuously sampling for antigen and migrate from peripheral tissues into draining lymph nodes to finally present processed peptides to T cells [6]. To convert immature, antigen-capturing DCs into fully mature, antigen-presenting DCs, some functional changes have to take place. Therefore, DCs stop sampling for antigens but instead (i) upregulate MHC to stimulate the TCR on T cells, (ii) upregulate co-stimulatory molecules like CD80 and CD86, binding to CD28 on T cells and (iii) secrete cytokines such as interleukin (IL)-12 for T cell polarization [7].

DCs can induce both, immunity and tolerance. It is assumed that the maturation state of DCs determines the outcome of T cell polarization, thus immature DCs induce tolerance while mature DCs induce immunity [8, 9]. However, it is also reported that mature DCs are mediating T cell tolerance by inducing Tregs [10] or unresponsive T cells [11]. Therefore, it is under debate whether the activation state, meaning which types of stimuli DCs receive, rather than the maturation state in terms of upregulation of costimulatory molecules, determines immunity versus tolerance induction.

3.1.1.1 Regulatory T cells

Regulatory T cells (Tregs) have been extensively studied due to their role in establishing and maintaining immune tolerance and therefore preventing autoimmune and inflammatory diseases. The main types of Tregs are CD4⁺ IL-10-producing type 1 Tregs, tumor growth factor β (TGF- β)-producing CD4⁺ Th3 cells and CD4⁺CD25⁺ forkhead box protein P3 (FoxP3)⁺ cells. We are focusing here only on CD4⁺CD25⁺FoxP3⁺ cells with Foxp3 as key transcription factor (TF) crucial for Treg development, function and homeostasis [12, 13, 14]. Mutations in the Foxp3 gene in both humans and mice have been shown to lead to fatal

autoimmune diseases such as fatal lymphoproliferative disorder of the scurfy mouse and the human equivalent immune dysregulation, polyendocrinopathy, enteropathy, X-linked inheritance syndrom [15, 16], demonstrating the crucial role of Tregs in peripheral tolerance.

FoxP3⁺ Tregs can be distinguished further into natural Tregs (nTregs) and induced Tregs (iTregs). While nTregs develop in the thymus upon the process of central tolerance, iTregs are generated in the periphery depending on environmental factors [17]. Therefore, it is obvious that the intestinal environment with its high amount of microbial antigens is the primary site of iTreg generation to sustain tolerance towards commensal bacteria and food-antigens, which cannot be represented in the thymus. To phenotypically differentiate iTregs from nTregs, surface markers such as Neuropilin-1 [18] and Helios [19] have been found to be preferentially expressed on nTregs. In addition, iTregs can be identified by the expression of retinoic acid-related orphan receptor γ t (ROR γ t), while they are negative for Helios [20].

3.2 Dendritic cells

Since DCs were first described by Ralph Steinman in 1973 in mouse spleen as cells with dendrite-shaped protrusions [21], this field of research, regarding DC origin, development and function got huge interest. As mentioned before, DCs are specialized cells sampling for antigens in peripheral tissues. Antigen-loaded DCs migrate into draining lymph nodes to prime antigen-specific T cells. Therefore, antigens are internalized and processed by DCs and peptides are finally loaded onto MHC molecules. Endogenous antigens are degraded by the proteasome and peptides are transported by the transporter associated with antigen processing into the endoplasmic reticulum to be loaded onto MHCI molecules [22] and presented to activate CD8⁺ T cells. In contrast, exogenous antigens are internalized by endocytosis and degraded in lysosomal compartments to be loaded onto MHCII molecules [23] and presented to activate CD4⁺ T cells. Next to these classical pathways, DCs show the property of cross-presentation, defined by the presentation of exogenous antigens also via MHCI [24, 25]. This concerns in particular viruses that are not infecting DCs directly or tumors [26].

Next to classical or conventional DCs (cDCs) described by Steinman, another subpopulation of DCs, plasmacytoid DCs, exists. These cells resemble plasma cells and produce large amounts of type I interferon in response to viral infections [27] but will not be discussed further in this thesis.

All DCs originate from hematopoietic stem cell-derived progenitors in the bone marrow and undergo several steps of differentiation. They differentiate from myeloid progenitors into granulocyte-macrophage precursors and further macrophage/DC progenitors, which are the origin for monocytes and the common DC precursors. Common DC precursors finally differentiate in the blood into plasmacytoid DCs and the precursor of cDCs which then enter lymphoid and non-lymphoid tissues to mature into cDCs. [28].

3.2.1 Conventional DCs

cDCs are divided into CD8a⁺ cells in lymphoid tissues and the equivalent population in non-lymphoid tissues, expressing the CD103 integrin marker, or CD11b⁺ cells [29]. CD8⁺ splenic DCs [30] as well as CD103⁺ DCs from non-lymphoid tissues [31] are specialized in cross-presentation. Further, CD8a⁺ splenic DCs are also described to secrete high amounts of IL-12p70 upon TLR stimulation [32].

CD11b⁺ DCs are present in all lymphoid organs except for the thymus and additionally in non-lymphoid tissues. In contrast to CD8⁺ DCs, the CD11b⁺ subset is more prominent to produce IL-6 and IL-23 and to induce CD4⁺ T cell responses instead of cross-presentation [33, 34, 35].

3.2.2 Intestinal DCs

DCs in the intestine are constantly exposed to foreign but also food- and commensal-derived antigens. Therefore, a tight regulation of intestinal DC function is indispensable to sustain tolerance towards commensal bacteria but at the same time protect from invading pathogens. Disturbance of intestinal homeostasis can result in chronic intestinal inflammation such as inflammatory bowel disease (IBD) [36].

Intestinal DCs are located in the gut-associated lymphoid tissue, consisting of peyer's patches (PPs) and isolated lymphoid follicles, as well as in mesenteric lymph nodes (mLNs) and throughout the intestinal lamina propria (LP) [37]. Intestinal DCs are defined as CD11c⁺ MHCII⁺ cells, lacking expression of CD64 to be distinguished from macrophages [38].

The three subpopulations of CD11c⁺MHCII⁺CD64⁻ intestinal DCs are CD103⁺CD11b⁻, CD103⁺CD11b⁺ and CD103⁻CD11b⁺ cells, whereby CD103⁺CD11b⁺ are most prominent in the small intestine LP [37]. This subset is reduced in the large intestine LP where CD103⁺CD11b⁻ and CD103⁻CD11b⁺ DCs are the major subsets instead [37].

It is assumed that the main antigen sampling cells in the intestine are resident C-X3-C motif chemokine receptor 1 (CX₃CR1)⁺ macrophages rather than CD103⁺ DCs [39, 40, 41].

Nevertheless, also DCs are able to acquire luminal antigens by several pathways. First, they can directly acquire antigens that actively invade the epithelium [40] or that are internalized by epithelial M cells [42]. Further, DCs can take over luminal antigen from CX₃CR1⁺ macrophages that previously acquired antigen via gap-junction proteins [43]. In addition, Farache et al. could visualize that upon bacterial challenge, CD103⁺ DCs are recruited from the intestinal LP into the epithelium to directly sample for luminal antigens by expanding their dendrites into the lumen [44]. As soon as DCs have acquired luminal antigen, they are able to migrate into draining lymph nodes where they initiate adaptive immune responses by T cell priming. Of note, all three intestinal DC subsets have the potential to migrate into mLNs in a CC-chemokine receptor 7-dependent manner [45, 46], but it is still not completely clear whether the different subsets are processing and presenting different luminal antigens and whether they prime different cells in the mLNs.

By presenting dietary antigens or antigens from commensal bacteria, intestinal DCs sustain gut homeostasis upon inducing oral tolerance. It was first shown by the group of Fiona Powrie that CD103⁺ DCs are the predominant subset to convert naïve T cells into Tregs and that this process depends on TGF- β and retinoic acid (RA) [47]. Therefore, CD103⁺ DCs highly express α v β 8 integrin to convert latent into active TGF- β as well as aldehyde dehydrogenase to metabolize vitamin A into RA [47, 48]. RA induces the expression of gut-homing receptors CC-chemokine receptor 9 and α 4 β 7 on T cells [49, 50]. So far, there are many contradictory studies, regarding the contribution of the different CD103⁺ DC subsets on the generation of peripheral iTregs. However, Esterhazy et al. could recently demonstrate that CD103⁺CD11b⁻ DCs are more efficient in inducing Tregs in the periphery rather than CD103⁺CD11b⁺ DCs [51].

As mentioned above, intestinal DCs are not only efficient in mediating tolerance but also effector responses. Also in the steady state, effector T cells are found in the intestine as result of previous pathogen encounter but also specific for commensals [52, 53]. In this context, CD103⁻ DCs are described to migrate into mLNs to induce effector T cells even in the

absence of further stimuli [46]. Hence, in the steady state, effector T cells can contribute to enhance the epithelial barrier [54] but are simultaneously controlled by CX₃CR1⁺ cells, anti-inflammatory cytokines and Tregs [55, 56].

By now, the conditions that convert tolerogenic into immunogenic DCs are not entirely known. As it is very likely that pathogen-associated molecular patterns from commensals are also encountered in the healthy intestine, it is comprehensible that a "second signal" might be critical for this conversion. So far, this second signal is not studied very well but a recent study by Hansen et al. supports this hypothesis. They show that IgA-containing immune complexes present after bacterial infection of the LP can convert tolerogenic into immunogenic human CD103⁻ DCs further inducing Th17 responses [57].

Another second signal that might be involved in conversion of tolerogenic into immunogenic DCs is CD40, which will be discussed in more detail below.

3.2.3 CD40-signaling in DCs

The costimulatory molecule CD40 is a transmembrane protein expressed on many cell types such as B cells, DCs, monocytes, epithelial cells, and endothelial cells [58]. CD40 is activated by CD40 ligand (CD40L), that is transiently expressed on activated CD4⁺ T cells [59] but also B cells, mast cells, basophils, eosinophils, DCs and platelets [60, 61].

CD40-CD40L interactions are critical mediators of immune responses and are also associated with the pathogenesis of IBD. Several human studies report higher levels of CD40L expression on T cells and platelets as well as elevated serum levels of soluble CD40L in IBD patients [62, 63, 64]. Further, patients suffering from Crohn's disease show CD40 overexpression on mucosal cells, endothelial cells and DCs [65, 66] and the treatment of Crohn's disease patients with an antagonistic CD40 monoclonal antibody (mAb) showed beneficial responses and remission rates [67].

In contrast to CD40-signaling on B cells that in particular induces proliferation [58], its impact on DCs is less well understood. It has been reported that CD40-signaling on DCs leads to

upregulation of MHCII and CD80/CD86, making them more effective in antigen presentation [68, 69, 70]. It has also been shown that CD40-ligation on DCs induces cytokine production such as IL-12 *in vitro* [71] and administration of agonistic anti-CD40 antibody has revealed immunostimulatory effects *in vivo* [72, 11]. However, other studies suggested that CD40-signaling needs further microbial stimuli, the TLR-ligands, to activate DCs completely for cytokine production [73, 74].

By using anti-CD40 mAb *in vivo*, the group of Fiona Powrie could show that CD103⁺ DCs were absent after administration of anti-CD40 mAb, resulting in colitis [75]. However, a big disadvantage of *in vivo* anti-CD40 antibody studies are the side effects as CD40 is also expressed on other cell types than DCs. For instance, CD40-signaling on B cells was reported to mediate necroinflammatory responses in the liver [76]. To study the direct effect of CD40 on DCs *in vivo*, avoiding the side effects upon anti-CD40 antibody usage, our group generated a mouse model with DC-specific constitutive CD40-signaling [77].

3.2.3.1 CD40-mediated non-canonical NF- κ B activation in DCs

Nuclear factor- κ B (NF- κ B) activation is essential for the expression of a variety of genes involved in survival, proliferation and immune responses [78]. For B cells, it is reported that constitutive CD40-signaling activates the non-canonical NF- κ B pathway, promoting lymphomagenesis [79]. As CD40-signaling in DCs is associated with their maturation state, the NF- κ B pathway also plays an important role in DCs.

NF- κ B activation can be achieved via two signaling pathways, the canonical and the non-canonical NF- κ B pathway. The canonical NF- κ B activation is mediated for instance by TLRs. The formation of the inhibitor of κ B kinase (IKK) complex, consisting of IKK1, IKK2 and NF- κ B essential modulator (NEMO), leads to phosphorylation and subsequent proteasomal degradation of inhibitor of κ B (I κ B), resulting in p50/RelA heterodimer translocation into the nucleus to finally activate target genes [80] (Fig.3.1).

In contrast, the non-canonical NF- κ B pathway can be activated by tumor necrosis factor receptor (TNFR) superfamily members such as CD40. TNFRs bear cytoplasmic motifs that

bind TNFR associated factor 2 and/or 3 which enable degradation of NF- κ B-inducing kinase (NIK) and thus initiation of the signaling cascade. Upon phosphorylation of p100 by activated IKK1, p52 is generated and leads to the nuclear translocation of the p52/RelB complex, subsequently inducing target gene transcription [81] (Fig.3.1). Previous studies, using the alymphoplasia mouse with a spontaneous single point mutation in the NIK gene and mice with DC-specific NIK-deficiency indicate that non-canonical NF- κ B activation is critical for DC cross-presentation but not necessarily for DC development or CD4⁺ T cell priming [82, 83]. The non-canonical NF- κ B pathway is also involved in tolerance induction by DCs. *In vitro*, using siRNA-mediated knockdown of NIK or IKK1 in human DCs, it was demonstrated that the non-canonical NF- κ B pathway leads to immunosuppressive indoleamine 2,3 dioxygenase expression in DCs to ensure their immune regulatory functions [84].

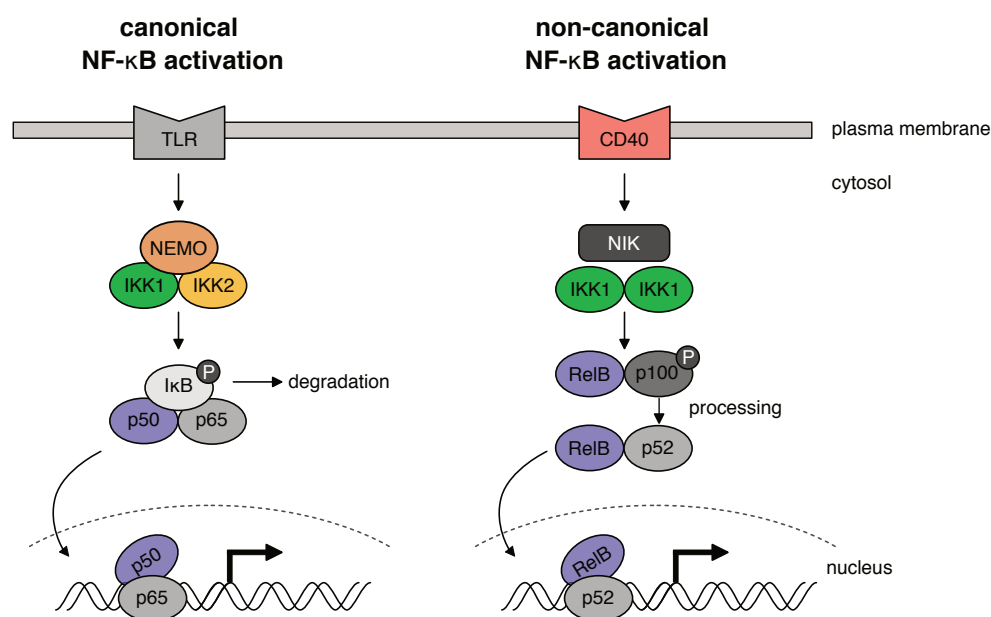


Figure 3.1: Schematic illustration of the canonical and non-canonical NF- κ B pathway in DCs. The canonical NF- κ B pathway (left) is activated upon TLR-stimulation on DCs. The complex, consisting of NEMO, IKK1 and IKK2, induces I κ B phosphorylation followed by degradation, finally releasing p50/p65 to activate target gene transcription. The non-canonical NF- κ B pathway (right) is activated upon CD40-signaling on DCs. Activated IKK1 induces phosphorylation and processing of p100. The resulting p52/RelB complex is translocated into the nucleus and activates transcription of target genes.

3.3 Gut microbiota

The role of gut microbiota in health and disease is an emerging field of research that has gained huge interest during the last years. In particular, 16S rRNA sequencing of luminal content provides much information about the bacterial composition in the mammalian gut [85, 86].

The mammalian gastrointestinal tract is shaped by highly diverse microbiota. More than 1000 species with about five million genes have been reported to exist in the human gut [87, 88], whereby the concentration increases from small intestine with 10^3 to 10^7 bacterial cells/g to large intestine with 10^{12} bacterial cells/g [89]. Of note, the microbial composition is influenced by multiple factors such as host genetics, age, diets, infections, and antibiotics [90]. From the first contact with bacteria at birth, bacterial diversity develops, whereby the phyla Bacteroidetes and Firmicutes predominate the adult mammalian intestine [91]. As mucosal immune cells are constantly exposed to harmless, so called commensals as well as harmful bacteria, a precise coordination between microbiota and host immune cells is indispensable to regulate the induction of tolerance or inflammatory responses in this environment.

3.3.1 Microbial-host interactions

The intestinal LP is home of a variety of host immune cells such as DCs, plasma cells, nTregs and iTregs as well as effector T cells like Th17 and Th1 cells (Fig.3.2). As described in chapter 3.2.2, intestinal DCs are constantly sampling luminal bacteria to transport bacterial antigen into draining mLNs where they prime naïve T cells to differentiate into Tregs or effector T cells in the LP. Further, secretory IgA (SIgA) is produced by intestinal plasma cells and transcytosed across the epithelium to coat bacteria in the lumen. However, if homeostasis is disturbed and microbial composition changes from symbiosis towards dysbiosis, microbial-host interactions might contribute to the development of inflammatory diseases like IBD.

Several studies could reveal that the gut microbiota is not only influencing a variety of metabolic and physiological functions of the host [92] but also effecting the host immune

system itself [93]. However, there are still major gaps in our understanding of the complex interaction between the microbial community and the host. One important question that still remains to be addressed is how the immune system regulates the microbiota and how the microbiota shape host immunity to finally reveal whether intestinal diseases are cause or consequence of altered bacterial compositions.

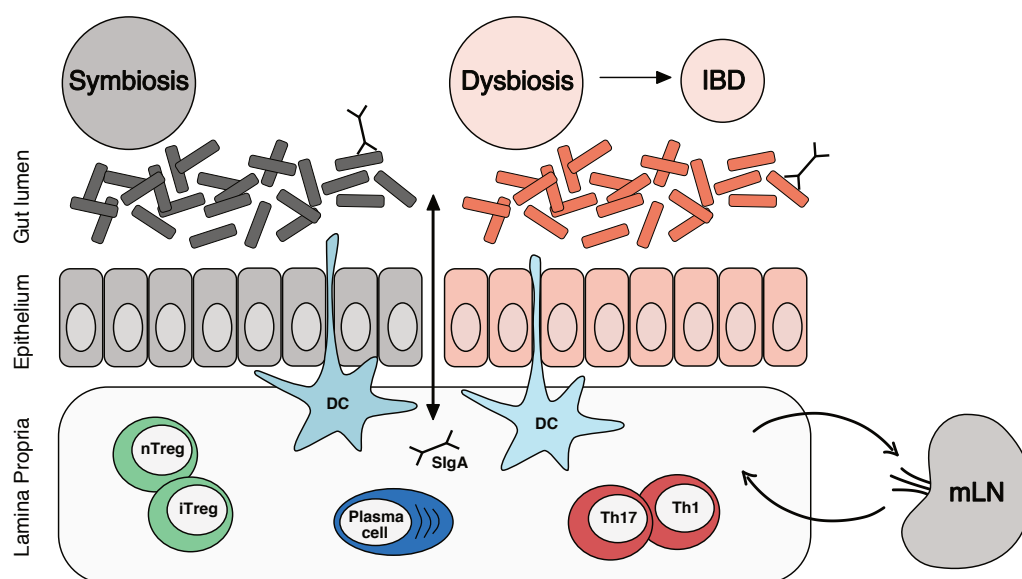


Figure 3.2: Microbial-host interactions during health and disease. Intestinal DCs sample for bacterial antigens and transport them into mLNs. Primed naïve T cells re-enter the LP to differentiate into Tregs or effector T cells to sustain tolerance during symbiosis in health or promote inflammatory responses upon dysbiosis, leading to IBD. SIgA produced by plasma cells in the LP is transported across the epithelium to bind luminal bacteria.

In a healthy gut, the host cells live in mutualistic symbiosis with the gut microbiota. Beneficial bacteria, termed commensals, are indispensable in the intestine with regard to digestion and nutrition. For instance, commensals provide us with short chain fatty acids such as acetate, propionate and butyrate from indigestible dietary fibers as source of energy and synthesize vitamin B and K [94]. Therefore, commensal bacteria must be tolerated while invading pathogens must be eliminated to prevent intestinal inflammation. To maintain this mucosal homeostasis, different levels of protection have evolved.

The epithelium represents a barrier, consisting of absorptive epithelial cells, goblet cells and paneth cells, separating the lumen from the LP but also cross-talking between both com-

partments. The structural epithelial integrity is sustained by cell-cell junctions such as tight junctions, adherens junctions and desmosomes [95]. Further, the epithelium is protected by a covering mucus layer whereby goblet cells, which are enriched in the large intestine, secrete mucins such as MUC2 to build an inner and an outer mucus layer [96]. Commensal bacteria are usually colonizing the outer mucus layer while the inner mucus layer separates the commensal bacteria from the epithelium [96]. The inner mucus layer can only be penetrated by some specialized bacteria such as *Clostridium*, *Lactobacillus* or *Enterococcus* [89]. Although the bacterial diversity is much higher in the lumen, mucosa-associated bacteria might be even more important in the context of interaction with host cells and thus mucosal homeostasis as they are in closer contact with epithelial cells [97].

Despite secreting mucins, antimicrobial peptides (AMPs), chemokines and cytokines [98], a recent study suggested that goblet cells might also play a critical role in luminal antigen delivery to CD103⁺ DCs in the LP by formation of goblet cell-associated antigen passages to induce oral tolerance in the steady state [99]. Another type of intestinal epithelial cells are paneth cells, in particular producing AMPs [100]. However, paneth cells are only present in the small intestine, thus the amount of AMPs in the large intestine is rather low [100].

Further, the epithelial barrier is influenced by immune cells. It was reported that secretion of IL-5 and IL-13 by Th2 cells contributes to colonic wound repair by macrophage activation followed by epithelial cell proliferation [101]. In contrast, a human study with patients suffering from Ulcerative Colitis did show that pro-inflammatory IL-13, that is upregulated in these patients, leads to apoptosis of epithelial cells and thus to barrier disruption [102].

3.3.1.1 The role of IgA

IgA is the predominating immunoglobulin (Ig) in the gut and the second most abundant isotype in the blood [103]. While serum IgA can be present as monomer as well as polymers, intestinal IgA is only found as dimer [104]. These IgA dimers bind to polymeric Ig receptor at the basolateral membrane of epithelial cells to be transported across the epithelium [105].

IgA is then released into the intestinal lumen, thereby containing the secretory component as part of the polymeric Ig receptor that provides stability of SIgA within the lumen and adhesion to mucus [105].

IgA is essential for mucosal homeostasis [106, 107] and the fact, that germ-free mice show 10-fold reduced numbers of IgA-producing cells [108] highlights the impact of the microbiota on host immune cells. SIgA is known to be involved in both maintenance of commensal bacteria as well as neutralization of invading pathogens [109, 110]. Although potential functions of IgA might include immune exclusion, neutralization, motility alteration, modulation of gene expression, niche occupancy, and antigen uptake via epithelial M cells [111], the diverse and complex functions of IgA are not fully understood so far.

IgA originates from B cells that undergo class switching and affinity maturation in organized follicular structures of the gut-associated lymphoid tissue as well as extrafollicularly in the LP [111]. The most prominent IgA-inductive sites are PPs, only present in the small intestine, but also mLNs, isolated lymphoid follicles in small and large intestine and the cecal patch [111]. These B cells home to the intestinal LP via the blood circulation and finally differentiate into IgA-secreting plasma cells. IgA⁺ plasma cells as well as both free IgA and IgA bound to bacteria are in particular found in the small intestine LP and only to a minor extent in the large intestine LP, while a small population of IgA⁺ plasma cells can be also found in extraintestinal tissues such as liver or bone marrow [111].

IgA can be induced in a T cell-dependent and T cell-independent manner. T cell-dependent induction requires the formation of germinal centers, thus PPs and mLNs are prone for this pathway. Here, T cell help provided by CD4⁺ T cells such as T follicular helper cells, Tregs and Th2 cells promote B cell proliferation, class switch recombination and somatic hypermutation via CD40-CD40L interaction and production of cytokines such as TGF- β 1, IL-4, IL-6 and IL-10, resulting in IgA-secreting plasma cells [112]. It is assumed that T cell-dependent IgA induction leads to high-affinity and monospecific IgA, responsible for neutralizing toxins and pathogens [111]. In contrast, IgA can also be induced T cell independently at follicular and extrafollicular sites in the LP without the need of germinal centers [111]. IgA induction

without T cell help is suggested to be of low-affinity and polyspecific nature to interact with commensal bacteria [111]. However, this differentiation is not absolute and needs further studies as there are reports that also high-affinity IgA is involved in the regulation of commensal microbiota [113] and that low-affinity IgA plays a role in protection against pathogens [114].

Increased coating of bacteria with IgA is reported for patients suffering from IBD as well as in mice [115, 116, 117]. The study by Palm and colleagues revealed that highly IgA-coated bacteria from IBD patients lead to colitis upon transfer into germ free mice [115]. For the human intestine, next to bacterial IgA-coating, also IgM- and IgG-coating is detectable [116]. Although IgM⁺ and IgG⁺ plasma cells are not observed in the murine intestine, serum IgM and IgG antibodies are reactive to bacteria and in particular for serum IgG it was shown that this isotype binds to a similar bacterial subset that is coated by IgA [118, 119].

In recent years, it became more widely accepted that the microbiota is influencing not only the mucosal but also the systemic IgA repertoire. For instance, serum IgA induced by commensals was reported to protect mice from fatal sepsis upon epithelial barrier breakdown [120]. Further, patients with IBD show higher levels of bacteria-specific serum IgA levels [121], whereby some studies observed serum IgA-reactivity for flagellin and autoantigens [122, 123, 124]. Interestingly, Iversen et al. recently revealed that serum IgA and intestinal IgA are specific for the same epitopes in patients suffering from celiac disease, suggesting that systemic and mucosal IgA-secreting plasma cells derive from the same B cell clone [125]. Furthermore, two studies demonstrated that commensals are able to induce serum IgG responses that could protect from systemic infection and influence mucosal T cell fate decisions [118, 119].

Although studies focusing on the role of IgA in microbial-host interactions could provide important insights, there is further research necessary to reveal the mutualistic relationship of bacteria and mucosal IgA. In particular, there is little known about the role of distinct bacterial species in inducing IgA class switch and the impact of IgA inductive sites on mucosal homeostasis [112].

3.3.1.2 Intestinal CD4⁺ T cells

CD4⁺ T cells are the most common T cells in the intestinal LP. As described in section 3.1.1.1, Tregs are the predominant intestinal subset in the steady state, maintaining tolerance towards food- and commensal-derived antigens. In contrast, a key component of intestinal inflammation is the infiltration of the LP by CD4⁺ effector T cells.

Naïve CD4⁺ T cells recognize their cognate antigen presented by MHCII on APCs. Upon TCR stimulation in combination with distinct cytokine combinations, naïve CD4⁺ T cells can not only differentiate into Tregs but also Th cells which are further classified into Th1, Th2 and Th17 cells. Th1 cells are the major subset that develops in response to intracellular pathogens such as bacteria and viruses upon stimulation with interferon- γ (IFN- γ) and IL-12 [126]. In addition to signal transducer and activator of transcription (STAT) 1 and STAT4, Th1 cells express the key TF T-bet, driving the production of the signature cytokine IFN- γ but also TNF- α and IL-2 [127]. Th1 cells are linked to autoimmunity as they are able to induce experimental autoimmune encephalomyelitis [128] as well as intestinal inflammation while naïve T cells with T-bet or STAT4 deficiency were not able to induce colitis upon adoptive transfer experiments in mice [129, 130]. In contrast, IL-4 and IL-2 drive the fate of Th2 cells in the context of extracellular pathogens and are key mediators, providing B cell help for antibody production. Th2 cells express the TF STAT5, STAT6 and GATA3 and predominantly secrete IL-4, IL-5 and IL-13 [126]. Th17 cells are induced by TGF- β , IL-6 and IL-21. This Th subset is characterized by the expression of the TF STAT3 and ROR γ t and production of the signature cytokines IL-17A, IL-17F and IL-22 [126]. While TGF- β alone is sufficient to induce FoxP3⁺ Tregs, Th17 cell differentiation needs IL-6 in addition, that leads to expression of IL-23R [126, 131]. These non-pathogenic Th17 cells are not able to induce autoimmune tissue inflammation as they also produce IL-10 [132]. However, upon further IL-23 stimulation, Th17 cells show a more pathogenic gene expression pattern, indicated by upregulation of T-bet, IL-23R, IL-7R and granulocyte-macrophage colony-stimulating factor, and are reported to contribute to experimental autoimmune encephalomyelitis [133, 134]. Of

note, so called pathogenic Th17 cells can also be induced independent of TGF- β 1 by IL-1 β , IL-6 and IL-23 or TGF- β 3 and IL-6 [133, 135]. A major hallmark of Th17 cells is their high plasticity as they are more prone for transdifferentiation as compared to Th1 and Th2 cells. Thus, Hirota et al. could demonstrate the property of Th17 cells to acquire a Th1-like phenotype by downregulation of IL-17 but upregulation of IFN- γ expression [136].

In the context of CD4⁺ T cell fate decisions, there is increasing evidence that gut microbiota has a major impact, thus eliciting pro- as well as anti-inflammatory responses. At the steady state, Th17 cells are abundant in the intestinal LP to ensure protection against pathogens such as *Candida albicans* [137]. However, the Th17 cell response is related to several autoimmune and inflammatory diseases such as rheumatoid arthritis, multiple sclerosis, psoriasis and IBD [138]. Interestingly, Th17 cells are not detectable in the intestine of germ free mice [52], demonstrating the requirement of microbial stimuli for Th17 differentiation. The most prominent strain known in this regard is segmented filamentous bacteria (SFB). These gram-positive bacteria, predominantly colonizing the small intestinal mucus layer, are potent inducers of Th17 cells in the small intestinal LP of mice [139]. In this context, serum amyloid A produced by SFB was shown to promote DCs to prime Th17 cells *in vitro* and SFB colonization could protect the host from the pathogen *Citrobacter rodentium*, suggesting SFB as a major part of Th17-mediated mucosal protection [139]. Further, it is reported that the Th17 effector function depends on the respective species triggering Th17 differentiation. For instance, Zielinski and colleagues reported IL-17A and IFN- γ production of human Th17 cells upon infection with *Candida albicans*, whereas *Staphylococcus aureus* leads to IL-17A and IL-10 producing human Th17 cells [140].

Tregs are also known to be affected by gut microbiota. For instance, the short chain fatty acid butyrate, as product of fiber utilization by commensals is essential for colonic Treg responses [141]. In particular, *Clostridium* cluster IV and XIVa are potent drivers of IL-10⁺Helios⁻ iTregs in the large intestine [142]. Further, Round and Mazmanian reported that the human commensal *Bacteroides fragilis* is capable of promoting mucosal tolerance. They could show

that the bacterial antigen polysaccharide A leads to differentiation of CD4⁺ T cells into IL-10 producing Tregs in the steady state but also under inflammatory conditions [143].

Of note, this interaction between microbiota and host immune cells is a bidirectional crosstalk, in which the microbiota is shaping the host immunity but also the host effector T cells have a major impact on the microbiota colonizing the gut. If these processes are not tightly regulated, inflammatory diseases like IBD can be the consequence.

3.3.2 Inflammatory Bowel Disease

IBD is a multifactorial chronic inflammatory disease that is dependent on a variety of environmental and genetic risk factors as well as on the microbiota, colonizing the gut, and the host immune cells [144]. Patients with IBD are either suffering from Crohn's disease, affecting different sites of the gastrointestinal tract or Ulcerative Colitis, confining to the large intestine [97].

The most common phyla colonizing the healthy colon are Firmicutes and Bacteroidetes [145]. However, certain circumstances such as infection, inflammation, dietary changes, immune deficiency or antibiotic treatment can disturb mucosal homeostasis, causing a shift in relative abundance of bacteria towards less diversity. This imbalance is termed dysbiosis and characteristic for the pathogenesis of IBD. In this regard, IBD patients show about 25 % less microbial genes as compared with healthy people [146]. The most prominent change during IBD is the "bloating" of *Enterobacteriaceae* of the phylum Proteobacteria, which are less frequently represented in the healthy gut [145]. However, the determination of species shifted during IBD is difficult to summarize as it depends on the age of patients, disease stage as well as type of tissue sample and analysis [97]. Nevertheless, data from the largest study so far revealed that the abundance of *Enterobacteriaceae*, *Pasteurellaceae*, *Veillonellaceae* and *Fusobacteriaceae* was increased in patients with Crohn's disease whereas the abundance of Erysipelotrichales, Bacteroidales and Clostridiales was reduced, correlating with severity of the disease status [147].

The most abundant anaerobic species in the human intestine, the *Bacteroides*, are described as pathobionts that are able to act as commensals but under certain conditions, these species can contribute to disease development [148]. Other pathobionts reported to be increased in patients with IBD are *Escherichia coli*, *Shigella*, *Rhodococcus*, *Stenotrophomonas maltophilia*, *Prevotellaceae*, *Clostridium difficile*, *Klebsiella pneumoniae*, *Proteus mirabilis* and *Helicobacter hepaticus* [97].

3.3.3 *Helicobacter hepaticus*

The finding that *Helicobacter* species are critical players in the context of IBD is not surprising as every species systematically examined to date is colonized by at least one *Helicobacter* species [149]. In 2005, Warren and Marshall received the Nobel price in physiology for the discovery of *Helicobacter pylori* in 1982 [150]. Since *H. pylori* infection is associated with gastritis, gastric carcinoma and mucosa-associated lymphoid tissue lymphoma in humans [149], many other *Helicobacter* species were discovered and raised the interest to study their potential impact on disease development. The *Helicobacter* genus comprises 26 formally named species, colonizing several hosts such as humans, cats, dogs, swine, sheep, birds, mice, rats and many more [149].

Fox and colleagues were able to isolate *Helicobacter hepaticus* (*Hh*) from liver but also from cecum and colon of mice [151]. *Hh* is a gram-negative, urease-positive as well as nitrate-reducing bacterium, growing under microaerobic and aerobic conditions. Further, *Hh* has a curved to spiral shape with bipolar flagella, thus being actively motile and able to colonize the mucus of cecum and colon [151]. Of note, *Hh* is found in many academic and commercial mouse colonies [152, 153] and infection is linked to chronic hepatitis as well as hepatocellular carcinoma [154, 155]. Most interestingly, *Hh* is able to elicit intestinal inflammation in immunodeficient or -compromized mice as demonstrated by several mouse models, mimicking human IBD. For instance, *Hh*-infected severe combined immunodeficiency mice reconsti-

tuted with naïve CD45RB^{hi}CD4⁺ T cells develop severe colitis [156]. Further, *Hh* infection of Rag2^{-/-} [157, 158], IL10-deficient [159] as well as TCR $\alpha\beta$ -deficient mice [160] has been used to model human IBD in mice and to study the role of this specific pathobiont regarding the complex interaction with both, innate as well as adaptive host immune cells. In the T-cell dependent colitis model used by Kullberg and colleagues, *Hh* infection of IL10-deficient mice induced pathogenic, *Hh*-specific T cells, expressing both IL-17 and IFN- γ [161]. Only recently, the group of Dan Littmann published a further study, using the *Hh* infection model of IL-10^{-/-} mice [162]. The data reveal the TF c-Maf in iTregs as key component to restrain colitogenic Th17 cells in *Hh*-positive mice [162].

However, while it is reported that *Hh* causes lesions in the liver by producing a cytotoxic protein [163], the underlying mechanism by which this pathobiont leads to the development of colitis is still a major gap in our knowledge. Thus, further research is indispensable to determine the properties and functions of *Hh*, making this pathobiont such a potent inducer of intestinal disease.

Of note, there is a group of proteins related to bacterial infections, that might be a key component in eliciting host pathology. These bacterial proteins are the chaperonins, associated with human diseases such as systemic lupus erythematosus, rheumatoid arthritis and Crohn's disease [164]. Chaperonins are a subgroup of molecular chaperones, the heat-shock proteins (Hsps), which are typically noticed as protein folders but emerging evidence highlights their function also in cell-cell signaling and therefore eliciting immune response [164]. Chaperonins are expressed on the cell surface of various prokaryotic and eukaryotic cells but can also be secreted to interact with several cell types such as leukocytes and epithelial cells or activate cytokine production [164].

The best studied chaperonins are chaperonin 60 (GroEL) and chaperonin 10 (GroES) from *E. coli* [165, 166]. Chaperonins are highly conserved among human and bacteria, therefore tolerance of bacterial chaperonins upon infection would be expected. However, chaperonins are known to be immunogenic in both human and animals. For instance, mice infected with

Mycobacterium tuberculosis showed T cells specific for the chaperonin 60.2 of this species [167]. In addition, anti-chaperonin antibodies, for instance serum antibodies, targeting Hsp70 of *Hh*, have been detected in mice with chronic active hepatitis [168]. However, the role of *Hh*-chaperonins and host cell interaction in the context of IBD has not been studied so far.

3.4 The DC-LMP1/CD40 mouse model

To study conditions that convert tolerogenic into immunogenic DCs, we previously generated a mouse model, where CD11c⁺ cells, mostly DCs, receive a constitutive CD40-signal [77]. Therefore, a floxed stop cassette, followed by the gene for the fusion protein LMP1/CD40, consisting of the transmembrane protein LMP1 of Epstein-Barr-Virus and the intracellular signaling domain of human CD40, was knocked into the transcriptionally active *rosa26* locus of LMP1/CD40^{fl/flSTOP} mice (Fig.3.3 A). Upon breeding these mice with mice expressing Cre-recombinase under the control of the CD11c promoter, DC-LMP1/CD40 mice express LMP1/CD40, thus receive ligand-independent, DC-specific CD40-signaling (Fig.3.3 A). In contrast to control littermates, DC-LMP1/CD40 animals develop severe colitis, macroscopically characterized by a strongly shortened and thickened colon (Fig.3.3 B, upper panels) as well as microscopically by immune cell infiltration, loss of crypts and reduction of goblet cells (Fig.3.3 B, lower panels). Further, spontaneous colitis in DC-LMP1/CD40 mice is fatal after some weeks, whereas 100 % of transgenic animals that were crossed onto *Rag1*^{-/-} background or treated with mixture of antibiotics (ABX), survived as compared with control littermates (Fig.3.3 C). In addition, DC-LMP1/CD40 animals but not transgenic mice on *Rag1*^{-/-} background or treated with ABX showed increased levels of fecal lipocalin-2, a sensitive, non-invasive marker for inflammation (Fig.3.3 D), suggesting that disease development in DC-LMP1/CD40 mice depends on T and B cells as well as on microbiota.

In DC-LMP1/CD40 mice, a huge reduction in frequency as well as absolute numbers of CD103⁺CD11b⁻ and CD103⁺CD11b⁺ DCs has been observed in the colonic LP (Fig.3.4 A) while CD103⁻CD11b⁺ DCs were increased when compared to control littermates. We further could demonstrate that this reduction in the colonic LP results from the migration of CD103⁺ DCs into mLNs where they undergo apoptosis (data not shown here). While overall FoxP3⁺CD4⁺ T cells did not differ between transgenic and control mice (data not shown here), due to the loss of CD103⁺ DCs, ROR γ t⁺Helios⁻ iTregs were significantly impaired in different organs, most importantly in the colonic LP of DC-LMP1/CD40 mice (Fig.3.4 B).

As a consequence of constitutive CD40-signaling on DCs, we did observe increased inflammatory IL-17⁺IFN- γ ⁺ Th17/Th1 and IFN- γ ⁺ Th1 cells in the colon of transgenic animals but not in control littermates (Fig.3.4 C).

In summary, our previously published data suggest that CD40-activation of DCs might serve as powerful tool to shut down immune tolerance by various CD40L-expressing immune cells.

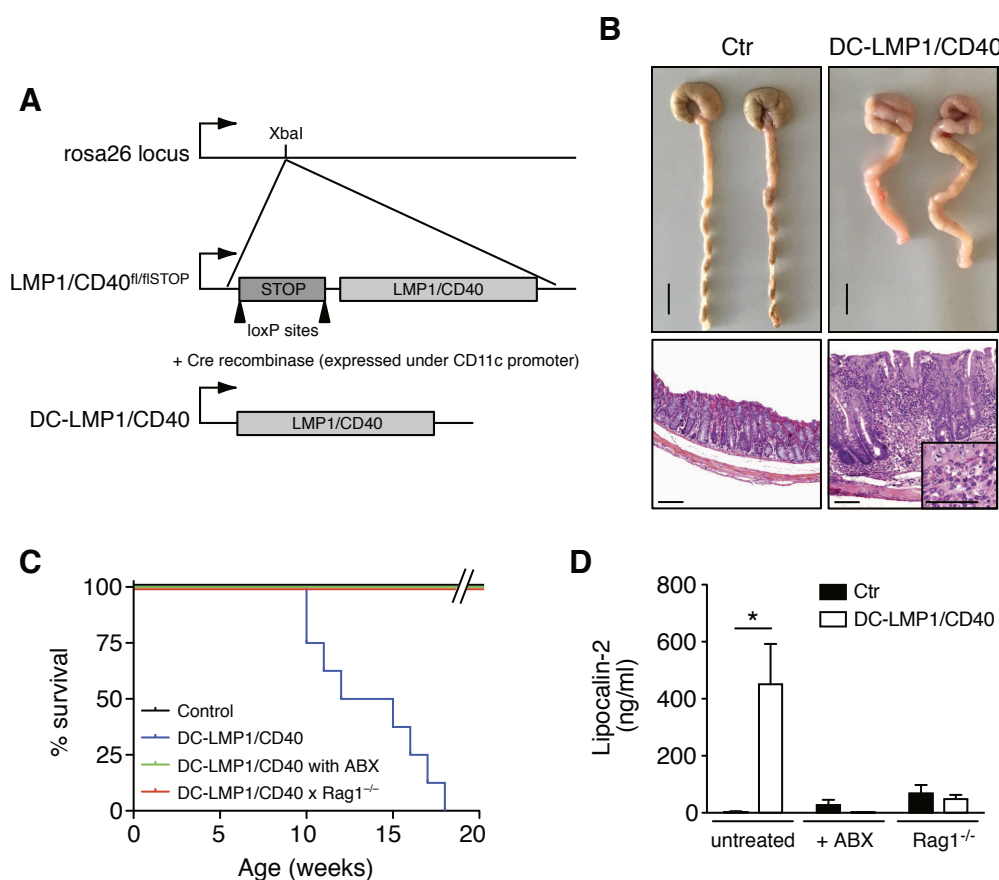


Figure 3.3: DC-LMP1/CD40 animals spontaneously develop fatal colitis.

A) Schematic representation of the *rosa26* locus in *LMP1/CD40^{fl/STOP}* and *DC-LMP1/CD40* mice. **B)** Macroscopic pictures of colons (upper panel, scale bars = 1 cm) and colon histopathology (lower panel, scale bars = 100 μ m) of control (Ctr) or *DC-LMP1/CD40* animals, showing severe colitis with thickening of the colon mucosa, extensive proprial infiltration of mixed inflammatory mononuclear cells, loss of crypts and reduction of goblet cells (paraffin sections, inset to *DC-LMP1/CD40*: GMA/MMA section, HE-staining). **C)** Kaplan-Meier plot showing survival of Ctr and untreated or ABX-treated *DC-LMP1/CD40* animals on C57BL/6 or *Rag1^{-/-}* background ($n \geq 6$). **D)** Levels of fecal lipocalin-2 as measured by ELISA in 8-10-week-old mice on different genetic backgrounds or treated with ABX. Bar graphs represent mean \pm SEM ($n \geq 3$ per group). Figure is adapted from Figure 2 in our recently published paper [77].

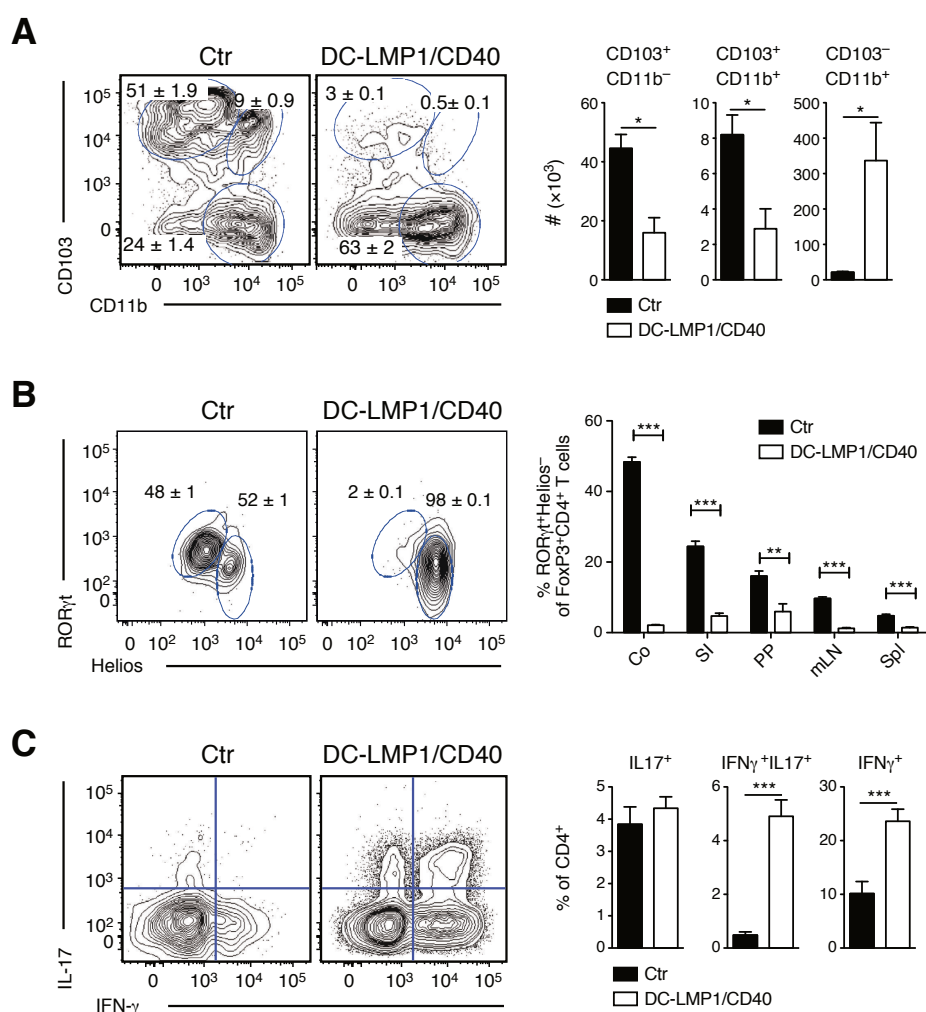


Figure 3.4: CD103⁺ DCs are strongly reduced in DC-LMP1/CD40 animals, leading to severely impaired iTreg induction and breakdown of T cell tolerance. **A)** DC subsets in the LP from Ctr and DC-LMP1/CD40 animals were gated on live, CD45⁺, CD11c⁺MHCII⁺, CD64⁻ cells. Representative FACS-plots are shown with numbers, indicating frequency of DC subsets and bar graphs show absolute numbers per colon (mean ± SEM, n=6). **B)** Single-cell suspensions from different organs were analyzed for Tregs. The representative FACS plots show nTreg (RORγt⁺Helios⁺) and iTreg (RORγt⁺Helios⁻) distribution within FoxP3⁺ T cells from colon LP. Cells are pre-gated on CD45⁺, CD3⁺CD4⁺, CD25⁺FoxP3⁺. Statistics of iTreg (RORγt⁺Helios⁻) distribution within FoxP3⁺ T cells in different organs pooled from two experiments are depicted as bar graphs (mean ± SEM, n=6). **C)** Single-cell suspensions were stimulated with PMA/Ionomycin and subsequently stained intracellularly for the production of IL-17 and IFN-γ. Shown are representative FACS plots for LP (gated on live, CD45⁺, CD3⁺CD4⁺ cells) as well as pooled statistics from more than five experiments (mean ± SEM, n=14-18). Figure is adapted from Figure 3, 4 and 5 in our recently published paper [77].

3.5 Aim of the thesis

We recently published a CD40-mediated mouse model of colitis, where CD11c-specific constitutive CD40-signaling leads to migration of CD103⁺ DCs from the colonic LP to draining lymph nodes followed by DC-apoptosis [77]. Loss of tolerogenic CD103⁺ DCs caused lack of ROR γ t⁺Helios⁻ iTregs and increase of inflammatory IL-17⁺IFN- γ ⁺ Th17/Th1 and IFN- γ ⁺ Th1 cells in the colon, resulting in breakdown of mucosal tolerance and early onset colitis that is fatal [77]. By crossing mice on Rag1^{-/-} background or by treatment with antibiotics, DC-LMP1/CD40 mice showed no signs of colitis, indicating that CD40-mediated colitis depends on both, T or B cells as well as on microbiota [77].

Nowadays, it is common knowledge that microbiota have critical impact on the pathogenesis of many diseases such as IBD. However, it is not known whether changes in the microbial composition during IBD are cause or rather consequence of inflammation. Further, underlying cellular and molecular mechanisms as well as specific bacterial proteins, contributing to disease development are rarely studied by now. Therefore, the aim of this study was to analyze microbial-host interactions in DC-LMP1/CD40 mice to determine how intestinal microbiota can modulate host immune response with impact on disease onset, progression and outcome in CD40-mediated colitis.

4 Material and Methods

4.1 Materials

4.1.1 Devices

Analytic scale (Adventurer, Ohaus Corp., Pine Brooks, NJ, USA), automatic pipettors (Integra Biosciences, Baar, Switzerland), bench centrifuge (Centrifuge 5415 D, Eppendorf, Hamburg, Germany), cell counter (CASY cell counter and analyzer, OMNI life science, Bremen, Germany), centrifuge (Rotixa RP, Hettich, Tuttlingen, Germany; Heraeus Multifuge X3R, Thermo Fisher Scientific, Waltham, MA, USA), chemical scale (Kern, Albstadt, Germany), ELISA-reader (ν max kinetic microplate reader, Molecular Devices, Biberach, Germany), tissue homogenizer (FastPrep-24, MP Biomedicals, Santa Ana, CA, USA), flow cytometer (FACSCalibur and FACSCantoII BD, Heidelberg, Germany), incubator (Hera cell, Heraeus Kendro Laboratory Products, Hanau, Germany), laminar airflow cabinet (Heraeus, Hanau, Germany), magnetic stirrer (Ika Labortechnik, Staufen, Germany), Molecular Imager Gel Doc XR+ (BIO-RAD, Hercules, CA, USA), NanoDrop SimpliNano (GE Healthcare), OPTIMAX X-ray film processor (Protec, Oberstenfeld, Germany), PCR-machine (Biometra, Goettingen, Germany), pH-meter (Inolab, Weilheim, Germany), pipettes (Gilson, Middleton, WI, USA), power supply (Amersham Pharmacia, Piscataway, NJ, USA), Qubit Fluorometer (Invitrogen, Carlsbad, CA, USA), Sonifier 150 Cell Disruptor (Branson/Emerson, St. Louis, MO, USA), vortex-Genie2 (Scientific Industries, Bohemia, NY, USA)

4.1.2 Consumables

BD Microtainer tube	BD, Franklin Lakes, NJ, USA
Disposable cell strainer (100 μ m nylon)	Falcon, Corning, NY, USA
Disposable injection needle (26 G x 1/2")	Terumo Medical Corporation, Tokyo, Japan

Disposable syringe (1+5 ml)	Braun, Melsungen, Germany
Disposable glass pasteur pipettes (150+230 mm)	VWR International, Leuven, Belgium
Laboratory gloves Latex Gentle Skin Grip	Meditrade, Kiefersfelden, Germany
Lysing matrix tubes (matrix A and E)	MP Biomedicals, Eschwege, Germany
Petri dish (94 x 16 mm)	Greiner Bio-One, Frickenhausen, Germany
PCR strips tubes (0.2 mL)	VWR International, Leuven, Belgium
Qubit assay tubes (0.5 mL)	Life technologies, Eugene, Oregon, USA
Reaction container 1.5 ml and 2 ml	Eppendorf, Hamburg, Germany
Reaction container 5 ml (FACS tubes)	BD, Franklin Lakes, NJ, USA
Reaction container 15 ml and 50 ml	Greiner Bio-One, Frickenhausen, Germany
Serological pipette, sterile (5, 10, 25, 50 ml)	Greiner Bio-One, Frickenhausen, Germany
TipOne filter tips (10, 200, 1000 μ l)	STARLAB, Hamburg, Germany
Tissue culture plates (96 wells-U, sterile)	Thermo Fisher Scientific, Waltham, MA, USA
Microtest staining plates (96 wells-U)	Sarstedt, Nümbrecht, Germany
Nunc MaxiSorp ELISA plates (96 wells, flat-bottom)	Thermo Fisher Scientific, Waltham, MA, USA

4.1.3 Chemicals

Unless stated otherwise, chemicals were purchased from Merck (Darmstadt, Germany), Roth (Karlsruhe, Germany) or Sigma-Aldrich (St. Louis, MO, USA). All buffers and solutions were prepared using double distilled water.

4.1.4 Buffer and media

ACK: 8.29 g NH_4Cl
1 g KHCO_3
37.2 mg Na_2EDTA
 H_2O ad 1 L
pH 7.4

FACS buffer: PBS
2 % (v/v) FCS
0.01 % NaN_3

HBSS: 137 mM NaCl
5.4 mM KCl
0.25 mM Na_2HPO_4
0.1 g glucose
0.44 mM KH_2PO_4
1.3 mM CaCl_2
1.0 mM MgSO_4
4.2 mM NaHCO_3

HBSS-EDTA: HBSS
8 % (v/v) FCS
10 mM EDTA
10 mM HEPES

PBS:	137 mM NaCl 2.7 mM KCl 10 mM Na ₂ HPO ₄ pH 7.4
50x TAE buffer:	242 g Tris-HCl 57.1 ml 100 % (v/v) acetic acid 100 ml 0.5 M EDTA (pH 8.0) H ₂ O ad 1 L
T cell-medium:	RPMI 10 % (v/v) FCS 100 U/ml Penicillin 100 g/ml Streptomycin 500 mM β-mercaptoethanol
10x Gitocher:	670 mM Tris pH 8.8 166 mM NH 65 mM MgCl ₂ 0.1 % (v/v) gelatin
1x Gitocher buffer:	5 μl 10x Gitocher buffer 2.5 μl 10 % Triton X-100 (v/v) 0.5 μl β-mecaptoethanol 3 μl proteinase K (10 mg/ml) 39 μl H ₂ O

Carbonate Coating Buffer	8.4 g NaHCO ₃ 3.56 g Na ₂ CO ₃ H ₂ O ad 1 L pH 9.5
5x SDS Loadingbuffer	250 mM Tris-HCL pH 6.8 500 mM β-mecaptoethanol 10 % (w/v) SDS 0.5 % Bromophenol blue sodium salt 50 % glycerol
5x Running Buffer	25 mM Tris 192 mM Glycin 0.1 % SDS
Transfer Buffer	25 mM Tris 192 mM Glycin 20 % Methanol 0.002 % SDS

4.1.5 Antibodies

Unless stated otherwise, anti-mouse antibodies were used.

epitope	conjugate	clone	manufacturer
CD3	AlexaFluor488	17A2	BioLegend
	PE-Cy7	17A2	BioLegend

Continued on the next page.

epitope	conjugate	clone	manufacturer
CD4	APC-Cy7	GK1.5	BioLegend
	PerCP	RM4-5	BioLegend
CD11b	APC-eFlour780	M1/70	Invitrogen
CD11c	PE-Cy7	N418	BioLegend
CD25	PerCP	PC61	BD Pharmingen
CD45	BV421	30-F11	BioLegend
CD64	APC	X54-5/7.1	BioLegend
CD103	PE	M290	BD Pharmingen
FoxP3	eFlour660	FJK-16s	eBioscience
Helios	FITC	22F6	eBioscience
human HSP60		LK-2	Enzo
IFN- γ	APC	XMG1.2	eBioscience
IgA	HRP		SouthernBiotech
	PE	mA-6E1	eBioscience
IgG	HRP		SouthernBiotech
IL-17A	PE	TC11-18H10.1	BioLegend
MHCII (I-A/I-E)	FITC	M5/114.15.2	BioLegend
ROR γ t	PE	AFKJS-9	eBioscience

4.1.6 Oligonucleotides

All oligonucleotides were purchased from Eurofins Genomics GmbH (Ebersberg, Germany).

target	primer	sequence 5' to 3'	application	reference
bacteria	universal_for	TCCTACGGGAGGC- AGCAGT	PCR	[169]
	universal_rev	GGACTACCAGGGT- ATCTAATCCTGTT		
<i>Helicobacter</i> spp.	hspp_for	TATGACGGGTATC- CGGC	PCR	[170]
	hspp_rev	ATTCCACCTACCT- CTCCCA		
<i>H. hepaticus</i>	hh_for	GCATTTGAAACTG- TACTCTG	PCR	[152]
	hh_rev	CTGTTTTCAAGCT- CCCC		
<i>H. typhlonius</i>	Ht_Franklin_for	TTAAAGATATTCT- AGGGGTATAT	PCR	[171]
	Ht_Franklin_rev	TCTCCATACTCT- AGAGTGA		

Continued on the next page.

target	primer	sequence 5' to 3'	application	reference
<i>H. rodentium</i>	Hr_Shen_for	GTCCTTAGTTGCT- AACTATT	PCR	[172]
	Hr_Shen_rev	AGATTTGCTCCAT- TTCACAA		
<i>H. bilis</i>	Hb_Fox_for	AGAACTGCATTTG- AAACTACTTT	PCR	[173]
	Hb_Fox_rev	GGTATTGCATCTC- TTTGTATG		
Cre	RO334	GGACATGTTTCAGG- GATCGCCAGGCG	genotyping	
	RO335	GCATAACCAGTGA- AACAGCATTGCTG		
LMP1/CD40	HL15	AAGACCGCGAAGA- GTTTGTCC	genotyping	
	HL54	TAAGCCTGCCAG- AAGACTCC		
	HL152	AAGGGAGCTGCAG- TGGAGTA		

Continued on the next page.

target	primer	sequence 5' to 3'	application	reference
IKK1	Ikk1FL-U	CGCTTAGTGTGAC- TGAGGAAC	genotyping	
	Ikk1FL-L	ATGAGCCCAACAT- TTAATCTT		
	Ikk1D-U	GGCATCAGAGTCC- GTGGGT		

4.1.7 Mouse strains

All mouse strains were bred and kept in the Institute for Immunology at the LMU Munich. Mice were housed under conventional conditions. In the course of move into a new animal facility, embryo transfer rederivation was performed by ENVIGO (Huntingdon, United Kingdom) and mice were subsequently housed under specific-pathogen-free (SPF) conditions. The following mouse strains have been used:

CD11c-Cre

The CD11c-Cre mouse strain was produced in the Lab of Boris Reizis and expresses the Cre recombinase under control of the CD11c promotor [174]. This mouse allows the deletion of floxed alleles in DCs and other CD11c-expressing cells. Mice were kept on the C57BL/6 genetic background.

DC-LMP1/CD40

To obtain DC-LMP1/CD40 animals, CD11c-Cre mice were crossed with LMP1/CD40^{fl/flSTOP} mice [79]. The latter mouse strain carries the knock-in of the LMP1/CD40 gene which is preceded by a floxed stop-codon into the rosa26 locus. The cre-mediated excision of the stop codon then leads to the constitutive expression of the fusion-protein between LMP1, derived from Epstein-Barr-Virus, and the intracellular signaling domain of human CD40.

The LMP1 domain anchors the protein in the plasma membrane and at the same time leads to a multimerization, which in turn leads to signaling by the CD40 molecule.

DC-LMP1/CD40 mice were previously published [77, 175, 187].

DC-LMP1/CD40 Δ IKK1

By additional DC-specific deletion of IKK1 as part of the non-canonical NF- κ B pathway, DC-LMP1/CD40 mice with impaired non-canonical NF- κ B signaling in DCs were generated. Therefore, LMP1/CD40^{fl/fl}^{flSTOP} mice were kept on IKK1^{fl/fl} background and crossed with CD11c-Cre mice on IKK1^{fl/fl} background to obtain DC-LMP1/CD40 ^{Δ IKK1} mice. In these mice, the CD11c-Cre allows the deletion of the floxed IKK1 alleles in DCs next to excision of the stop codon, leading to the constitutive expression of CD40 in DCs.

4.2 Methods

4.2.1 Immunological and cell biology methods

4.2.1.1 Harvesting of organs and single cell preparation

Animals were euthanized in a CO₂ chamber or sacrificed by cervical dislocation after they had been sedated using Isoflurane. Organs were removed using scissors and fine tweezers and put into phosphate buffered saline (PBS). Spleen and lymph nodes were mashed through a 100 μ m cell strainer and washed with ice cold PBS. Red blood cells were lysed using 1 ml ACK buffer for 5 min at room temperature. Cells were washed once again with PBS, counted using the CASY-counter (OMNI life science) and stored on ice for further analysis.

To analyze cells from the colonic LP, the colon was cleaned from fecal content, opened longitudinally and cut into pieces about 5 mm in size. The pieces were incubated with Hank's balanced salt solution (HBSS)-ethylenediaminetetraacetic acid (EDTA) for 10 min on a shaker at 37°C and the supernatant containing epithelial cells was discarded. The pieces were then digested once for 30 min and twice for 20 min with a mixture of Collagenase IV (157

Wuensch units/ml, Worthington, reconstituted in HBSS with 8% fetal calf serum (FCS)), DNase I (0.2 mg/ml) and Liberase (0.65 Wuensch units/ml, both from Roche, reconstituted in H₂O). The supernatant was collected after each digestion and cells were always washed with PBS. Collected cells were enriched for immune cells with Percoll gradient centrifugation. Therefore, cells were resuspended in 40 % Percoll (GE Healthcare) and underlayered with a 80 % Percoll solution using a glass pasteur pipette. After centrifugation for 20 min at 1800 rpm and 4°C (acceleration set to 3, deceleration set to 0), cells at the interphase were collected, washed once, counted using the CASY-counter and stored on ice for further analysis.

4.2.1.2 Flow Cytometry staining

For flow cytometric analysis, 2×10^6 cells per staining and per well were aliquoted into a 96 well plate. Cells were stained for 20 min at 4°C in the dark in 50 μ l of antibody mix diluted in fluorescence-activated cell sorting (FACS) buffer. After incubation, cells were washed once with 150 μ l FACS buffer and directly acquired at the FACS device.

For intracellular stainings, cells were fixed and permeabilized after they have been stained for all surface markers. Cells were fixed/permeabilized with a Cytofix/Cytoperm kit (BD) for 30 min at 4°C in the dark, according to manufacturer's instructions. After washing, cells were stained for intracellular markers for additional 30 min at 4°C in the dark.

For intranuclear staining of FoxP3 and Helios, cells were washed once and then resuspended in 200 μ l 1x Fixation/Permeabilization solution (eBioscience) for 30 min at 4°C in the dark. Cells were collected by centrifugation, the supernatant was removed and the cells were washed twice with 1x Permeabilization Buffer (eBioscience). Cells were then stained with either FoxP3- or Helios-specific antibody in 50 μ l Permeabilization Buffer for 30 min at 4°C in the dark. Afterwards, cells were washed once and acquired by FACS.

Acquisition was performed using a FACSCalibur or a FACSCantoII (BD). Data analysis was performed using the FlowJo software (version 9 and 10, TreeStar, Ashland, OR, USA).

4.2.1.3 Fecal IgA flow cytometry

To analyze IgA-binding of bacteria by flow cytometry, 2-3 fecal pellets from 8- to 15-week-old mice were homogenized by bead beating and fecal bacteria were stained with anti-mouse IgA as described previously [115]. Therefore, feces were placed into Matrix D tubes and incubated in 500 μ l PBS for 1 h on ice. Afterwards, homogenization was performed using the FastPrep-24 Instrument (MP Biomedicals) for 5 sec at maximum speed, followed by centrifugation at 50 x g for 15 min at 4°C. 100 μ l of fecal bacteria in the supernatant were washed with PBS/1 % bovine serum albumin (BSA) and centrifuged at 8000 x g for 5 min at 4°C. After an additional wash, bacterial pellets were resuspended in 100 μ l PBS/1 % BSA/20 % rat serum and incubated for 20 min on ice. Finally, bacteria were stained with 100 μ l PBS/1 % BSA containing a PE anti-mouse IgA antibody (1.3 μ g/ml, eBioscience) for 30 min on ice. Bacteria were washed three times with PBS and analyzed by flow cytometry.

4.2.1.4 Depletion of commensal bacteria

To deplete as many commensal bacteria as possible, animals were provided a mixture of antibiotics (ABX), containing ampicillin sodium salt (1 g/l), vancomycin hydrochloride (500 mg/l), neomycin sulfate (1 g/l) and metronidazole (1 g/l) in the drinking water for at least 3 weeks before analysis [176].

4.2.1.5 *Ex vivo* T cell restimulation

To assess the cytokine secretion potential of a polyclonal T cell population, animals were sacrificed and single cell suspensions of spleen, mLNs or colon LP were prepared as described in section 4.2.1.1. 2×10^6 cells per well were aliquoted into 96 well plates and unspecifically stimulated for 4 h at 37°C with phorbol-12-myristate-13-acetate (PMA) (40 ng/ml final) and ionomycin (1 μ g/ml final) in T cell-medium in the presence of 2 μ M Monensin (Golgi-Stop, BD). Afterwards, cells were washed twice with FACS buffer, stained extra- and intracellularly and acquired by FACS as described in section 4.2.1.2.

4.2.1.6 Lipocalin-2 ELISA

Fecal samples were prepared as published previously [177] but adjusted for a smaller amount of starting material. Therefore, 2-3 fecal pellets were collected, weighed and reconstituted in 100 μ l PBS containing 0.1 % Tween20 per 10 mg feces. The fecal homogenate was centrifuged at 100 x g for 15 min at 4°C and 100 μ l of the supernatant were transferred into a new tube containing 10 μ l protease inhibitor (cOmplete ULTRA Tablets, Roche). After centrifugation at 10,000 x g for 10 min at 4°C, the supernatant was stored at -20°C until use.

Samples were diluted 1:200 to 1:600 in Calibrator Diluent RD5-24 (1X) and lipocalin-2 was measured according to manufacturer's instructions using the Quantikine enzyme-linked immunosorbent assay (ELISA) for mouse Lipocalin-2/NGAL (R&D Systems).

4.2.1.7 Determination of fecal and serum antibody concentrations

Fresh feces were used to prepare fecal homogenates as described in section 4.2.1.6.

Blood from mice was collected by terminal cardiac puncture and transferred into a microtainer tube (BD). After incubation at room temperature for at least 3 h, the coagulated blood was centrifuged at 8,000 rpm for 5 min at room temperature and serum was frozen at -20°C until further use.

Fecal or serum antibody concentrations were determined using the Mouse IgG total Ready-SET-Go! or the Mouse IgA Ready-SET-Go! ELISA (eBioscience) according to the manufacturer's instructions.

4.2.1.8 Preparation of commensal bacterial lysate

The cecum of C57BL/6 mice was removed, opened longitudinally, transferred into a 2 ml tube, containing 1.5 ml PBS and cecal content was expelled by vigorous vortexing to get rid of the cecal tissue. Remaining cecal content was transferred into Lysing Matrix E tubes (MP Biomedicals) and then homogenized using the FastPrep-24 Instrument (MP Biomedicals) for 45 sec at maximum speed. Samples were spun down and supernatant was collected, filtered

and spun again at maximum speed. The protein concentration was determined according to the manufacturer's instructions using the Qubit Protein Assay Kit and Fluorometer (Invitrogen) and the cecal bacterial lysate (CBL) was stored at -20°C until use.

4.2.1.9 Culture and lysate preparation of *Helicobacter hepaticus*

The *Helicobacter hepaticus* strain *Hh-2* (ATCC 51448, [151]) was purchased from the Leibniz Institute DSMZ-German Collection of Microorganisms and Cell Cultures (DSM No.: 22909) and kindly cultivated by the group of Prof. Dr. Bärbel Stecher (Max von Pettenkofer-Institute, LMU Munich). Bacteria from cryo stock were resuspended in brain heart infusion medium and put onto blood agar plates (Columbia agar with 5% sheep blood, BD). Plates were incubated in a chamber with anaerobic conditions (83 % N₂, 10 % CO₂, 7 % H₂) for 4 days at 37°C. A subculture was cultivated further on in brain heart infusion medium with 3% sheep serum in a culture flask in the chamber with anaerobic conditions for additional 4 days at 37°C.

For lysate preparation, bacterial cells were harvested and washed 2-3 times with PBS. Cell pellets were resuspended in PBS and lysed by sonification with the Sonifier 150 Cell Disruptor (Branson/Emerson) 6 times for 3 min at level 3 on ice. Lysed cells were centrifuged at 20,000 x g for 30 min at 4°C and the supernatant was mixed with protease inhibitor (cOmplete ULTRA Tablets, Roche). The protein concentration was determined according to the manufacturer's instructions using the Qubit Protein Assay Kit and Fluorometer and the lysate was stored at -20°C until used for ELISA or immunoblotting.

4.2.1.10 ELISA for commensal- or *Helicobacter hepaticus*-specific antibodies

CBL was prepared as described in section 4.2.1.8 and diluted in Carbonate Coating Buffer to a final concentration of 1 µg/ml. Lysate from *Hh* (*HhL*) was prepared as described in section 4.2.1.9 and diluted in Carbonate Coating Buffer to a final concentration of 0.1 µg/ml. 100 µl of diluted lysate were coated per well over night at room temperature. Wells were washed five

times with PBS/0.05 % Tween20 followed by blocking of unspecific binding sites using 200 μ l PBS/0.5 % nonfat dried milk for 2 h at room temperature and again washing five times.

Differences in serum antibody concentrations between Ctr and DC-LMP1/CD40 mice (as determined in 4.2.1.7) were adjusted by using 2.5 μ g/ml serum IgG or 6.5 μ g/ml serum IgA for each sample.

100 μ l of diluted serum were added per well, incubated for 2 h at room temperature and washed again five times with PBS/0.05 % Tween20. For detection, isotype-specific antibodies coupled to horseradish peroxidase (HRP) were used at a dilution of 1:4,000 in PBS/0.5 % nonfat dried milk for 2 h at room temperature. After washing, the ELISA was developed using 100 μ l of 3,3',5,5'-tetramethylbenzidine solution. The reaction was stopped by adding 50 μ l 2 N H₂SO₄ and the optical density (OD) was measured at a wavelength of 450 nm with 630 nm as a reference wavelength, using the ELISA reader (ν max kinetic microplate reader, Molecular Devices).

4.2.1.11 Immunoblotting

Serum IgG or IgA reactivity towards CBL or *HhL* was analyzed by immunoblotting. CBL prepared as described in section 4.2.1.8 (30 μ g per lane or 600 μ g for Mini-PROTEAN II Multiscreen Apparatus (Bio-Rad)) or *HhL* prepared as described in section 4.2.1.9 (20 μ g per lane or 200 μ g for Mini-PROTEAN II Multiscreen Apparatus) were separated by sodium dodecyl sulfate-polyacrylamide gel electrophoresis (SDS-PAGE) at 90 V for 1-3 h in 1x Running Buffer and transferred to a nitrocellulose membrane, using the tank blot method.

Proteins were transferred to a nitrocellulose membrane by blotting at 30 V O/N at 4°C in Transfer Buffer. Membranes were blocked for unspecific binding with PBS/5 % nonfat dried milk for 1 h and then incubated with sera as primary antibodies in PBS/1 % nonfat dried milk for 1 h at room temperature or O/N at 4°C. Differences in serum antibody concentrations between Ctr and DC-LMP1/CD40 mice (as determined in 4.2.1.7) were adjusted by using 2.5 μ g/ml serum IgG or 1 μ g/ml serum IgA for each sample.

In some experiments, mouse IgG1 anti-human heat shock protein 60 (α HSP60) mAb (clone

LK-2) was additionally used as primary antibody (1:10,000 in PBS/1 % nonfat dried milk). Membranes were washed with PBS/1 % nonfat dried milk 3 times for at least 15 min each and incubated with HRP-coupled secondary antibodies (goat anti-mouse IgG-HRP or goat anti-mouse IgA-HRP, 1:10,000 in PBS/1 % nonfat dried milk) for 1 h at room temperature or O/N at 4°C, followed by additional washing as described above. Western Lightning Plus-ECL Detection Reagent (PerkinElmer) and X-ray films (Amersham) were used for protein detection at the OPTIMAX X-ray film processor (Protec).

4.2.1.12 Immunoprecipitation of potential antigens

Identification of bacterial antigens within CBL was performed by using serum antibodies from control and DC-LMP1/CD40 mice for immunoprecipitation followed by label-free liquid chromatography tandem mass spectrometry (LC-MS/MS). Therefore, 50 μ l protein G beads (Dynabeads Protein G, Invitrogen) were coupled with 2.5 μ g serum IgG from control or DC-LMP1/CD40 mice for 10 min at room temperature. 1600 μ g CBL were added to the coated beads, incubated for 30 min at room temperature, and the complex was washed three times with PBS/Tween 0.02 % followed by additional 3 rounds of washing with 50 mM NH_4HCO_3 . Samples were stored at -20°C until LC-MS/MS was performed in the Protein Analysis Unit (Biomedical Center, LMU Munich).

4.2.1.13 On-beads trypsin digest and Mass Spectrometry

Following the immunoprecipitation procedure, beads were incubated with 100 μ l of a 10 ng/ μ l trypsin solution in 1 M Urea and 50 mM NH_4HCO_3 for 30 min at 25°C for trypsin digestion. The supernatant was collected, beads washed twice with 50 mM NH_4HCO_3 and all three supernatants collected together and incubated overnight at 25°C at 800 rpm after addition of dithiothreitol to 1 mM. Iodoacetamide was added to a final concentration of 27 mM and samples were incubated at 25°C for 30 min in dark. One μ l of 1 M dithiothreitol was added to the samples and incubated for 10 min to quench the iodoacetamide. Finally, 2.5 μ l of trifluoroacetic acid were added to the samples and the samples were subsequently

desalted using C18 Stage tips. Samples were evaporated to dryness, resuspended in 15 μl of 0.1 % formic acid solution and injected in an Ultimate 3000 RSLCnano system (Thermo), separated in a 15 cm analytical column (75 μm ID home-packed with ReproSil-Pur C18-AQ 2.4 μm from Dr. Maisch) with a 50 min gradient from 5 to 60 % acetonitrile in 0.1 % formic acid. The effluent from the HPLC was directly electrosprayed into a Qexactive HF (Thermo) operated in data dependent mode to automatically switch between full scan MS and MS/MS acquisition. Survey full scan MS spectra (from m/z 375 - 1600) were acquired with resolution $R = 60,000$ at m/z 400 (AGC target of 3×10^6). The 10 most intense peptide ions with charge states between 2 and 5 were sequentially isolated to a target value of 1×10^5 , and fragmented at 27 % normalized collision energy. Typical mass spectrometric conditions were: spray voltage, 1.5 kV; no sheath and auxiliary gas flow; heated capillary temperature, 250°C; ion selection threshold, 33,000 counts. MaxQuant 1.5.2.8 was used to identify proteins and quantify by intensity-based absolute quantification (iBAQ) with the following parameters: Database, uniprot_proteomes_Bacteria_151113.fasta; MS tol, 10 ppm; MS/MS tol, 0.5 Da; Peptide FDR, 0.1; Protein FDR, 0.01 Min. peptide Length, 5; Variable modifications, Oxidation (M); Fixed modifications, Carbamidomethyl (C); Peptides for protein quantitation, razor and unique; Min. peptides, 1; Min. ratio count, 2. Identified proteins were considered as interaction partners if their MaxQuant iBAQ values were greater than \log_2 2-fold enrichment and p -value 0.05 (ANOVA) when compared to the control.

4.2.1.14 Infection with *Helicobacter hepaticus* by oral gavage

Bacterial suspensions cultured as described in section 4.2.1.9 were used for oral infection of mice. *Hh* identity was confirmed by sequencing prior to infection. Bacterial density was determined by OD measurements at 600 nm. Appropriate amount of suspension was washed with PBS and then adjusted to OD(600) 3.0. Mice were inoculated with 100 μl of the suspension by oral gavage at d0, d3 and d5, for a total of 3 doses. Animals were analyzed 40 days post inoculation (p.i.).

4.2.2 Molecular biology methods

4.2.2.1 Isolation of genomic DNA

In order to isolate genomic deoxyribonucleic acid (DNA) for genotyping, a little piece of mouse tail tip or ear was put into a 50 μ l 1x Gitocher buffer and incubated at 55°C for 6 h, followed by a 5 min incubation at 95°C for proteinase K inactivation.

Isolation of bacterial DNA from fecal pellets was performed with the QIAamp Fast DNA Stool Mini Kit (Qiagen) according to the manufacturer's instructions.

4.2.2.2 Polymerase chain reaction

To determine the genotype of mice, template DNA from tail or ear, isolated as described in section 4.2.2.1, was used. The region of interest was amplified using the respective primers (listed in 4.1.6) and respective polymerase chain reaction (PCR) programs at the PCR-machine (Biometra):

Reaction mix - genotyping

DNA template	1 μ l
5x MyTaq Red Reaction buffer (Bioline)	5 μ l
Primer for (100 pmol/ μ l)	0.1 μ l
Primer rev (100 pmol/ μ l)	0.1 μ l
MyTaq Polymerase (Bioline)	0.15 μ l
H ₂ O	18.65 μ l

PCR conditions - genotyping

	CD11c-Cre		LMP1/CD40
initialization	95 °C 5 min		94 °C 2 min
denaturation	95 °C 30 sec] 35 cycles	94 °C 10 sec
annealing	55 °C 30 sec		62 °C 30 sec
elongation	72 °C 45 sec		72 °C 30 sec
final elongation	72 °C 5 min		72 °C 2 min
final hold	4 °C		4 °C

To screen mice for bacterial colonization, bacterial DNA was isolated from fecal pellets as described in section 4.2.2.1, concentration was measured at the NanoDrop (GE Healthcare) and adjusted to 2 ng/ μ l. Amplification of the region of interest was performed, using 5-10 ng DNA and the respective primers (listed in 4.1.6) with the following PCR programs:

PCR conditions - bacterial colonization

			annealing temperature
initialization	94 °C 4 min		
denaturation	94 °C 1 min] 35 cycles	universal bacteria 58 °C
annealing	55-61 °C 1 min		<i>H. spp, H. hepaticus</i> 61 °C
elongation	72 °C 1 min		<i>H. bilis, H. rodentium</i> 55 °C
final elongation	72 °C 7 min		<i>H. typhlonius</i> 55 °C
final hold	4 °C		

4.2.2.3 Agarose gel electrophoresis

To visualize and separate DNA fragments according to size, samples were subjected to agarose gel electrophoresis. The gel consisted of 1 - 2 % agarose dissolved in 1x TAE buffer with addition of ethidium bromide at a final concentration of 0.5 μ g/mL. Separation of fragments on the gel was achieved with a constant voltage (90 V) applied to an electrophoresis chamber containing a conductive buffer (1x TAE). For size estimation of fragments, a 100 bp ladder was used (New England Biolabs). The DNA samples were visualized by examination under ultraviolet light at 312 nm, using the Molecular Imager Gel Doc XR+ (BIO-RAD).

4.2.2.4 16S rRNA amplicon sequencing and taxonomic profiling

Analysis of the intestinal microbiota of mouse fecal samples was based on the recently developed dual-index strategy for sequencing on the MiSeq Illumina platform [178]. Briefly, genomic DNA was extracted from stool samples using the phenol-chloroform extraction technique with mechanical disruption [179]. Inserts were PCR-amplified in duplicate using multiplexed 8 forward x 12 reverse primers targeting the V3-V4 variable regions of the 16S ribosomal ribonucleic acid (rRNA) gene [180] and purified using the Agencourt AMPure XP PCR Purification system (Beckman Coulter). Purified amplicons were combined in equimolar amounts in one pool and sent to Eurofins Genomics (Ebersberg, Germany) for library quality control and sequencing on the Illumina MiSeq v.3 as 300-bp paired-end runs. Sequencing output was pre-processed to retain only high-quality reads, which were then analyzed with QIIME v1.8 [181]. Open-reference operational taxonomic unit (OTU) clustering and taxonomy assignment of sequences were done with UCLUST [182] against the Silva database Release 111 [183] at the 97 % similarity level. Alpha diversity was calculated on rarefied OTU tables using the observed OTUs metric. 16S rRNA amplicon sequencing data have been deposited in the NCBI Sequence Read Archive under Accession Number SRX1799186.

4.2.2.5 Statistics

For statistical analysis, the PRISM software (version 5 and 7, GraphPad, La Jolla, CA, USA) was used. If not mentioned otherwise, bar graphs represent mean \pm standard error of mean (SEM) and p -values were calculated with two-tailed unpaired Student's t -test, with $*P < 0.05$, $**P < 0.01$, $***P < 0.001$ and $****P < 0.0001$.

5 Results

5.1 Role of the non-canonical NF- κ B pathway in DC-LMP1/CD40 animals

To study the effect of CD40-signaling on DCs, we generated a mouse model with constitutive CD40-signaling on DCs. These transgenic DC-LMP1/CD40 mice develop early-onset colitis that is fatal [77]. We could demonstrate that the generation of ROR γ t⁺Helios⁻ iTregs in the large intestine of DC-LMP1/CD40 mice is impaired due to the loss of tolerogenic CD103⁺ DC subsets in the colonic LP and the mLNs [77].

As it is known that CD40 can activate the non-canonical NF- κ B pathway [81], we asked whether this is the predominant downstream signaling pathway in our CD40-mediated model of colitis. Therefore, we generated mice not only with DC-specific constitutive CD40-signaling but also with DC-specific deletion of IKK1, a critical component for p100 phosphorylation (Fig.5.1 A). As a consequence, p100 is neither phosphorylated nor processed into p52, and the p52/RelB complex is not assembled to be translocated into the nucleus for subsequent target gene transcription. Thus, constitutive CD40-signaling in DCs cannot activate the non-canonical NF- κ B pathway in DC-LMP1/CD40 Δ IKK1 animals.

In contrast to control and DC-LMP1/CD40 mice, DC-LMP1/CD40 Δ IKK1 animals did show enlarged spleens and mLNs (Fig.5.1 B) with significantly elevated total cell numbers (Fig.5.1 C). Surprisingly, we did neither observe macroscopic signs of colitis (Fig.5.1 B) nor elevated total cell numbers in the colonic LP (Fig.5.1 C) and no increase in fecal lipocalin-2 levels (Fig.5.1 D) in DC-LMP1/CD40 Δ IKK1 mice when compared to control littermates. This pathological phenotype was only detected in DC-LMP1/CD40 mice. Further, DC-LMP1/CD40 Δ IKK1 mice showed even significantly reduced colon LP cell numbers (Fig.5.1 C) and fecal lipocalin-2 levels (Fig.5.1 D) similar to controls, confirming a non-inflammatory environment in DC-LMP1/CD40 Δ IKK1 animals.

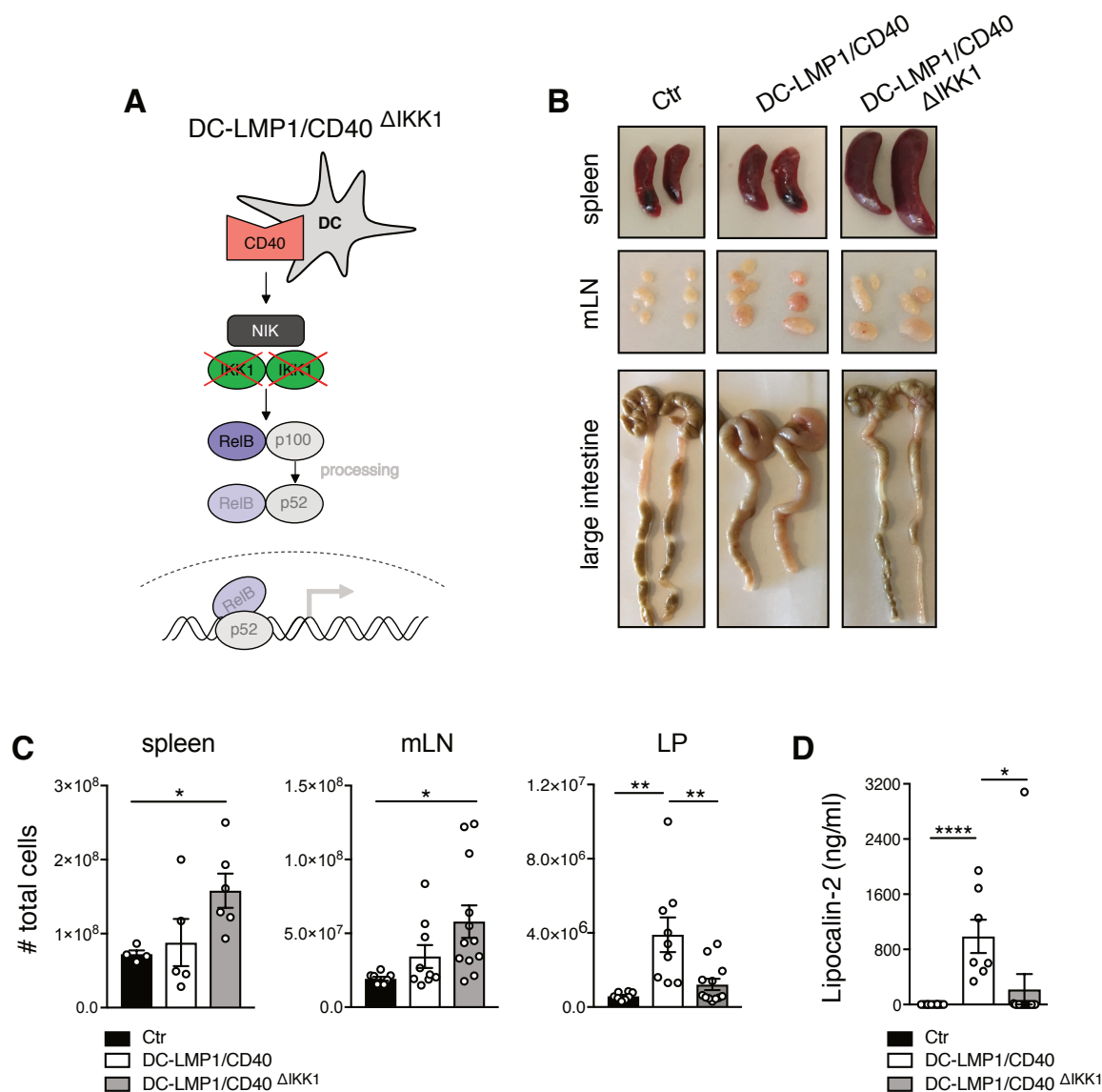


Figure 5.1: DC-LMP1/CD40 Δ IKK1 animals show enlarged spleens and mLNs but no colitis. **A)** Schematic illustration of the impaired non-canonical NF- κ B pathway in DCs of DC-LMP1/CD40 Δ IKK1 animals upon IKK1 deletion. **B)** Macroscopic pictures of spleen, mLN and colon from Ctr, DC-LMP1/CD40 and DC-LMP1/CD40 Δ IKK1 animals. Shown are two representative organs per group. **C)** Bar graphs show total spleen, mLN and colon cell numbers in Ctr, DC-LMP1/CD40 and DC-LMP1/CD40 Δ IKK1 animals from two pooled experiments for spleen (mean \pm SEM, n=4-6) and four pooled experiments for mLN and LP (mean \pm SEM, n=8-12). **D)** Levels of fecal lipocalin-2 were measured by ELISA in Ctr, DC-LMP1/CD40 and DC-LMP1/CD40 Δ IKK1 animals. Shown are data from two pooled experiments as mean \pm SEM, n=7-14.

5.1.1 Loss of colonic iTregs in DC-LMP1/CD40 animals depends on CD40-activated non-canonical NF- κ B signaling

To reveal the impact of non-canonical NF- κ B activation in our CD40-mediated colitis model in further detail, we analyzed cell subsets in the spleen, mLNs and colonic LP of DC-LMP1/CD40 Δ IKK1 animals.

Most interestingly, we have found some changes in the colonic LP of DC-LMP1/CD40 Δ IKK1 animals. CD103⁺ DCs were strongly reduced in DC-LMP1/CD40 Δ IKK1 animals, similar to DC-LMP1/CD40 animals (Fig.5.2 A). However, although not statistically significant, DC-LMP1/CD40 Δ IKK1 mice showed a tendency towards increased frequency of CD103⁺CD11b⁻ DCs when compared to DC-LMP1/CD40 animals (Fig.5.2 A).

When we analyzed Tregs in the colonic LP, the frequency of FoxP3⁺CD25⁺ Tregs was similar in control, DC-LMP1/CD40 as well as DC-LMP1/CD40 Δ IKK1 animals (Fig.5.2 B, upper panel). As we previously published ([77], Fig.3.4 B), DC-LMP1/CD40 animals showed an almost complete loss of ROR γ t⁺Helios⁻ iTregs. Surprisingly, DC-LMP1/CD40 Δ IKK1 animals were able to induce ROR γ t⁺Helios⁻ iTregs (Fig.5.2 B, lower panel). Here, iTregs were still reduced in frequency when compared to controls, but strongly increased when compared to DC-LMP1/CD40 animals (Fig.5.2 B, lower panel).

The analysis of effector T cells in the large intestine revealed a strong increase in IL-17-producing Th17 cells in DC-LMP1/CD40 Δ IKK1 animals (Fig.5.2 C). Notably, IL-17⁺ Th17 cells in DC-LMP1/CD40 Δ IKK1 animals were accumulating but not transdifferentiating into IL-17⁺IFN- γ ⁺ Th17/Th1 or IFN- γ ⁺ Th1 cells (Fig.5.2 C). This transdifferentiation of Th17 cells was only observed in DC-LMP1/CD40 animals as also shown previously ([77], Fig.3.4 C). Therefore, pathogenic effector T cells are not induced in the colon LP when CD40-activated DCs are deficient in non-canonical NF- κ B signaling.

Further, DC-LMP1/CD40 Δ IKK1 animals showed some signs of splenic inflammation as indicated by granulocytes increased in frequency and number (data not shown), causing macroscopically enlarged spleens in these animals as shown in Fig.5.1 B. We did not find any

differences in the mLNs of DC-LMP1/CD40 Δ IKK1 and DC-LMP1/CD40 animals, meaning CD103⁺CD11b⁻ as well as CD103⁺CD11b⁺ DCs were similarly reduced as we showed for DC-LMP1/CD40 animals but not control littermates (data not shown). Of note, ROR γ t⁺Helios⁻ iTregs were also significantly reduced in mLNs of DC-LMP1/CD40 Δ IKK1 as previously seen in DC-LMP1/CD40 animals (data not shown).

Taken together, CD40-signaling is activating the non-canonical NF- κ B pathway in DCs that seems to be crucial for the pathogenesis in our colitis model. Our data suggest that the impaired non-canonical NF- κ B pathway in CD40-activated DCs preserves some characteristics that are sufficient to generate iTregs in DC-LMP1/CD40 Δ IKK1 animals. This improved induction of iTregs in turn restrains pathogenic effector T cells in the large intestine, preventing development of colitis.

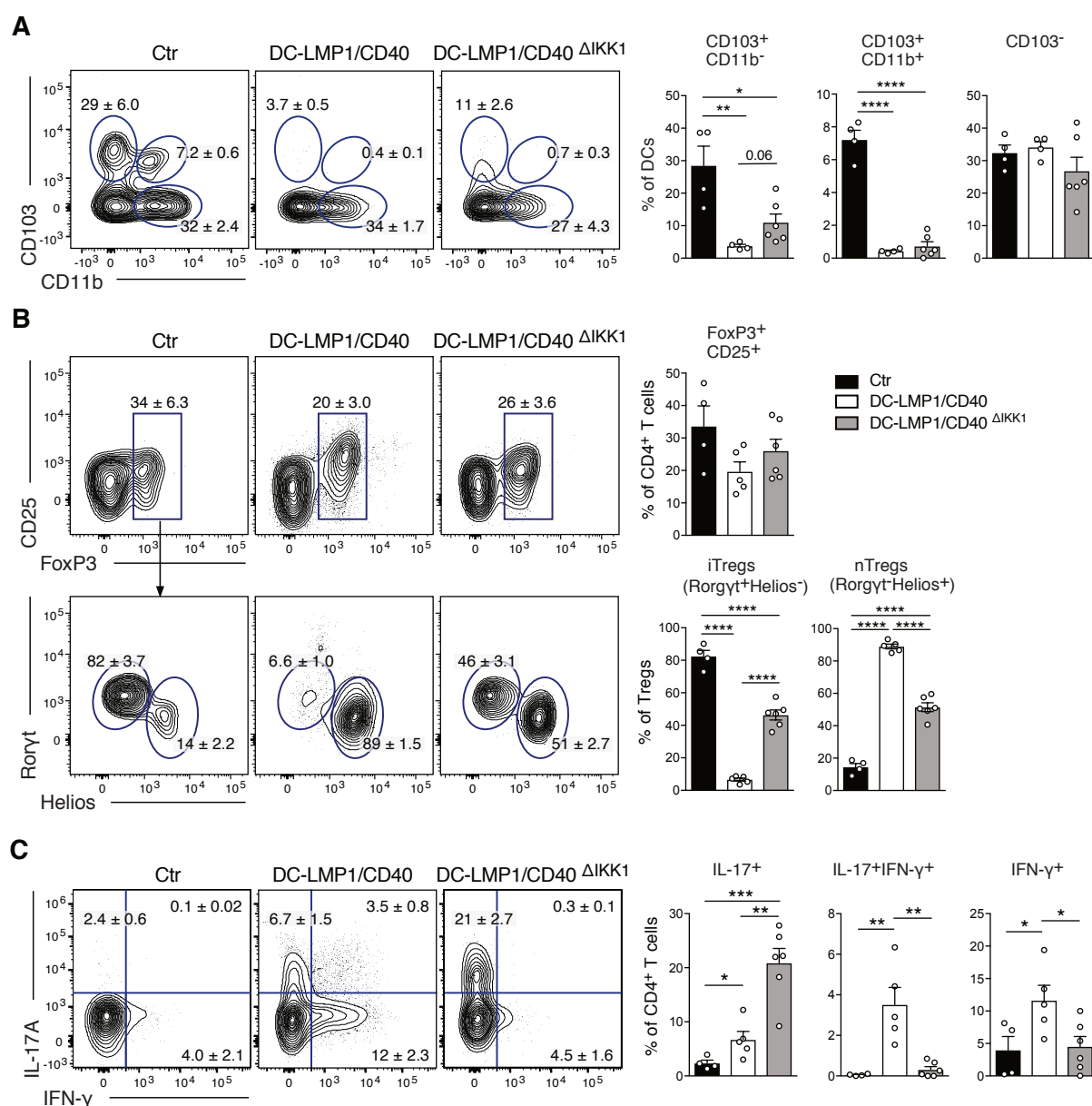


Figure 5.2: Deficiency of non-canonical NF- κ B signaling in DCs leads to generation of iTregs and IL-17⁺ effector T cells in the colonic LP. A-C) Different cell subsets in the colonic LP were analyzed in Ctr, DC-LMP1/CD40 and DC-LMP1/CD40 Δ IKK1 animals. Shown are representative FACS-plots as well as pooled statistics from two experiments (mean \pm SEM, n=4-6), illustrating frequencies of the indicated cell subsets within the gates. **A)** DCs were gated on single, live, CD45⁺, MHCII⁺CD11c⁺, CD64⁻ cells. **B)** Tregs were gated on single, live, CD45⁺, CD3⁺CD4⁺, FoxP3⁺CD25⁺ (upper panel) and for further differentiation on ROR γ t⁺Helios⁻ (iTregs) or ROR γ t⁻Helios⁺ (nTregs) (lower panel). **C)** Single-cell suspensions were stimulated with PMA/Ionomycin and subsequently stained intracellularly for IL-17 and IFN- γ production. CD4⁺ T cells were pre-gated on single, live, CD45⁺, CD3⁺CD4⁺ cells.

5.2 Analysis of gut microbiota in DC-LMP1/CD40 mice

As transgenic animals treated with ABX or crossed onto Rag1^{-/-} background do not suffer from intestinal inflammation, colitis development clearly depends on T or B cells as well as on microbiota [77]. It is well known that microbiota shape the host immune system and have a relevant impact on health and disease. To maintain mucosal homeostasis, a balance between appropriate immune responses to invading pathogens and tolerance to dietary and commensal antigens is essential. Disturbed balances, dysbiosis, can result in severe inflammatory disorders like IBD. To evaluate the role of microbiota within the CD40-mediated colitis model, we studied changes of microbiota during disease development.

To get further insights into the complex microbiota responsible for shaping adaptive immunity and inflammation in CD40-mediated colitis, we first determined the disease onset in DC-LMP1/CD40 mice by measuring fecal lipocalin-2, a sensitive non-invasive inflammatory marker [184]. In contrast to non-transgenic littermates, lipocalin-2 levels in DC-LMP1/CD40 mice were significantly increased starting in week 5 after birth (Fig.5.3 A), indicating a very early disease onset due to constitutive CD40-signaling in DCs as published previously [77]. In addition, neither ABX-treated control nor transgenic animals did show elevated lipocalin-2 levels (Fig.5.3 A), confirming our previous results that colitis development depends on microbiota [77].

As a first hint for bacterial changes during disease development, we determined the fecal bacterial load of DC-LMP1/CD40 mice at different ages. We plated fecal content onto MacConkey agar, which is selective for gram-negative bacteria. Therefore, mainly *Enterobacteriaceae* are represented, the bacterial load of which can be determined as colony-forming units (cfu). We already observed a tendency towards higher bacterial load in 4-week-old DC-LMP1/CD40 mice when compared to cohoused control littermates (Fig.5.3 B). This difference became more obvious upon colitis onset in 5-week-old DC-LMP1/CD40 mice and finally statistically significant in 8-week-old DC-LMP1/CD40 mice (Fig.5.3 B). The so-called "*Enterobacteriaceae* blooming" in DC-LMP1/CD40 mice indicates dysbiosis, a hallmark of colitis [145]. Of note,

all ABX-treated mice showed almost no bacterial load, confirming successful treatment.

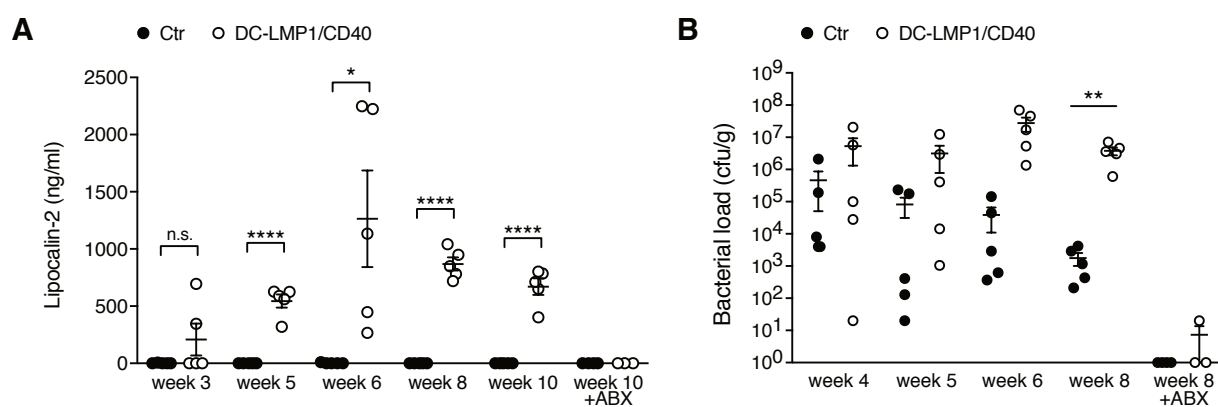


Figure 5.3: DC-LMP1/CD40 animals show "Enterobacteriaceae blooming" upon colitis onset. **A)** Levels of fecal lipocalin-2 were measured by ELISA in untreated or ABX-treated Ctr and DC-LMP1/CD40 mice at the indicated time points. Data is shown as mean \pm SEM (n=3-5). **B)** Fecal bacterial load of untreated or ABX-treated Ctr and DC-LMP1/CD40 mice at the indicated time points. Fecal content was plated onto MacConkey agar and cfu were calculated. Data represents mean \pm SEM (n=3-5 per group).

5.2.1 Dysbiosis in DC-LMP1/CD40 animals

To reveal more detailed changes in the microbial composition upon disease development in DC-LMP1/CD40 animals, we performed 16S rRNA gene sequencing of fecal bacteria in collaboration with the group of Prof. Dr. Bärbel Stecher (Max von Pettenkofer-Institute, LMU Munich), amplifying the variable region V3-V4 (Fig.5.4 A). We analyzed the intestinal microbiota in fecal samples from 3-week-old DC-LMP1/CD40 animals, which did not show any signs of colitis as well as 8-week-old DC-LMP1/CD40 animals, suffering from colitis (Fig.5.3 A).

We have determined the microbiota within-group (alpha-) diversity at the operational taxonomic unit (OTU) level upon amplicon sequencing of the 16S rRNA gene regions V3-V4. Here, our data revealed a strong and statistically significant decrease in the number of observed OTUs in 8-week-old DC-LMP1/CD40 mice as compared with cohoused control littermates (Fig.5.4 B), indicating a shift in microbiota diversity further confirming dysbiosis in transgenic animals.

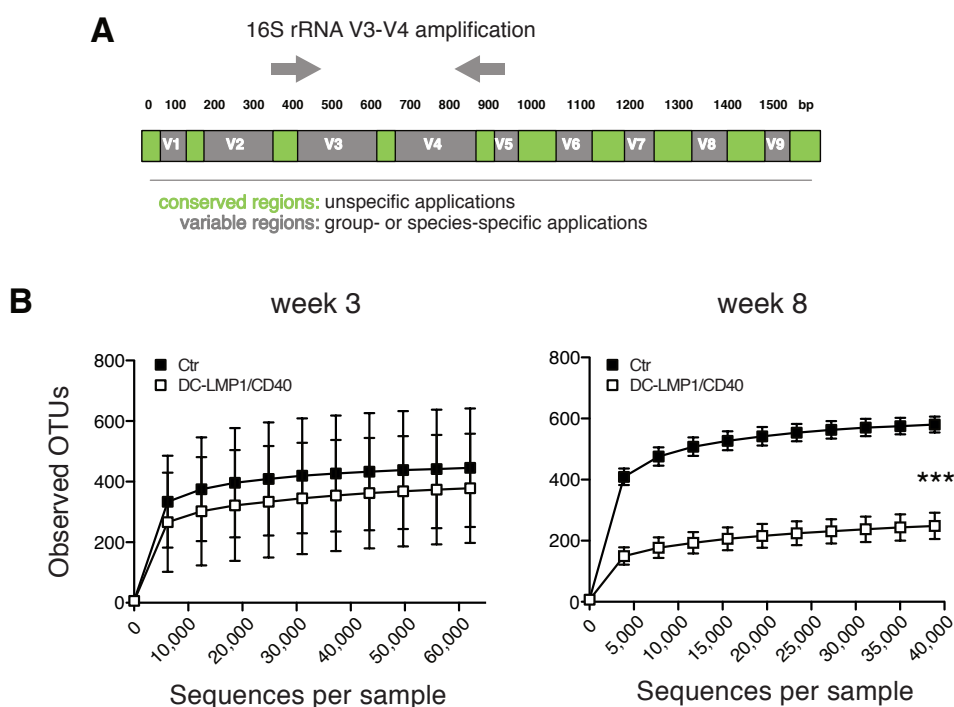


Figure 5.4: DC-LMP1/CD40 animals show reduced numbers of OTUs. **A)** Schematic representation of the variable region 3-4 of the 16S rRNA gene used for sequencing. **B)** Rarefaction plots illustrating within-group (alpha-) diversity of Ctr and DC-LMP1/CD40 mice at the indicated time points. On the basis of 16S rRNA gene sequencing of the V3-V4 regions, the number of observed OTUs versus sequencing depth are shown. Data indicate mean \pm standard deviation (n=5 per group). Figure is adapted from Figure 5 in our published paper [77].

We further analyzed the samples for taxa composition at the family level. Changes observed in 3-week-old mice were littermate-dependent (Fig.5.5 upper panel) while changes in 8-week-old mice were genotype-dependent (Fig.5.5 middle panel). Here, DC-LMP1/CD40 mice showed distinct fecal microbial compositions when compared to control littermates. Consistent with our findings in Fig.5.3 B, 8-week-old DC-LMP1/CD40 mice showed an increase in the abundance of the Proteobacteria *Enterobacteriaceae* (Fig.5.5 middle panel). Further, abundance of Firmicutes *Clostridiaceae*, *Erysipelotrichaceae* and *Peptostreptococcaceae* was increased whereas abundance of Firmicutes *Ruminococcaceae* and *Lachnospiraceae* was reduced (Fig.5.5 middle panel). When mice were treated with ABX, we did not detect a complex taxa composition as in untreated animals (Fig.5.5 lower panel). Here, we did find mainly *Mycoplasmataceae* in both control and DC-LMP1/CD40 animals, which were resistant to the antibiotics cocktail we used.

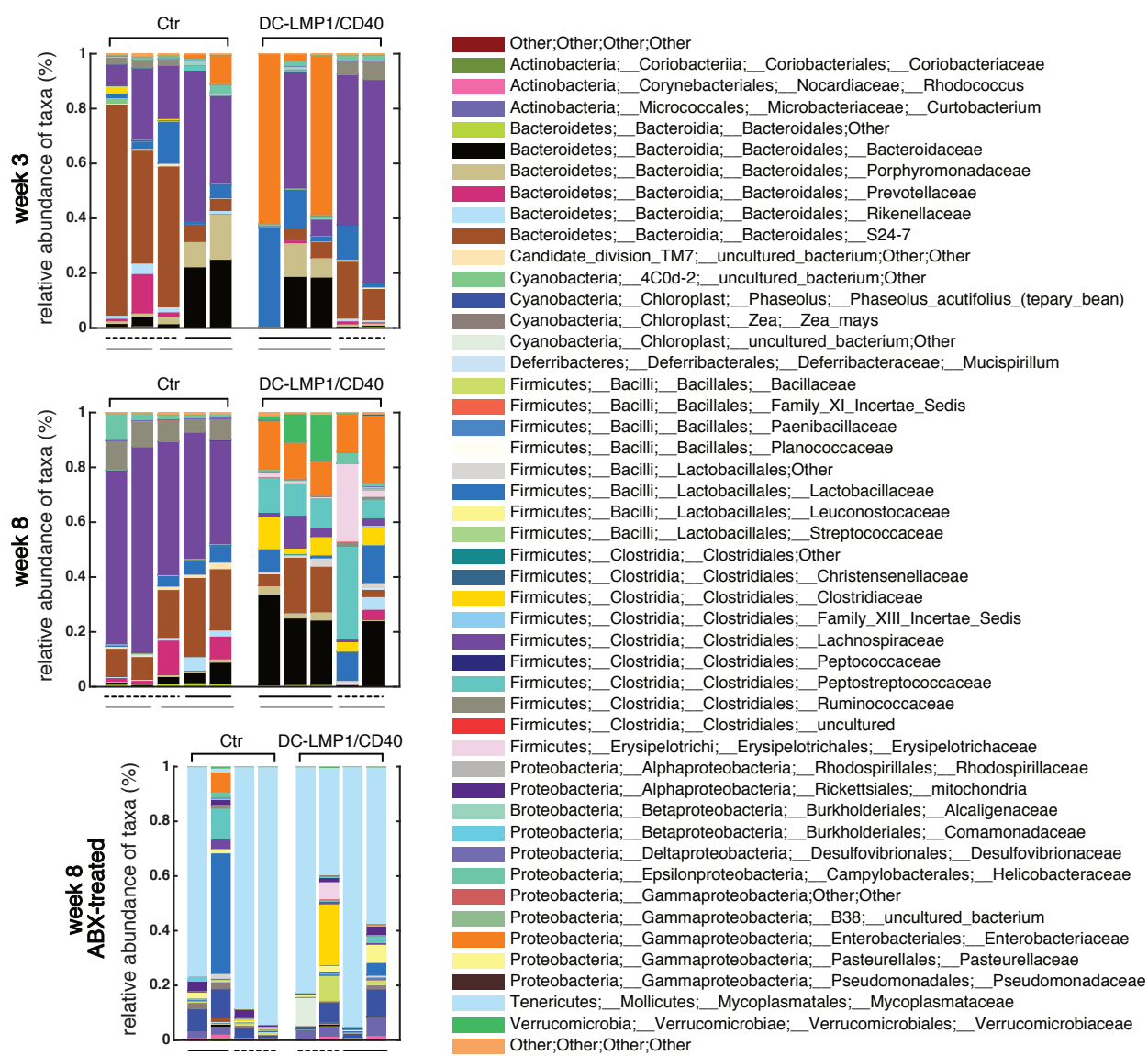


Figure 5.5: DC-LMP1/CD40 animals show changes in taxa composition upon colitis onset. Analysis of composition of intestinal microbiota in fecal samples from untreated or ABX-treated Ctr and DC-LMP1/CD40 mice at the indicated time points was based on sequencing the V3-V4 variable regions of the 16S rRNA gene (Illumina MiSeq; open-reference OTU picking, reference database SILVA, UCLUST). Shown is the relative abundance of taxa at family level with each bar representing one animal ($n=4-5$ per group). Underline codes indicate littermates (dashed or solid black line) or caging (solid grey lines).

5.3 Microbial-host interactions

Due to the fact that we observed major changes in taxa composition during disease progression, we asked whether and to what extent adaptive immune responses have the potential to modulate microbiota or how and to what extent microbiota impact host immunity in the CD40-mediated colitis model. Therefore, we analyzed microbial-host interactions in DC-LMP1/CD40 animals to subsequently identify mechanisms and/or species driving disease development.

5.3.1 Fecal bacteria in DC-LMP1/CD40 mice are highly IgA-coated

Palm et al. previously showed that in particular highly IgA-coated bacteria have the potential to drive intestinal inflammation [115]. Therefore, we measured fecal IgA-levels by ELISA. We detected elevated fecal IgA-levels in DC-LMP1/CD40 mice starting at week 5 (Fig.5.6 A). These levels further increased with age but were entirely abolished if the mice were treated with ABX (Fig.5.6 A). We further monitored bacterial IgA-coating by flow cytometry, whereby a higher percentage of intestinal microbiota was IgA-coated and also more IgA was bound per microbe in DC-LMP1/CD40 animals (Fig.5.6 B), indicating that highly IgA-coated bacteria are driving the disease in transgenic animals.

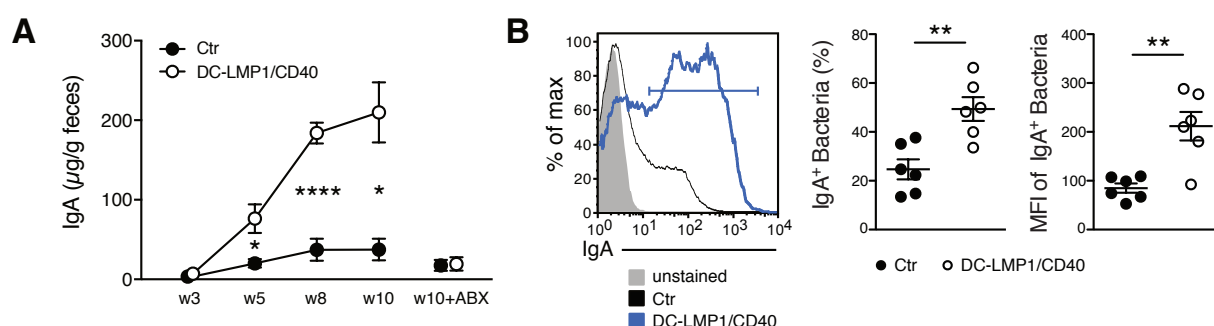


Figure 5.6: Fecal bacteria from DC-LMP1/CD40 animals are highly coated by IgA. **A)** Fecal IgA concentrations in Ctr and DC-LMP1/CD40 animals at different time points and treated as indicated were measured by ELISA. Data is represented as scatter plot (mean \pm SEM, $n=3-5$). **B)** Feces homogenates from Ctr and DC-LMP1/CD40 mice were stained with α -mouse IgA and analyzed by flow cytometry. Data shows one representative histogram and scatter plots with percentage or MFI of IgA⁺ bacteria (mean \pm SEM for two pooled experiments, $n=6$). Figure is adapted from Figure 5 in our published paper [77].

5.3.2 DC-LMP1/CD40 mice produce commensal-specific antibodies

We next analyzed IgG and IgA serum levels in DC-LMP1/CD40 animals during colitis progression. Compared with control littermates, DC-LMP1/CD40 mice showed elevated total serum IgG-levels already at 6 weeks of age (Fig.5.7, left panel). These levels further increased with age. Also IgA-levels were elevated in DC-LMP1/CD40 animals at every age tested and strongly increased further with age (Fig.5.7, right panel).

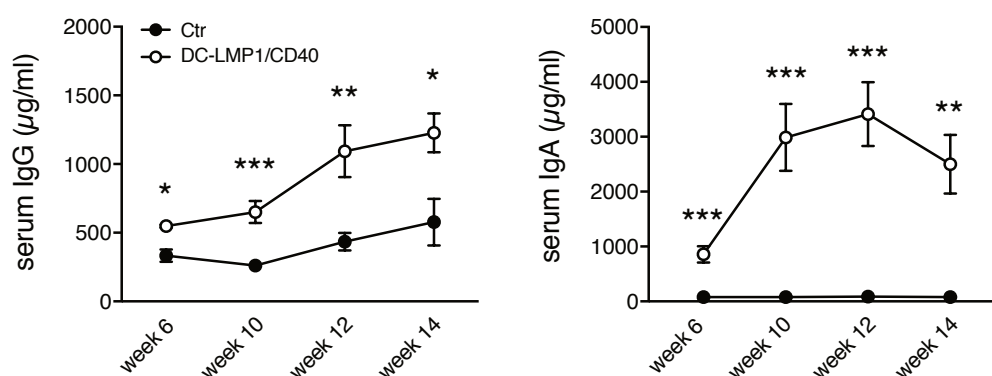


Figure 5.7: DC-LMP1/CD40 mice show elevated serum IgG- and IgA-levels upon colitis onset. Total IgG (left panel) or IgA (right panel) concentrations in sera from Ctr and DC-LMP1/CD40 animals at the indicated time points were measured by ELISA. Data from two pooled experiments are shown as mean \pm SEM (n=3-13).

As mice with spontaneous colitis have the propensity to develop antibody responses against commensal bacteria [185], we next set out to identify antibody specificities in DC-LMP1/CD40 mice. To this end we used cecal bacterial lysate (CBL) from non-transgenic C57BL/6 mice, representing normal intestinal microbiota [185] for ELISA (Fig.5.8 A). In DC-LMP1/CD40 mice, serum IgG response to commensal antigens was significantly increased at the 10-week time point when compared to control littermates (Fig.5.8 A, left panel). In contrast, we detected significantly higher serum IgA reactivities in mice at the age of 10, 12 and 14 weeks (Fig.5.8 A, right panel).

To further visualize the whole variety of bacterial antigens potentially recognized by serum Ig from DC-LMP1/CD40 mice, we tested these sera also by immunoblotting (Fig.5.8 B). Serum IgG from both, DC-LMP1/CD40 mice and control littermates, detected some proteins

of different sizes ranging from 10 to 250 kDa (Fig.5.8 B, left panel). However, in contrast to sera from controls, each serum IgG sample from DC-LMP1/CD40 mice showed reactivity with a protein of about 60 kDa (Fig.5.8 B, left panel). This reactivity was increasing with the age of the mice (Fig.5.8 B, left panel). Serum IgA from 10-, 12- and 14-week samples of DC-LMP1/CD40, but not control mice, selectively detected proteins around 60 kDa (Fig.5.8 B, right panel).

Summarized, our data reveal that DC-LMP1/CD40 mice produce more serum antibodies upon colitis onset and that serum antibodies are specific for bacterial antigens present in CBL from healthy mice.

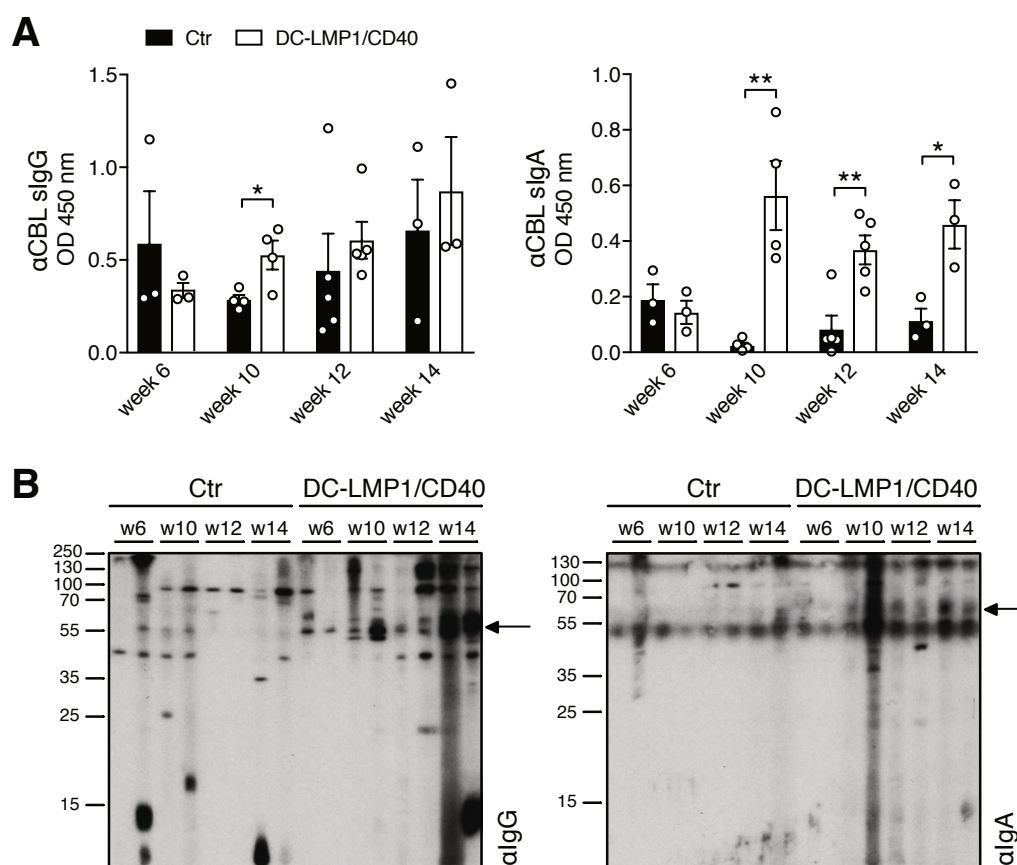


Figure 5.8: DC-LMP1/CD40 mice show commensal-specific antibodies. A-B) Serum IgG (left) and IgA (right) response in Ctr and DC-LMP1/CD40 mice towards commensal antigens within the CBL was determined by (A) ELISA (mean \pm SEM, n=3-5 per group and time point) or (B) immunoblotting at the indicated time points (n=2 per group and time point, each lane represents one serum sample from Ctr or DC-LMP1/CD40 mice). Goat α -mouse IgG-HRP or goat α -mouse IgA-HRP were used as secondary antibodies. Arrows indicate 60 kDa.

5.3.3 Identification of bacterial antigens by serum antibody reactivity

To identify bacterial antigens recognized by serum antibodies in DC-LMP1/CD40 animals, we performed label-free liquid chromatography tandem mass spectrometry (LC-MS/MS) (Fig.5.9 A). For this approach, serum antibodies were coupled to beads and incubated with CBL for binding of potential target proteins. Upon immunoprecipitation we performed on-bead digestion of bead-bound proteins followed by LC-MS/MS. The resulting peak intensities were finally used for intensity-based absolute quantification (iBAQ). Proteins identified with a fold change > 2 and a p -value < 0.05 were considered for further analyses. Interestingly, the results provided only five proteins precipitated by serum antibodies from DC-LMP1/CD40 mice and two proteins by control serum antibodies that met these requirements (Fig.5.9 B). We focused on proteins precipitated by serum antibodies from DC-LMP1/CD40 animals with the highest fold change and lowest p -value. These were (i) the 60 kDa chaperonin GroEL (Hsp60) from *Hh* (CH60_HELHP, 8.36 fold change, p -value < 0.00001) (ii) the probable peroxiredoxin from *H. pylori* (TSAA_HELPJ, 9.93 fold change, p -value < 0.000001). The data analysis for the number of precipitated peptides (Fig.5.9 C, upper panels) and the percentage of sequence coverage of the proteins (Fig.5.9 C, lower panels) revealed that CH60_HELHP was identified by 1-21 peptides with a sequence coverage ranging from 2.4 % up to 43.7 %. In contrast, TSAA_HELPJ was identified by only one peptide and with a sequence coverage of only 5.6 % for every single DC-LMP1/CD40 serum sample (Fig.5.9 C). To exclude biased results due to differences in serum antibody amounts from DC-LMP1/CD40 and control animals bound by protein G beads, samples were adjusted by calculating equal amounts of serum IgG before coupling onto the beads and also the peak intensities of Ig-related proteins were quantified within the same experiment. Here, DC-LMP1/CD40 and control serum samples showed no differences in Ig-related protein intensities (Fig.5.9 D), indicating equal coupling of serum antibodies from both control and transgenic mice.

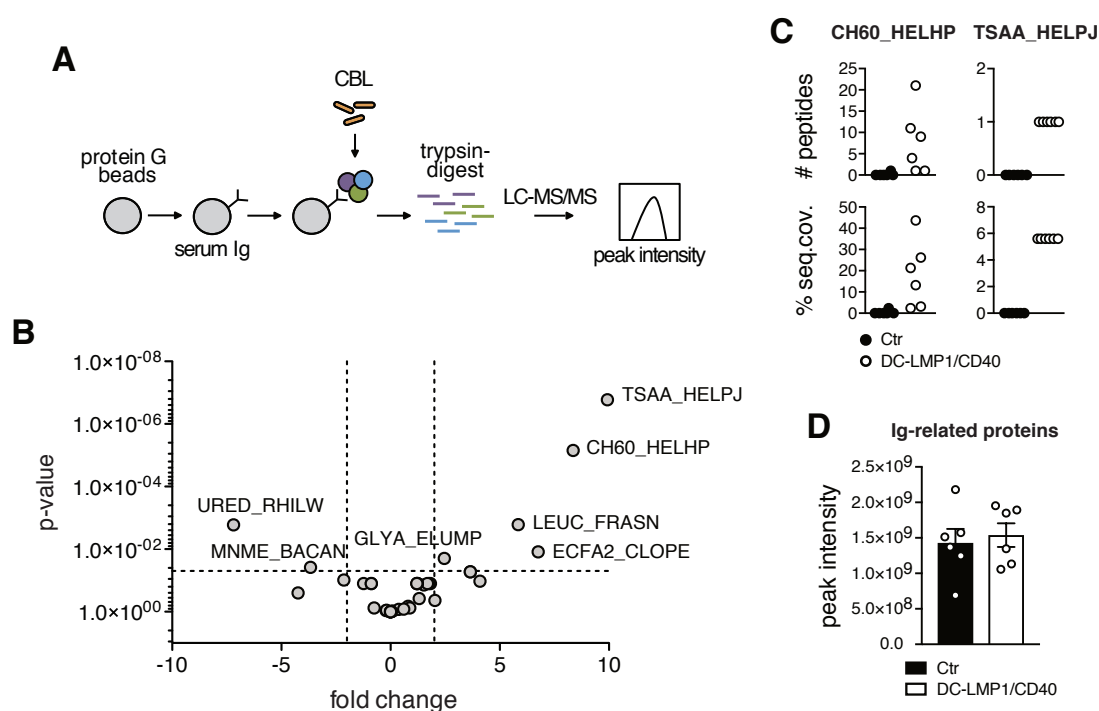


Figure 5.9: Serum antibodies from DC-LMP1/CD40 mice are specific for a protein from *Hh*. **A)** Schematic illustration of sample preparation for LC-MS/MS. Protein G beads were coupled with 2.5 μ g serum IgG from Ctr or DC-LMP1/CD40 mice (as determined in Fig.5.7) to bind commensal antigens within the CBL. Upon immunoprecipitation, proteins were trypsin-digested, analyzed by LC-MS/MS and the resulting peak intensity was used for iBAQ (pooled results from two experiments, n=6). **B)** Results obtained by iBAQ are illustrated by the volcano plot. Identified proteins were considered as interaction partners if their MaxQuant iBAQ values were greater than log₂ 2-fold enrichment and p-value 0.05 (ANOVA) when compared to the control. **C)** Data illustrate the number of peptides (upper panel) and the percentage of protein sequence coverage (lower panel) of the identified proteins CH60_HELHP and TSAA_HELPJ from B). Each symbol represents one single mouse. **D)** Experiment was performed as in A), but data were filtered for Ig-related proteins only. Intensities of all Ig-related proteins, detected by LC-MS/MS within every single Ctr or DC-LMP1/CD40 sample, are illustrated by bar graphs as mean \pm SEM (two pooled experiments, n=6).

The fact, that a protein from *Hh* was precipitated with this approach was plausible as the mice were housed under conventional conditions, increasing the probability that the mouse colony might have been endemically infected with *Hh*.

We next tested the serum antibody reactivity from DC-LMP1/CD40 mice towards whole *Hh* lysate (*Hh*L) by ELISA (Fig.5.10 A) and immunoblotting (Fig.5.10 B, C). Indeed, both serum IgG as well as IgA from DC-LMP1/CD40 mice showed a strong reactivity towards *Hh*L when compared to sera from control littermates by ELISA (Fig.5.10 A). To detect GroEL from *Hh* by immunoblotting, we used the anti-human Heat shock protein 60 (α HSP60) mAb

(clone LK-2, mouse IgG1 isotype) as positive control, recognizing both human HSP60 and the bacterial homologue GroEL [186]. As expected, in Western blot analyses LK-2 detected recombinant GroEL from *E.coli* (rGroEL (*Ec*)) and GroEL in CBL and *HhL* (Fig.5.10 B, left panel), confirming the specificity of this antibody and the presence of GroEL in CBL and *HhL* used for this screening. Furthermore, in contrast to sera from control littermates (Fig.5.10 B, middle panel), sera from DC-LMP1/CD40 (Fig.5.10 B, right panel) detected a band of the same size in CBL as well as *HhL*. Interestingly, we did detect the 60 kDa protein in *HhL* with serum IgG from DC-LMP1/CD40 with every age tested and this reactivity was increasing with the age of the mice (Fig.5.10 C). Further, detection of the 60 kDa protein in *HhL* with serum IgA from DC-LMP1/CD40 mice was only observed in mice at the age of 14 weeks and older (Fig.5.10 C). In contrast, there was no 60 kDa protein-specific signal detected neither with serum IgG nor IgA from control mice (Fig.5.10 C).

Taken together, we identified the 60 kDa chaperonin GroEL from *Hh* as potential antigen recognized by the immune system during early colitis onset, indicating that *Hh* might be a disease driver in the DC-LMP1/CD40 colitis model.

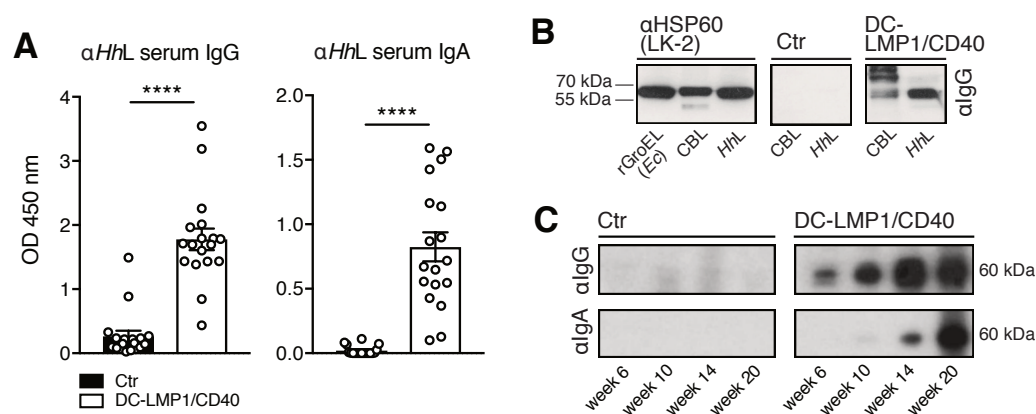


Figure 5.10: Serum antibodies from DC-LMP1/CD40 mice are specific for a 60 kDa protein from *Hh*. **A)** Serum IgG (left) and IgA (right) response in Ctr and DC-LMP1/CD40 mice towards *HhL* was determined by ELISA (mean \pm SEM, n=18). **B)** Detection of the 60 kDa protein in *HhL* and CBL by immunoblotting. 20 μ g *HhL*, 50 μ g CBL or 0.5 μ g rGroEL (*Ec*) were separated by SDS-PAGE. α HSP60 (left, clone LK-2) and sera from Ctr (middle) or DC-LMP1/CD40 mice (right) were used as primary Abs. α mouse-IgG-HRP was used as secondary Ab. **C)** Detection of the 60 kDa protein by immunoblotting with serum IgG (upper panel) or IgA (lower panel). 200 μ g *HhL* were separated by SDS-PAGE and sera from Ctr or DC-LMP1/CD40 mice at indicated age were used as primary Abs with each lane representing one serum sample. α mouse-IgG-HRP or α mouse-IgA-HRP was used as secondary Ab.

5.4 *Helicobacter hepaticus* as disease driver

The pathobiont *Hh* is associated with IBD and known to induce spontaneous colitis in immunodeficient mice with severe combined immunodeficiency or IL-10-deficiency [156, 159].

To determine the infection rates of conventionally-housed mice used in this study, we screened fecal contents from mice at week 3 and week 10 after birth for presence of *Helicobacter* by genus-specific (*Hspp*) and species-specific PCR (Fig.5.11 A).

We did find *Hspp* throughout all DC-LMP1/CD40 and control littermates (Fig.5.11 A). Moreover, all control littermates were consistently colonized with *Hh* (Fig.5.11 A). Surprisingly, young DC-LMP1/CD40 mice showed already reduced infection rates (week 3, 57.1 % *Hh*-positive transgenic animals, Fig.5.11 B), whereas *Hh* was hardly detectable in older DC-LMP1/CD40 mice (week 10, 8.3 % *Hh*-positive transgenic animals, Fig.5.11 B). Of note, we obtained similar results for colonization with *H. typhlonius* (*Ht*) and all animals tested were also colonized with *H. rodentium* (*Hr*), explaining consistent *Hspp* positive results (Fig.5.11 A). In contrast, none of the animals was tested positive for *H. bilis* (*Hb*) (Fig.5.11 A).

Taken together, conventionally-housed mice were endemically infected with *Hh*. The fact, that DC-LMP1/CD40 animals show loss of *Hh* colonization in particular upon colitis progression suggests that this pathobiont is eliminated by either ongoing immune response against *Hh*, *Hh* transition from the lumen into the LP upon manifestation of dysbiosis and inflammation or *Hh* displacement by other bacteria during dysbiosis.

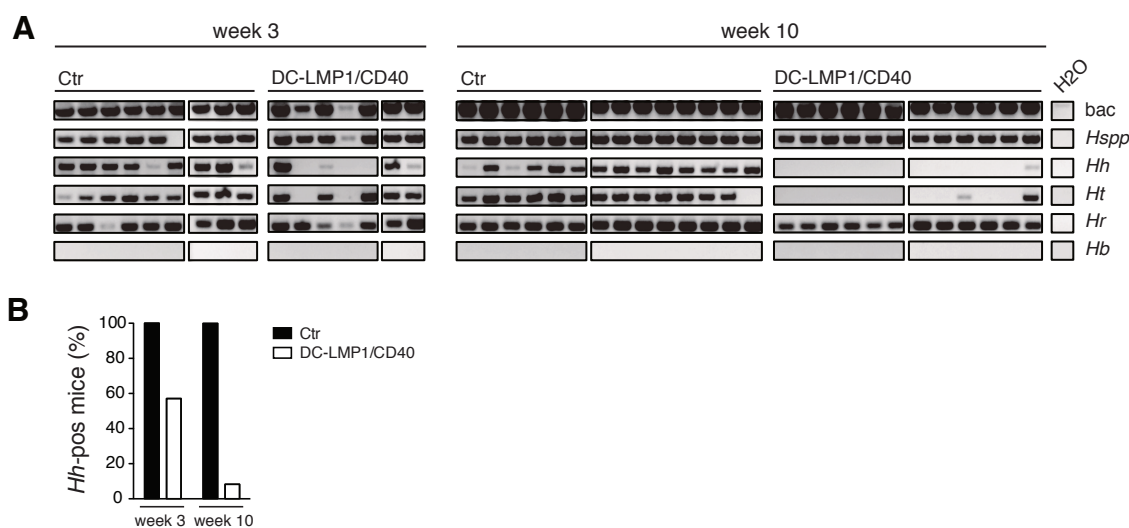


Figure 5.11: DC-LMP1/CD40 mice show loss of *Hh* colonization upon disease progression. **A)** Bacterial DNA was extracted from fecal samples from Ctr or DC-LMP1/CD40 mice at the indicated time points. 16S rRNA gene primers were used to detect the species indicated (n=7-14). **B)** Data from A) is represented as bar graphs, illustrating the percentage of 3- or 10-week-old *Hh*-pos Ctr or DC-LMP1/CD40 animals. bac: universal bacteria; *Hspp*: *Helicobacter species*; *Hh*: *H. hepaticus*; *Ht*: *H. typhlonius*; *Hr*: *H. rodentium*; *Hb*: *H. bilis*

5.4.1 *Helicobacter hepaticus*-free DC-LMP1/CD40 mice are protected from early disease onset

By embryo transfer rederivation, we rendered mice *Hh*-free and maintained them under specific-pathogen-free (SPF) conditions. We confirmed *Hh*-colonization status by genus-specific and species-specific PCR with fecal content from 6- and 10-week-old mice (Fig.5.12). Notably, all animals were tested negative for *Hh* as well as *Ht*, *Hr* and *Hb*.

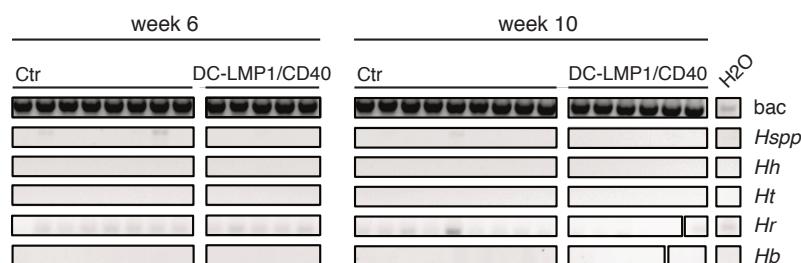


Figure 5.12: Control and DC-LMP1/CD40 animals are no longer colonized with *Helicobacter* after embryo transfer rederivation. Bacterial DNA was extracted from fecal samples from Ctr or DC-LMP1/CD40 mice after rendering them *Hh*-free at the indicated time points. 16S rRNA gene primers were used to detect the species indicated (n=5-9).

None of the *Hh*-free DC-LMP1/CD40 animals showed elevated fecal lipocalin-2 levels at the age of 8 or 14 weeks (Fig.5.13 A, lower panel), in contrast to *Hh*-positive DC-LMP1/CD40 mice, which already had significantly elevated fecal lipocalin-2 levels (Fig.5.13 A, upper panel). Interestingly, we did detect significantly increased fecal lipocalin-2 levels only at much later time points in some but not all *Hh*-free DC-LMP1/CD40 mice (Fig.5.13 A, lower panel). At week 20, 55.5 % and at week 25 only 30.8 % of *Hh*-free transgenic mice showed elevated lipocalin-2 levels. Of note, *Hh*-free DC-LMP1/CD40 mice not only showed less morbidity but also a remarkably improved survival rate. Compared to *Hh*-positive DC-LMP1/CD40 mice, which usually die between 10 to 18 weeks of age (Fig.5.13 B, [77]), none of *Hh*-free DC-LMP1/CD40 animals died before week 25 (Fig.5.13 B), the time point we sacrificed the mice for analyses.

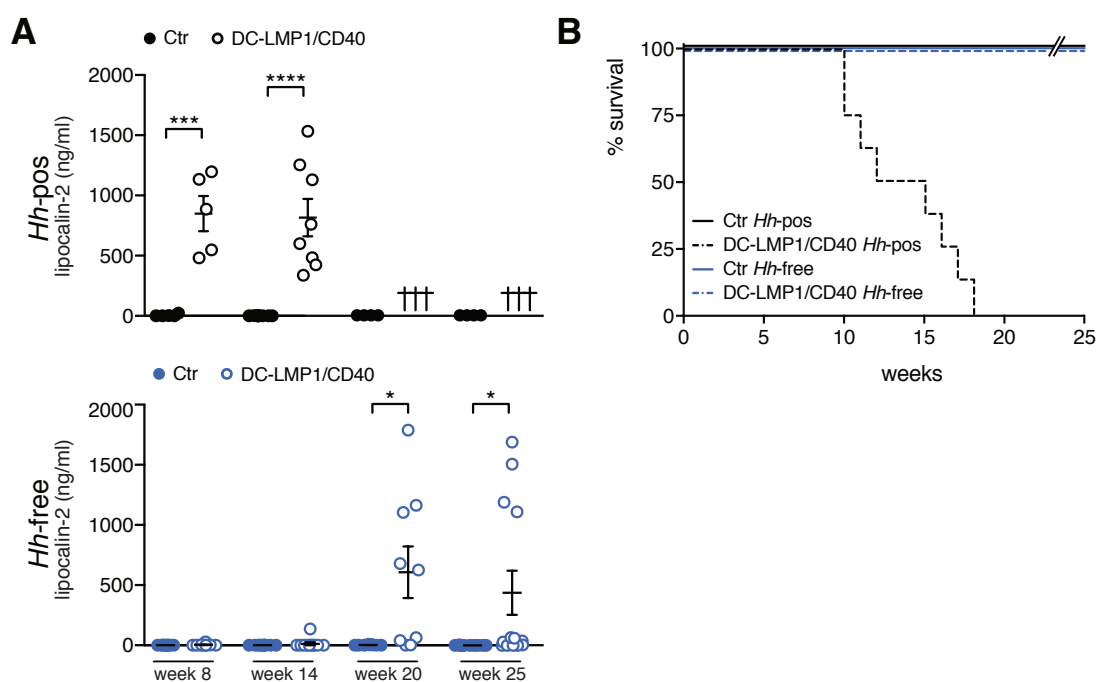


Figure 5.13: *Hh*-free DC-LMP1/CD40 mice show delayed inflammation with prolonged survival. **A)** Levels of fecal lipocalin-2 were measured by ELISA in *Hh*-pos (upper panel) or *Hh*-free (lower panel) Ctr and DC-LMP1/CD40 mice at the indicated time points. Shown are data from two pooled experiments for *Hh*-pos animals (n=5-9) and for *Hh*-free animals (n=9-13) as mean \pm SEM. Crosses represent animals already dead at the indicated time points. **B)** Kaplan-Meier plot showing survival of *Hh*-free or *Hh*-pos Ctr and DC-LMP1/CD40 animals (n=6-10). Data for *Hh*-pos animals were taken from Figure 2 in our previous publication [77].

When we compared the phenotype of *Hh*-pos and *Hh*-free animals at the age of 14 weeks, *Hh*-pos DC-LMP1/CD40 mice already suffered from acute colitis, indicated by shortened and thickened colon as well as strong increase in total colonic cell numbers (Fig.5.14 upper left panel, [77]). In contrast, we observed neither macroscopic signs of colitis, nor elevated total infiltrate cell numbers in the colonic LP of 14-week-old *Hh*-free DC-LMP1/CD40 animals (Fig.5.14 lower left panel). However, in aged mice of 25 weeks, again some but not all *Hh*-free DC-LMP1/CD40 mice showed an inflamed phenotype with shortened and thickened colon as well as increased cell numbers, infiltrating the colon LP (Fig.5.14 right panel). Our data show a substantial delay in disease onset as well as less morbidity of *Hh*-free DC-LMP1/CD40 mice, indicating a crucial role for this pathobiont in disease initiation and outcome in CD40-mediated colitis.

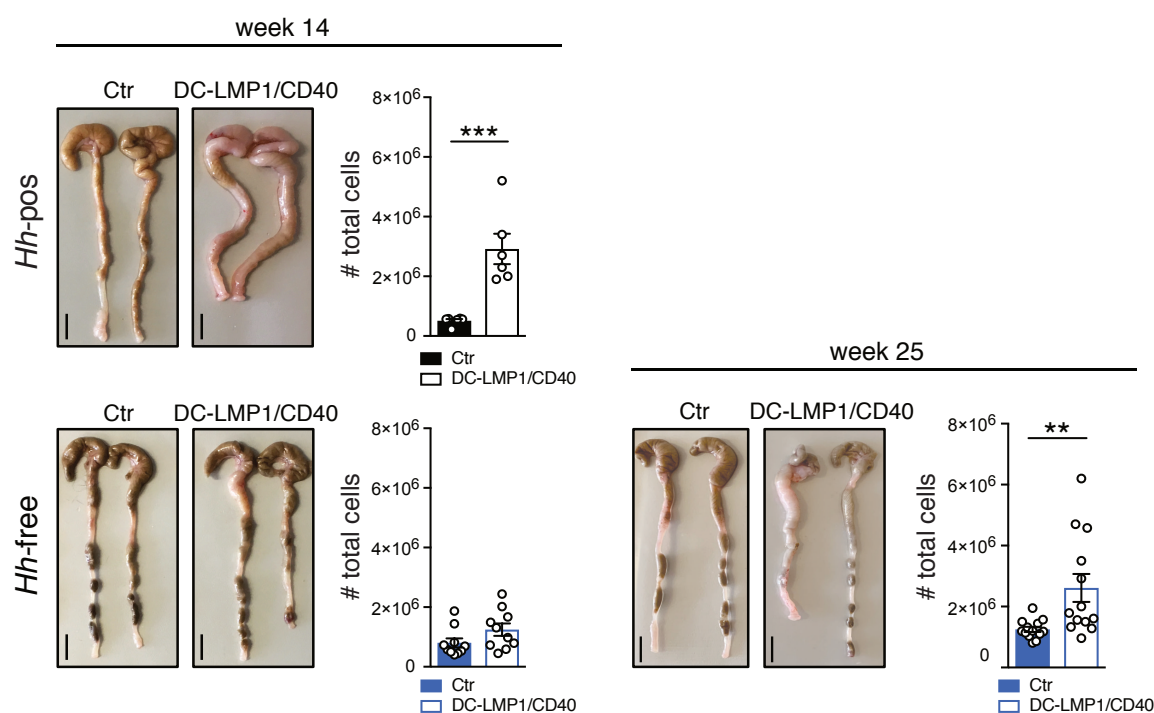


Figure 5.14: *Hh*-free DC-LMP1/CD40 mice show delayed inflammation and less morbidity. Macroscopic pictures of colons from *Hh*-pos (upper panel) or *Hh*-free (lower panels) Ctr and DC-LMP1/CD40 mice at the indicated time points. Shown are two representative colons per group with scale bars = 1 cm. Bar graphs show total colon LP cell numbers in Ctr and DC-LMP1/CD40 mice from three pooled experiments (mean \pm SEM, n=6-13).

5.4.2 DC-LMP1/CD40 mice rapidly develop strong intestinal inflammation upon reinfection with *Helicobacter hepaticus*

To further investigate the role of *Hh* in disease initiation, we reinfected *Hh*-free animals with *Hh* (strain ATCC 51448, [151]) by oral gavage (Fig.5.15 A).

Already at day 21 post inoculation (p.i.), all DC-LMP1/CD40 mice and control littermates, but not PBS-treated mice were *Hh*-positive as shown by species-specific PCR from feces (Fig.5.15 B). Also at day 40 p.i., when animals were finally sacrificed for analysis, all *Hh*-reinfected mice were still colonized with *Hh* (Fig.5.15 B). Of note, all mice were negative for the other most relevant *Helicobacter* species, confirming mono-colonization with *Hh* by oral gavage (Fig.5.15 B).

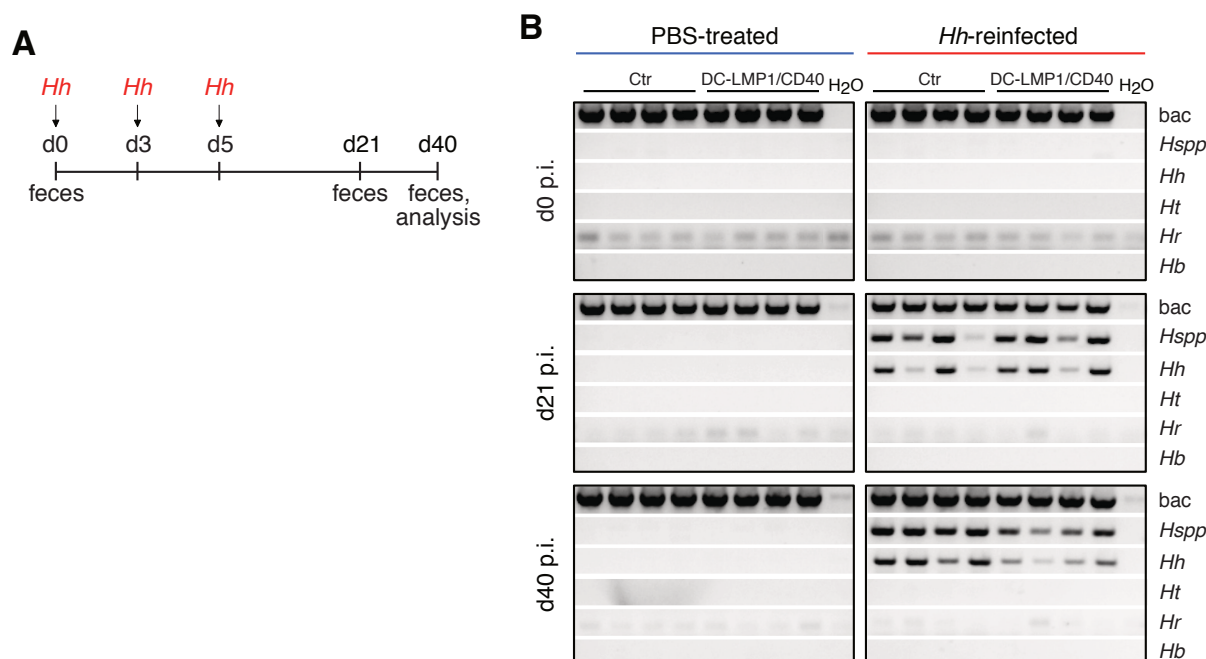


Figure 5.15: Oral gavage with *Hh* leads to rapid mono-colonization of *Hh*-free Ctr and DC-LMP1/CD40 mice. A) Schematic illustration of reinfection of *Hh*-free Ctr and DC-LMP1/CD40 mice with cultured *Hh* by oral gavage at the indicated time points. Feces were collected at the indicated time points and animals were sacrificed 40 d p.i. B) Bacterial DNA was extracted from fecal samples from either PBS-treated or *Hh*-reinfected Ctr and DC-LMP1/CD40 mice at the indicated time points. *Hh*-colonization was confirmed by PCR as in Fig.5.11 A and 5.12. Shown is one representative experiment out of two (n=4). bac: universal bacteria; *Hspp*: *Helicobacter species*; *Hh*: *Helicobacter hepaticus*; *Ht*: *Helicobacter typhlonius*; *Hr*: *Helicobacter rodentium*; *Hb*: *Helicobacter bilis*

Furthermore, only *Hh*-reinfected DC-LMP1/CD40 mice did show significantly elevated fecal lipocalin-2 levels already 21 d p.i. when compared to controls, indicating a rapid disease onset upon reinfection with *Hh* (Fig.5.16 A). By d40 p.i., *Hh*-reinfected DC-LMP1/CD40 animals but not control littermates showed not only increased fecal lipocalin-2 levels (Fig.5.16 A) but also a huge increase in cells infiltrating the colonic LP as well as a shortened and thickened colon (Fig.5.16 B), indicating acute colitis. In contrast, PBS-treated DC-LMP1/CD40 and control mice did not have elevated lipocalin-2 levels in their feces (Fig.5.16 A), neither did they show elevated cell numbers nor macroscopic changes of the large intestine (Fig.5.16 B) as also observed previously in 14-week-old *Hh*-free transgenic mice (Fig.5.13, 5.14).

Thus, our data reveal that *Hh* is rapidly provoking strong intestinal inflammation in DC-LMP1/CD40 mice, indicating that this bacterial stimulus combined with CD40-signaling in DCs is needed for the development of early onset colitis.

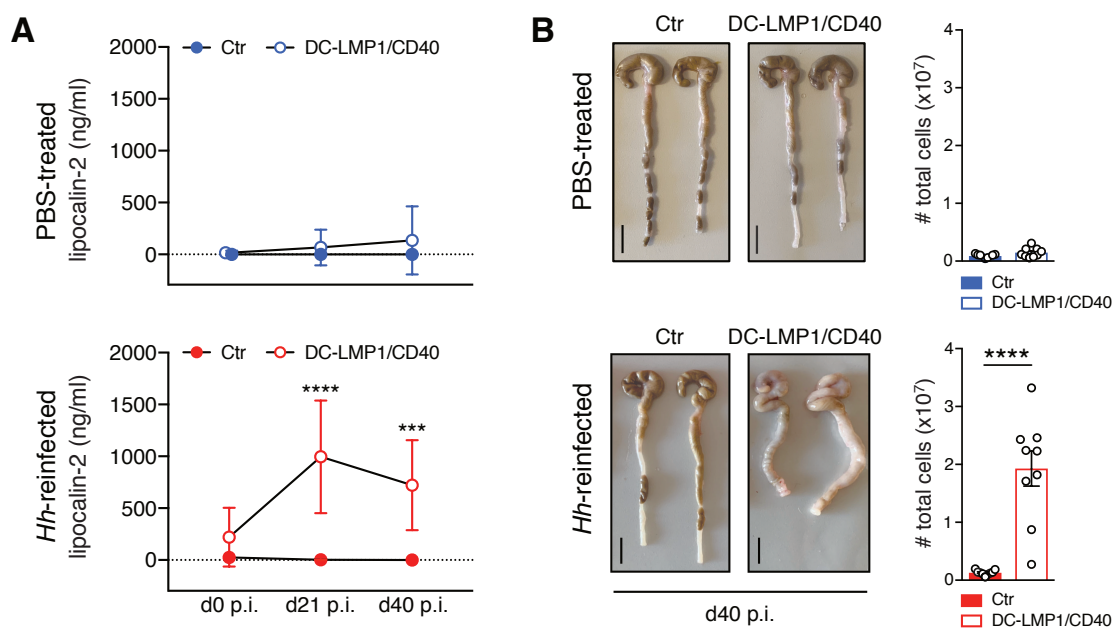


Figure 5.16: *Hh*-reinfection leads to rapid colitis onset in DC-LMP1/CD40 mice. **A)** Fecal lipocalin-2 levels in untreated (upper panel) or *Hh*-reinfected (lower panel) Ctrl and DC-LMP1/CD40 mice were measured by ELISA at the indicated time points. Data is shown as scatter plot with mean \pm SEM for two pooled experiments (n=9). **B)** Untreated (upper panel) or *Hh*-reinfected (lower panel) Ctrl and DC-LMP1/CD40 mice were sacrificed at day 40 p.i.. Shown are macroscopic pictures of two representative colons per group (scale bars = 1 cm) as well as bar graphs, representing total colon LP cell numbers from two pooled experiments with mean \pm SEM (n=9).

5.4.3 *Helicobacter hepaticus* affects colonic CD4⁺ T cell differentiation

We previously reported the effect of constitutive CD40-signaling on intestinal DCs [77]. Transgenic animals showed a strong reduction of tolerogenic CD103⁺ DC subsets in the colonic LP and mLNs. As a consequence, ROR γ t⁺Helios⁻ iTreg generation was drastically impaired in the large intestine of DC-LMP1/CD40 mice. As the conventionally-housed mouse colony used for our previous study was endemically infected with *Hh* (Fig.5.11), we wondered whether *Hh* affects DC subpopulations and/or CD4⁺ T cell differentiation in the CD40-mediated colitis model.

Therefore, we next analyzed cell subsets in the colonic LP of *Hh*-free DC-LMP1/CD40 mice and control littermates (Fig.5.17). We did find a strong reduction in the frequencies of CD103⁺CD11b⁻ as well as CD103⁺CD11b⁺ intestinal DCs in both 14- and 25-week-old *Hh*-free DC-LMP1/CD40 animals but not control littermates (Fig.5.17 A), similar to what we previously described for *Hh*-pos animals [77]. Further, ROR γ t⁺Helios⁻ iTregs were significantly reduced in 14- as well as 25-week-old *Hh*-free DC-LMP1/CD40 mice but not control animals (Fig.5.17 B) comparable with our previous findings in *Hh*-pos animals [77].

Of note, it seemed that CD103⁺CD11b⁻ DCs of *Hh*-free DC-LMP1/CD40 animals (Fig.5.17 A) were not as strongly reduced as in *Hh*-pos animals [77]. However, this level of preserved CD103⁺CD11b⁻ DCs was not sufficient for the generation of iTregs in the colonic LP of *Hh*-free DC-LMP1/CD40 mice (Fig.5.17 B).

We conclude that reduction of CD103⁺ DCs and impaired iTreg generation are rather a consequence of the transgene expression in DCs, suggesting that *Hh* has no direct impact on DC or Treg differentiation in this model.

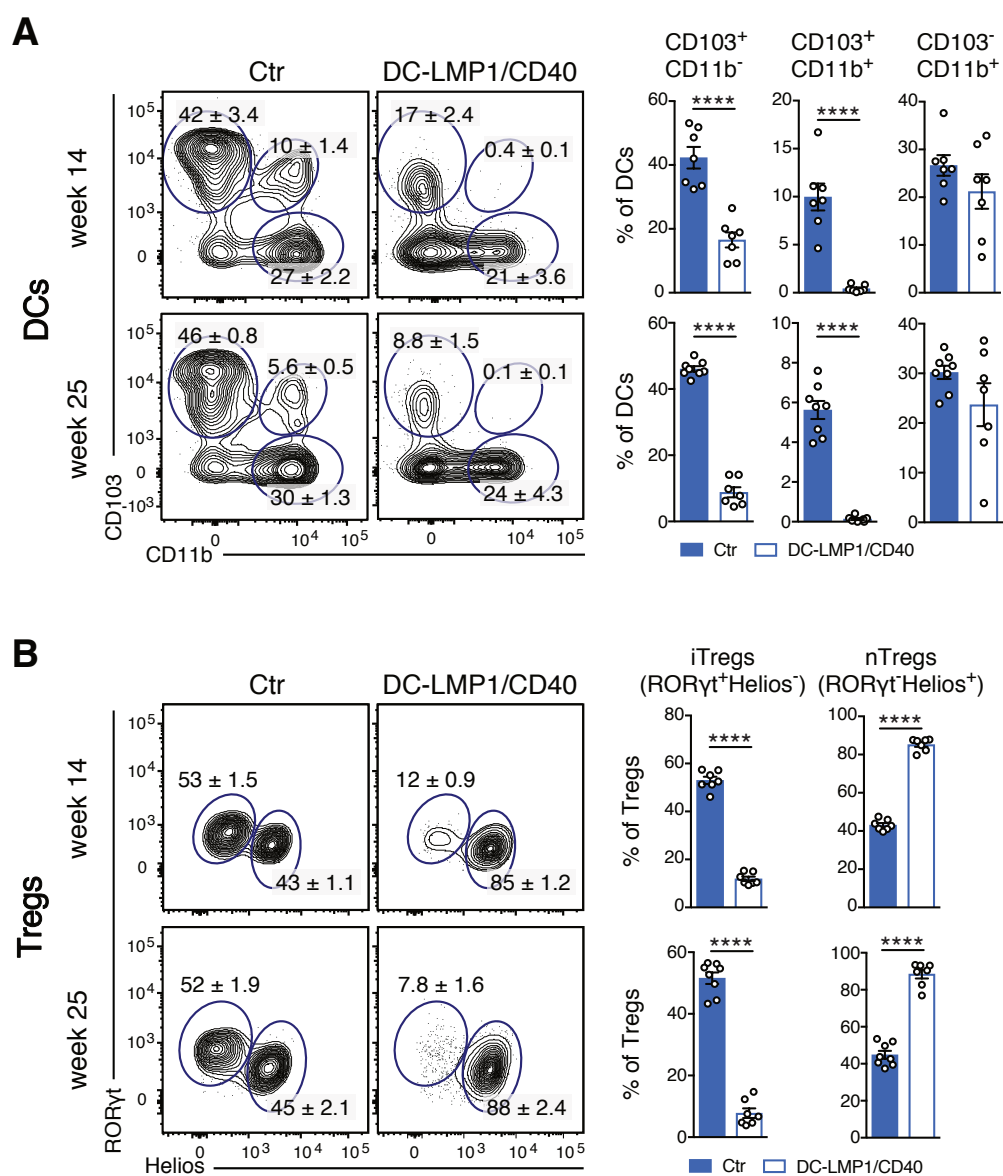


Figure 5.17: Loss of CD103⁺ DCs and iTregs in DC-LMP1/CD40 animals is not induced by *Hh*. A-B) Different cell subsets in the colonic LP were analyzed in *Hh*-free Ctr and DC-LMP1/CD40 animals at the indicated time points. Shown are representative FACS-plots as well as pooled statistics from two experiments for week 14 (mean ± SEM, n=7) and week 25 (mean ± SEM, n=7-8), illustrating frequencies of the indicated cell subsets. **A)** DCs were pre-gated on single, live, CD45⁺, MHCII⁺CD11c⁺, CD64⁻ cells. **B)** Tregs were gated on single, live, CD45⁺, CD3⁺CD4⁺, FoxP3⁺CD25⁺, RORγt⁺Helios⁻ (iTregs) or RORγt⁻Helios⁺ (nTregs).

We also know from our previous study that DC-LMP1/CD40 mice show a strong increase in IL-17⁺IFN-γ⁺ Th17/Th1 and IFN-γ⁺ Th1 cells in the colonic LP, indicating that non-pathogenic Th17 cells in DC-LMP1/CD40 mice are differentiating into pathogenic Th1 cells [77]. To evaluate the role of *Hh* in this CD4⁺ T cell differentiation process in DC-LMP1/CD40

animals, we compared IL-17 and IFN- γ producing CD4⁺ T cells in different mice (Fig.5.18). We did not detect significant differences in the frequency of IL-17⁺CD4⁺ T cells between DC-LMP1/CD40 and control animals neither in *Hh*-free nor in *Hh*-reinfected animals (Fig.5.18 A). However, at day 40 p.i., *Hh*-reinfected DC-LMP1/CD40 mice had significantly increased frequencies and total numbers of IL-17⁺IFN- γ ⁺ Th17/Th1 and IFN- γ ⁺ Th1 cells when compared to 14- or 25-week-old *Hh*-free DC-LMP1/CD40 mice (Fig.5.18 A). The increase in cell numbers of all three CD4⁺ T cell subsets detected in *Hh*-reinfected DC-LMP1/CD40 mice results from the huge increase in total cell numbers in the colonic LP of these mice as shown in Fig.5.16 B. Of note, also *Hh*-free DC-LMP1/CD40 mice showed some induction of IL-17⁺IFN- γ ⁺ Th17/Th1 and IFN- γ ⁺ Th1 cells in the colonic LP when compared to appropriate control littermates (Fig.5.18 A). However, when we analyzed the mean fluorescence intensity (MFI) of IFN- γ expression in IFN- γ ⁺CD4⁺ T cells, only Th1 cells from *Hh*-reinfected DC-LMP1/CD40 mice produced significantly higher amounts of IFN- γ when compared to *Hh*-free transgenic animals (Fig.5.18 B).

In the context of constitutive CD40-signaling in DCs, we could show that *Hh* has the potential to rapidly initiate the transdifferentiation of non-pathogenic Th17 into pathogenic Th1 cells in the colonic LP. However, this might not be an exclusive property of *Hh* but could also be accomplished in *Hh*-free mice by other commensals at slower rates.

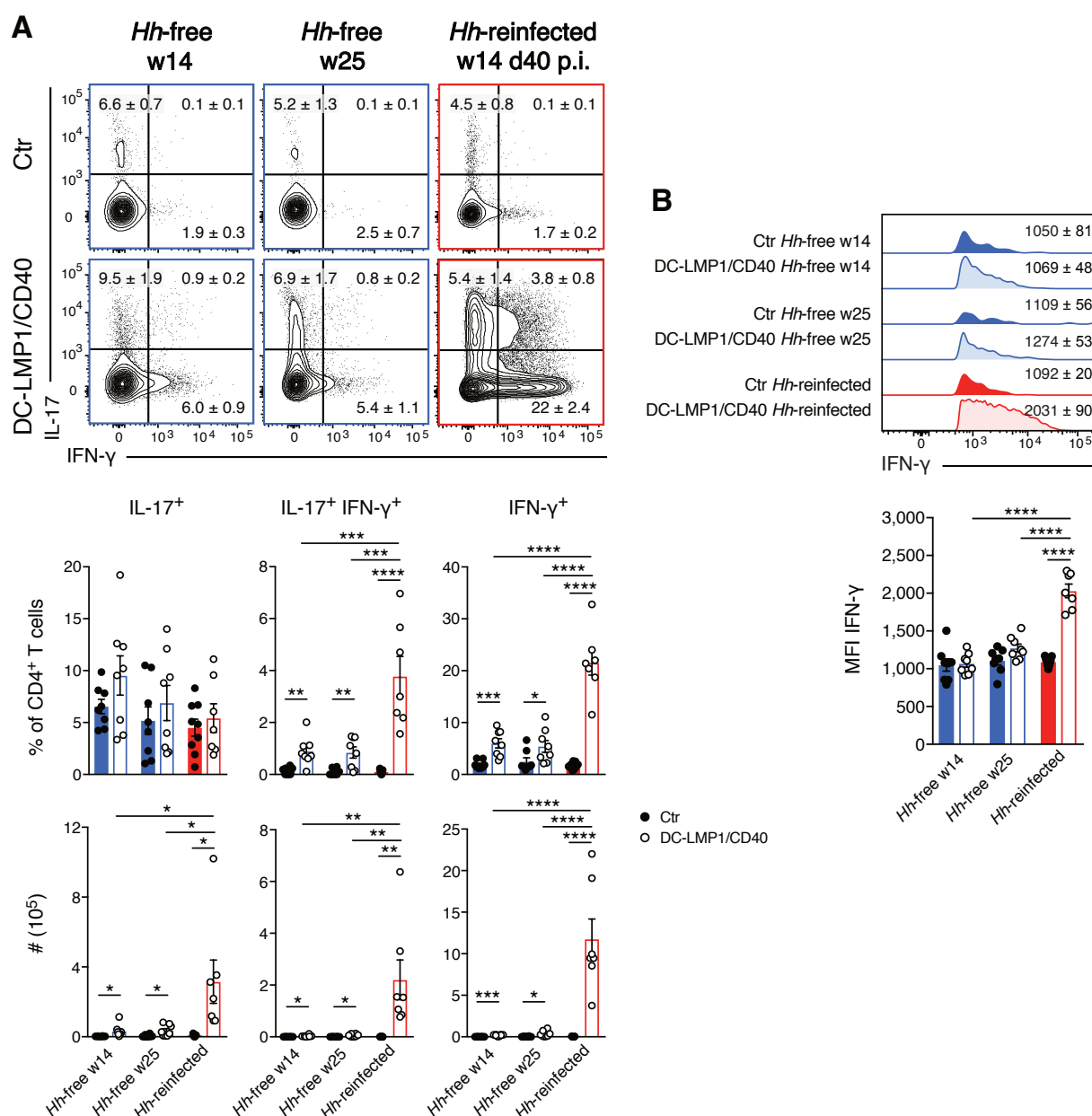


Figure 5.18: *Hh*-reinfection leads to rapid transdifferentiation into pathogenic Th1 effector cells in DC-LMP1/CD40 mice. A-B) Single-cell suspensions of the colonic LP from *Hh*-free or *Hh*-reinfected Ctrl and DC-LMP1/CD40 animals were stimulated with PMA/Ionomycin and subsequently stained intracellularly for IL-17 and IFN- γ production at the indicated time points. Bar graphs represent pooled statistics from two experiments (mean \pm SEM, n=7-9). **A)** T cells were pre-gated on single, live, CD45⁺, CD3⁺CD4⁺ cells. Shown are representative FACS-plots as well as bar graphs, illustrating the frequencies and numbers of indicated cell subsets within the CD4 T cell population. **B)** Shown are representative histograms as well as bar graphs, illustrating the MFI of IFN- γ expression within IFN- γ ⁺CD4⁺ T cells from A) as median \pm SEM.

6 Discussion

The microbiota is known as critical player in the context of IBD and bacterial infections are commonly used in colitis mouse models [156, 157, 158, 159, 162]. However, it is not fully understood how the microbiota modulates host immune cells and how the host is interacting with and discriminating between commensal and pathogenic bacteria present in the gut.

We studied microbial-host interactions in our previously published CD40-mediated model of colitis as DC-LMP1/CD40 mice did not show any signs of colitis if they were crossed onto Rag1^{-/-} background or if they were treated with antibiotics, indicating that disease development depends on the presence of T or B cells as well as on microbiota.

In the present study, we could identify the pathobiont *Helicobacter hepaticus* as disease driver with impact on disease onset, progression and outcome in our colitis model.

6.1 Role of the non-canonical NF- κ B pathway in DC-LMP1/CD40 animals

To determine the signaling pathway upon CD40 activation of DCs, IKK1 as part of the non-canonical NF- κ B pathway was knocked out in DCs of DC-LMP1/CD40 mice.

These DC-LMP1/CD40 ^{Δ IKK1} animals showed enlarged spleens and mLNs due to infiltrating granulocytes. However, these animals did not develop colitis as DC-LMP1/CD40 mice, indicating that the non-canonical NF- κ B pathway is the predominant signaling pathway upon CD40 activation of DCs. Our data further showed that DC-LMP1/CD40 ^{Δ IKK1} animals are protected from disease as iTregs were generated and accumulating Th17 cells did not transdifferentiate into pathogenic Th1 cells in the colon LP.

We previously published that DC-LMP1/CD40 animals on C57Bl/6 x Balb/c background (F1DC-LMP1/CD40) develop only mild colon inflammation that is not fatal [187]. In F1DC-LMP1/CD40 animals, CD103⁺CD11b⁻ DCs were not completely lost, iTregs were increased in frequency and transdifferentiation of Th17 cells into Th17/Th1 and Th1 cells was

attenuated [187]. Similarly, the impaired non-canonical NF- κ B pathway in DCs might preserve some level of CD103⁺CD11b⁻ DC induction in the colon LP of DC-LMP1/CD40 ^{Δ IKK1} animals that might be sufficient to generate iTregs and therefore protect these animals from disease [187]. Further, the deficiency of IKK1 as well as the expression of LMP1/CD40 in DC-LMP1/CD40 ^{Δ IKK1} animals is under control of the CD11c-Cre promoter. Thus, the non-canonical NF- κ B pathway might also be impaired in CD11c-expressing macrophages in these animals. As we showed previously in DC-LMP1/CD40 mice, intestinal macrophages express elevated levels of Il1a and Il1b, delivering survival signals to effector T cells [187]. Therefore, we can not exclude that also macrophages with deficiency of non-canonical NF- κ B signaling might contribute to protection from colitis.

However, our findings are in contrast to the results published by Tas et al. [84] where it was shown at least *in vitro* that the non-canonical NF- κ B pathway is involved in tolerance induction by DCs. In this study, the non-canonical NF- κ B pathway was impaired *in vitro* in human DCs by siRNA-mediated knockdown of NIK or IKK1. Here, they showed that the non-canonical NF- κ B pathway is essential for indoleamine 2,3 dioxygenase expression in DCs to control proinflammatory cytokine production and Treg induction [84]. However, for this *in vitro* study, human DCs were stimulated with CD40L and of course, tissue-specific DC analysis is not possible with this setup, hence the results are not completely comparable with our *ex vivo* analyses.

Of note, we did not analyze DC ^{Δ IKK1} mice with DC-specific deletion of IKK1 but no expression of the LMP1/CD40 transgene. However, DC ^{Δ IKK1} animals were previously studied by the group of Prof. Dr. Marc Schmidt-Supprian, demonstrating that IKK1 deletion in DCs has no significant effect neither on DC development nor on DC subsets in spleen and LNs (data not published). This is at least in parts in line with studies using alymphoplasia mice with a single point mutation in the NIK gene or mice with DC-specific NIK-deficiency, demonstrating that the non-canonical NF- κ B activation is critical for DC cross-presentation but not necessarily for DC development or CD4⁺ T cell priming [82, 83].

However, as we could demonstrate that both iTregs and effector T cells are affected in DC-LMP1/CD40^{ΔIKK1} mice which finally leads to protection from colitis, our data suggest that the non-canonical NF- κ B activation also impacts DCs in CD4⁺ T cell priming.

6.2 Dysbiosis in DC-LMP1/CD40 mice

To study the impact of microbiota on disease development in our CD40-mediated colitis model, we analyzed the microbial composition in healthy and sick mice. DC-LMP1/CD40 mice start to develop colitis very early in life, already at the age of 5 weeks. Concomitant with disease onset, they showed higher bacterial loads in feces, which was significantly increased in transgenic mice with the age of 8 weeks, when they suffer from severe colitis. As fecal content was plated onto MacConkey agar which is selective for gram-negative bacteria, gram-negative *Enterobacteriaceae* are mainly represented using this method. We also confirmed this "blooming" of *Enterobacteriaceae* in DC-LMP1/CD40 mice by 16S rRNA gene sequencing. Our results are in line with the literature as "*Enterobacteriaceae* blooming" is also reported as common phenomenon in both IBD patients as well as IBD mouse models [145].

We could also confirm dysbiosis in the CD40-mediated colitis model by analyzing the microbiota alpha-diversity at the OTU level in control and DC-LMP1/CD40 mice. Only in 8-week-old transgenic animals a strong reduction in the number of OTUs was observed. This reduced microbial diversity we observed in DC-LMP1/CD40 mice is very typical for colitis and also reported for IBD patients which show about 25 % less microbial genes when compared to healthy people [146].

By analyzing the 16S rRNA gene sequencing data at the family level, taxa differences turned out to be littermate-dependent at the age of 3 weeks but genotype-dependent in 8-week-old sick animals. Hence, our data suggest microbial changes observed in DC-LMP1/CD40 mice upon colitis onset as direct effect of the transgene and/or indirect effect of inflammation but not as direct environmental effect. Further, our data reveal an increase of the relative

abundance of the Proteobacteria *Enterobacteriaceae* and a decrease of the phylum Firmicutes such as *Lachnospiraceae* and *Ruminococcaceae* in DC-LMP1/CD40 mice suffering from severe colitis, which is also reported by the largest study so far which analyzed human IBD samples [147]. In contrast, we also detected an increase in *Clostridiaceae* and *Peptostreptococcaceae* which also belong to the phylum Firmicutes but which have not been reported in the study mentioned. Also in contrast to this study with IBD patients is our finding of an increase in *Erysipelotrichaceae* in 8-week-old DC-LMP1/CD40 mice while this family is decreased in IBD patients as reported by Gevers et al [147]. Of note, specific microbial changes in our model are difficult to compare with other studies as results are very much dependent on the region of amplification of the 16S rRNA gene and the bioinformatic analysis as well as the type of database used. Another limitation is also the fact that different studies discuss abundancies of taxa at different taxonomic levels which hampers the comparison of results. Further, even if same taxonomic level is discussed, it is difficult to compare results of studies with IBD patients as human samples are very heterogenous, depending on the age, disease stage as well as the type of sample and analysis [97].

6.3 Microbial-host interactions

6.3.1 Fecal bacteria in DC-LMP1/CD40 mice are highly IgA-coated

We observed that fecal IgA-levels were significantly elevated upon colitis onset and further increasing with age in DC-LMP1/CD40 mice. As expected, we did not detect fecal IgA in ABX-treated animals, indicating that the amount of IgA we measured in untreated mice was bound to bacteria. Further, flow cytometry analysis of fecal bacteria revealed not only higher percentages of bacteria coated by IgA but also more IgA bound per microbe in DC-LMP1/CD40 animals. It is known that IBD patients show higher percentage of IgA- but also IgG- and IgM-coated bacteria as compared to healthy people [116]. More recently, Palm and colleagues reported that potential disease drivers in IBD could be identified by their

IgA-coating level [115]. More in detail, germ-free mice were colonized with either IgA⁺ or IgA⁻ bacteria isolated from IBD patients. Surprisingly, highly IgA-coated bacteria from IBD patients were not able to cause disease in the steady state of germ-free mice but increased susceptibility and severity of dextran sodium sulfate-induced colitis in germ-free mice [115]. Of note, they found also highly IgA-coated bacteria in healthy people which do not show any pathology, indicating that potential bacterial disease drivers marked by high IgA-coating need a predisposing environment further contributing to disease development [115].

The cause for higher mucosal IgA-levels detected in DC-LMP1/CD40 mice could be that maybe more IgA is produced in response to certain bacteria that are hidden by others during homeostasis. However, upon dysbiosis, when microbial diversity decreases, these bacteria might be in closer contact to the epithelium and could therefore be actively recognized by intestinal immune cells. These bacteria could now also be able to even cross the epithelial barrier, which would lead to active recognition by immune cells in the LP. Of note, it seems that increased mucosal IgA, which is coating bacteria, is not effective enough to restore dysbiosis and stop ongoing inflammation in the CD40-mediated colitis model.

Hence, our data suggest that highly IgA-coated bacteria are potential disease drivers in DC-LMP1/CD40 mice.

6.3.2 DC-LMP1/CD40 mice produce commensal-specific antibodies

We did demonstrate that DC-LMP1/CD40 animals show both elevated serum IgG as well as serum IgA levels as soon as colitis onset was detectable and these levels were further increasing with the age of mice. While control animals showed also measurable IgG levels, serum IgA was entirely absent in this group, suggesting that serum IgA production is an exclusive hallmark of mice suffering from colitis.

The serum IgG reactivity towards commensal antigens tested by ELISA was only significant for DC-LMP1/CD40 animals at the age of 10 weeks. In contrast, significantly higher commensal-specific serum IgA was detected in DC-LMP1/CD40 animals at the age of 10,

12 and 14 weeks. However, proteins with approximately 60 kDa in size were more clearly detectable with serum IgG from DC-LMP1/CD40 mice at every age when tested by immunoblotting.

Although IgA is mainly produced locally in the gut, we also did detect elevated serum IgA levels and increased anti-commensal serum IgA in DC-LMP1/CD40 mice when compared to control littermates. The presence of commensal-specific serum antibodies in DC-LMP1/CD40 mice suggests that compartmentalization might be partly broken in mice suffering from colitis, leading to a systemic antibody response. This hypothesis is also supported by human studies, reporting elevated serum antibody levels in IBD patients [188, 189]. To ensure mucosal homeostasis, the gut sustains tolerance towards commensal bacteria by restraining them with the epithelium and the mucus layer, secreting protective AMPs and bacteria-specific IgA. Nevertheless, also under homeostatic conditions, contact between bacteria and host cells is not excluded but antigens are enclosed at mucosal sites. In particular, DCs in the intestinal LP are constantly sampling the lumen with their dendrites and transport antigen into draining mLN for B and T cell priming. In line with this, Konrad and colleagues confirmed that serum antibodies against bacteria are not detectable in SPF-housed mice [190]. However, if this tightly regulated balance is disturbed, bacteria can be delivered outside from mLN to induce systemic responses [191]. This is the case for instance when Tregs are missing, upon removal of mLN, chemical disruption of the epithelium, but also upon infection with pathogens, which can also actively spread beyond mLN and thus bacteria-specific antibodies can be systemically detectable [191].

However, our data also show some level of bacteria-specific serum IgG in control littermates. One explanation for this observation might be that we used conventionally- but not SPF-housed mice for this experiment. This hypothesis is supported by the fact that also for healthy humans which are of course not reaching SPF status, some level of systemic bacteria-specific IgG is reported, with levels further increasing during IBD [191]. During inflammatory conditions as in patients suffering from IBD, it is well known that systemic antibodies are

produced as a consequence of mucosal barrier dysfunction and thus increased exposure of commensals to systemic sites [191]. For instance, increased systemic IgG as well as IgA specific for *E. coli* outer membrane porin (OmpC) or CBir1-flagellin are detectable in IBD patients [189].

We observed (i) elevated serum IgG- and IgA-levels upon colitis onset that are further increasing with age of DC-LMP1/CD40 mice and (ii) commensal-specific serum IgG and IgA in DC-LMP1/CD40 mice. This might reflect the time of antigen exposure and further the degree of disease due to concomitant increased gut permeability. Only recently, it was reported by Wilmore and colleagues that in particular members of Proteobacteria are able to induce T cell-dependent serum IgA responses in conventional mice to protect them from lethal sepsis [120]. They identified the commensal *Helicobacter muridarum* as driving species, inducing mucosal IgA-secreting plasma cells as well as IgA⁺ bone marrow plasma cells [120].

Our data suggest that dysbiosis in DC-LMP1/CD40 mice affects dissemination of bacteria, inducing systemic IgG as well as IgA production.

6.3.3 Identification of bacterial antigens by serum antibody reactivity

We were able to identify a 60 kDa protein from *Hh* recognized by serum antibodies in DC-LMP1/CD40 mice upon colitis onset. Although five proteins were precipitated by serum antibodies from transgenic mice but not control littermates, only two proteins, a protein from *H. pylori* and a protein from *Hh*, were precipitated with high fold change and low *p*-value when analyzed with iBAQ.

However, the protein from *H. pylori* was not considered for further analyses as both the numbers of peptides as well as the percentage of protein sequence coverage were not reliable. One explanation for recovering a protein from *H. pylori* next to *Hh* with this approach might be the fact that about 50 % of total proteins from *Hh* have orthologs in *H. pylori* [192] and therefore might arise by the analysis within the bacterial database used for iBAQ.

The fact that only the 60 kDa chaperonin from *Hh* was identified with this method with high fold change and low *p*-value when compared to control sera and by showing up reliable numbers of peptides and percentage of protein sequence coverage was quite surprising with respect to the high number and variety of bacteria in CBL. Of note, for this approach we used protein G beads that mainly bind IgG, thus bacterial antigens recognized by other isotypes might not be considered here. Therefore, immunoprecipitation with protein A or protein L beads might identify further bacterial antigens by serum antibodies, in particular by serum IgA, in our colitis model. However, both serum IgG as well as serum IgA response was detected when we tested whole lysate from *Hh* by ELISA. Moreover, we could also detect a 60 kDa protein within the lysate with both serum IgG as well as serum IgA by immunoblot. Although we were not able to test the 60 kDa chaperonin from *Hh* directly, we used LK-2 as positive control, recognizing both human HSP60 and the bacterial homologue GroEL [186]. Our data indicate that serum antibodies from transgenic animals are specific for the 60 kDa chaperonin GroEL from *Hh*, confirming the data obtained by mass spectrometry.

The fact that we identified a bacterial chaperonin as target antigen in DC-LMP1/CD40 mice is supported by the literature as heat shock proteins are reported as immunodominant antigens, inducing humoral and cellular immune responses to several diseases in humans and mice. For instance, α Hsp60 antibodies are found in patients with tuberculosis as well as in mice infected with *Mycobacterium tuberculosis* [193, 194]. Further, it was demonstrated that pathogen-derived 60 kDa chaperonin induces pro-inflammatory cytokines *in vitro* [195], that mice infected with *Yersinia enterocolitica* produce 60 kDa chaperonin-specific T cells involved in anti-pathogenic immune response [193], and serum antibodies specific for Hsp60 from *H. pylori* are reported in patients with gastric cancer [196].

Our data suggest that *Hh* is involved in disease development and that the 60 kDa chaperonin we identified in *Hh* might be a potential immunodominant antigen in our CD40-mediated colitis model. Further work using the 60 kDa chaperonin from *Hh* in an *ex vivo* T cell restimulation assay would reveal whether effector T cells in the colonic LP of DC-LMP1/CD40

mice are specific for this bacterial antigen.

6.4 *Helicobacter hepaticus* as disease driver

With respect to the results we obtained by mass spectrometry upon immunoprecipitation of bacterial antigens with serum antibodies from DC-LMP1/CD40 mice, we studied the role of *Hh* in our colitis model in more detail.

Hh is known as pathobiont, endemic in many mouse colonies [152, 153], which is able to elicit intestinal inflammation in immunodeficient or -compromized mice as demonstrated by several mouse models, mimicking human IBD [156, 159]. The screening of fecal samples from DC-LMP1/CD40 animals and control littermates confirmed that our conventionally housed mouse colony was endemically infected with the *Helicobacter* genus. Of note, only control mice were consistently positive for *Hh*. In contrast, young DC-LMP1/CD40 mice showed already reduced infection rates while *Hh* was hardly detectable in older DC-LMP1/CD40 mice.

One reason for this phenomenon might be the clearance of *Hh*, indicated by increased anti-*Hh*L serum IgG and IgA we observed. However, DC-LMP1/CD40 mice show ongoing disease once colonized with *Hh* and finally die from severe colitis before the age of 20 weeks. This would rather suggest that serum antibodies from transgenic animals show cross-reactivity with a GroEL homologue from other bacteria after clearance of *Hh*. Another explanation would be that *Hh* is able to cross the epithelial barrier in DC-LMP1/CD40 mice more easily due to dysbiosis and inflammation and therefore this species would not be detectable anymore in the luminal content. Screening of tissue biopsies from the colon LP would be helpful to confirm this hypothesis. Another possibility would be that *Hh* is simply displaced by other bacteria such as *Enterobacteriaceae* which bloom during dysbiosis in DC-LMP1/CD40 animals, indicated by the data we obtained from 16S rRNA gene sequencing of fecal samples. However, this would suggest that *Hh* is needed for disease initiation but not maintenance and progression.

6.4.1 *Helicobacter hepaticus*-free DC-LMP1/CD40 mice are protected from early disease onset

Upon embryo transfer rederivation, animals were bred and maintained under SPF conditions, thus all DC-LMP1-CD40 mice and control littermates were negative for the *Helicobacter* genus. As expected, *Hh*-free DC-LMP1/CD40 mice did not show any signs of colitis at the age of 8 or 14 weeks when *Hh*-positive transgenic animals were already suffering from severe colitis. However, some but not all *Hh*-free transgenic animals developed intestinal inflammation at the age of 20 or 25 weeks when *Hh*-positive transgenic animals had already died from the disease. Interestingly, also Kullberg and colleagues reported that IL-10-deficient mice developed intestinal inflammation when maintained under SPF conditions but with delayed onset and less severity as indicated by less infiltrating lymphocytes in 5- to 6-month old animals [159]. Consistent with Kullberg et al., also Xu and colleagues have shown that *Hh*-free transgenic mice with Treg-specific c-Maf deficiency developed mild spontaneous colitis at a later age of 6 to 12 month [162].

The protection from early disease onset in *Hh*-free DC-LMP1/CD40 mice suggests that *Hh* might be a very potent disease driver in the CD40-mediated colitis model. However, as some of the *Hh*-free DC-LMP1/CD40 animals show intestinal inflammation, although with strong delay, also other bacteria may be considered as disease driving species in these animals. Of note, none of *Hh*-free animals died before the end of the experiment in week 25 after birth, indicating that those *Hh*-free transgenic animals which show signs of intestinal inflammation suffer from a milder degree of disease than *Hh*-positive DC-LMP1/CD40 animals did.

To finally reveal the cause of less morbidity in *Hh*-free DC-LMP1/CD40 mice, we plan to perform 16S rRNA gene sequencing of fecal content also with *Hh*-free animals as well as immunoprecipitation of potential bacterial antigens with serum antibodies from *Hh*-free mice.

6.4.2 DC-LMP1/CD40 mice rapidly develop strong intestinal inflammation upon reinfection with *Helicobacter hepaticus*

Upon reinfection of *Hh*-free animals with *Hh* using oral gavage, this species but not any other *Helicobacter* genus was rapidly detectable from day 21 p.i. in fecal samples from treated animals, confirming effective oral infection. Concomitant with mono-colonization by *Hh*, DC-LMP1/CD40 animals rapidly developed severe colitis, determined by elevated fecal lipocalin-2 levels, thickened and shortened colon as well as strong infiltration of the colonic LP with immune cells. Thus, our data suggest *Hh* as potent disease driver in our colitis model.

As mentioned before, many studies have applied *Hh* infection to immunodeficient or immunocompromized mice to elicit spontaneous colitis [156, 157, 158, 159, 162]. For instance, SPF-housed IL-10 deficient mice rapidly developed strong intestinal inflammation upon experimental infection with *Hh* [159].

6.4.3 *Helicobacter hepaticus* affects colonic CD4⁺ T cell differentiation

While we determined *Hh* as disease driver in our CD40-mediated colitis model, this pathobiont did not have a direct impact on DC subset composition or Treg differentiation in the colon LP. CD103⁺ DCs were reduced in both 14- and 25-week-old *Hh*-free transgenic animals, comparable with our previous findings in *Hh*-pos DC-LMP1/CD40 animals [77].

However, it seemed that CD103⁺CD11b⁻ DCs in *Hh*-free DC-LMP1/CD40 mice were not as strongly reduced as in *Hh*-pos animals [77]. This level of CD103⁺CD11b⁻ DCs was not sufficient for the induction of iTregs in the colonic LP of *Hh*-free DC-LMP1/CD40 mice as ROR γ t⁺Helios⁻ iTregs were similarly reduced in both *Hh*-free as well as *Hh*-pos DC-LMP1/CD40 mice.

As IBD is well known as multifactorial disease [144], it is difficult to determine the causative factor in this context. One main difference was the housing of mice. While *Hh*-free animals

were raised under SPF conditions, *Hh*-pos mice were conventionally housed, suggesting that the mice show an overall different microbial composition that also might impact the DC-iTreg axis. Thus, 16S rRNA gene sequencing of fecal content from *Hh*-free animals is planned as also mentioned before.

In contrast, we could demonstrate that CD4⁺ effector T cell differentiation in the colon LP is directly affected by *Hh*. Upon *Hh*-reinfection, DC-LMP1/CD40 mice showed significantly increased frequencies and total numbers of IL-17⁺IFN- γ ⁺ Th17/Th1 and IFN- γ ⁺ Th1 cells as compared to 14- or 25-week-old *Hh*-free DC-LMP1/CD40 mice.

Of note, we were only able to perform unspecific *ex vivo* T cell restimulation with PMA/ionomycin. Although we failed to stimulate CD4⁺ T cells using whole *Hh* lysate to detect *Hh*-specific T cells, also other studies have shown *Hh* to induce colitogenic effector T cells [161, 162]. Kullberg et al. demonstrated that *Hh*-infection of IL-10-deficient mice led to the induction of pathogenic, *Hh*-specific T cells, expressing both IL-17 and IFN- γ [161]. Further, only recently, the group of Dan Littmann used *Hh* infection of IL-10^{-/-} mice to study microbial-host interactions [162]. By generating TCR transgenic mice with T cells specific for the *Hh* transmembrane protein porin, they identified the TF c-Maf in iTregs as key component to restrain colitogenic Th17 cells in *Hh*-positive IL-10^{-/-} mice [162].

Our data revealed that the intestinal microbiota is able to modulate the host immune response with impact on disease onset, progression and outcome. Here, we identified the pathobiont *Hh* as disease driver in our CD40-mediated model of colitis. In the context of constitutive CD40-signaling in DCs, we could show that *Hh* has the potential to induce early onset colitis, concomitant with initiation of the transdifferentiation of non-pathogenic Th17 cells into pathogenic Th1 cells in the colonic LP. Our results are also of relevance for other studies using conventionally housed mice as *Hh* is endemic in many mouse colonies.

Our data further confirm the important role of the gut microbial composition during health and disease and reveal that single bacterial species can dramatically affect host immunity.

Nevertheless, the identification of other potential disease driving bacteria as well as specific

bacterial antigens and underlying mechanisms in IBD is central. This would further contribute to understand the complex interaction of microbiota and host immune cells to develop and improve in particular personalized therapeutic strategies in IBD.

Bibliography

- [1] Y. Xing and K. A. Hogquist, “T-Cell Tolerance: Central and Peripheral,” *Cold Spring Harbor Laboratory Press*, pp. 1–16, 2012.
- [2] L. Klein, B. Kyewski, P. M. Allen, and K. A. Hogquist, “Positive and negative selection of the T cell repertoire: what thymocytes see and don’t see,” *Nature Reviews Immunology*, vol. 14, no. 6, pp. 377–391, 2014.
- [3] C. Bouneaud, P. Kourilsky, and P. Bousso, “Impact of Negative Selection on the T Cell Repertoire Reactive to a Self-Peptide,” *Immunity*, vol. 13, no. 6, pp. 829–840, 2004.
- [4] D. Lo, L. Burkly, R. Flavell, R. Palmiter, and R. Brinster, “Tolerance in transgenic mice expressing class II major histocompatibility complex on pancreatic acinar cells,” *Journal of Experimental Medicine*, vol. 170, no. 1, pp. 87–104, 1989.
- [5] R. M. Steinman, “Dendritic cells: versatile controllers of the immune system,” *Nature Medicine*, vol. 13, no. 10, pp. 1155–1159, 2007.
- [6] R. Förster, A. Braun, and T. Worbs, “Lymph node homing of T cells and dendritic cells via afferent lymphatics,” *Trends in Immunology*, vol. 33, no. 6, pp. 271–280, 2012.
- [7] M. L. Kapsenberg, “Dendritic-cell control of pathogen-driven T-cell polarization,” *Nature Reviews Immunology*, vol. 3, no. 12, pp. 984–993, 2003.
- [8] M. V. Dhodapkar, R. M. Steinman, J. Krasovsky, C. Munz, and N. Bhardwaj, “Antigen-Specific Inhibition of Effector T Cell Function in Humans after Injection of Immature Dendritic Cells,” *The Journal of Experimental Medicine*, vol. 193, no. 2, pp. 233–238, 2001.
- [9] M. de Heusch, G. Oldenhove, J. Urbain, K. Thielemans, C. Maliszewski, O. Leo, and M. Moser, “Depending on their maturation state, splenic dendritic cells induce the differentiation of CD4⁺ T lymphocytes into memory and/or effector cells in vivo,” *European Journal of Immunology*, vol. 34, no. 7, pp. 1861–1869, 2004.

-
- [10] V. Verhasselt, O. Vosters, C. Beuneu, C. Nicaise, P. Stordeur, and M. Goldman, "Induction of FOXP3-expressing regulatory CD4^{pos} T cells by human mature autologous dendritic cells," *European Journal of Immunology*, vol. 34, no. 3, pp. 762–772, 2004.
- [11] D. Hawiger, K. Inaba, Y. Dorsett, M. Guo, K. Mahnke, M. Rivera, J. V. Ravetch, R. M. Steinman, and M. C. Nussenzweig, "Dendritic cells induce peripheral T cell unresponsiveness under steady state conditions in vivo.," *The Journal of experimental medicine*, vol. 194, no. 6, pp. 769–79, 2001.
- [12] S. Hori, T. Nomura, and S. Sakaguchi, "Control of regulatory T cell development by the transcription factor Foxp3," *Science.*, vol. 299, no. 5609, pp. 1057–1061, 2003.
- [13] J. D. Fontenot, M. A. Gavin, and A. Y. Rudensky, "Foxp3 programs the development and function of CD4⁺CD25⁺ regulatory T cells," *Nature immunology*, vol. 198, no. 3, pp. 986–992, 2003.
- [14] R. Khattri, T. Cox, S. A. Yasayko, and F. Ramsdell, "An essential role for Scurfin in CD4⁺CD25⁺T regulatory cells," *Nature immunology*, vol. 198, no. 3, pp. 993–998, 2003.
- [15] M. E. Brunkow, E. W. Jeffery, K. A. Hjerrild, B. Paeper, L. B. Clark, S.-A. Yasayko, J. E. Wilkinson, D. Galas, S. F. Ziegler, and F. Ramsdell, "Disruption of a new forkhead/winged-helix protein, scurfin, results in the fatal lymphoproliferative disorder of the scurfy mouse," *Nature genetics*, vol. 27, no. 1, pp. 68–73, 2001.
- [16] R. S. Wildin, F. Ramsdell, J. Peake, F. Faravelli, J.-L. Casanova, N. Buist, E. Levy-Lahad, M. Mazzella, O. Goulet, L. Perroni, F. D. Bricarell, G. Byrne, M. McEuen, S. Proll, M. Appleby, and M. E. Brunkow, "X-linked neonatal diabetes mellitus, enteropathy and endocrinopathy syndrome is the human equivalent of mouse scurfy," *Nature genetics*, vol. 27, no. january, pp. 2–4, 2001.

-
- [17] A. M. Bilate and J. J. Lafaille, “Induced CD4⁺ Foxp3⁺ Regulatory T Cells in Immune Tolerance,” *Annual Review of Immunology*, vol. 30, no. 1, pp. 733–758, 2012.
- [18] J. M. Weiss, A. M. Bilate, M. Gobert, Y. Ding, M. A. Curotto de Lafaille, C. N. Parkhurst, H. Xiong, J. Dolpady, A. B. Frey, M. G. Ruocco, Y. Yang, S. Floess, J. Huehn, S. Oh, M. O. Li, R. E. Niec, A. Y. Rudensky, M. L. Dustin, D. R. Littman, and J. J. Lafaille, “Neuropilin 1 is expressed on thymus-derived natural regulatory T cells, but not mucosa-generated induced Foxp3⁺ T reg cells,” *The Journal of Experimental Medicine*, vol. 209, no. 10, pp. 1723–1742, 2012.
- [19] A. Thornton, P. Korty, D. Tran, E. Wohlfert, P. Murray, Y. Belkaid, and E. Shevach, “Expression of Helios, an Ikaros Transcription Factor Family Member, Differentiates Thymic-Derived from Peripherally Induced Foxp3,” *J Immunol.*, vol. 184, no. 7, pp. 3433–3441, 2010.
- [20] C. Ohnmacht, J.-h. Park, S. Cording, J. B. Wing, K. Atarashi, Y. Obata, V. Gaboriau-Routhiau, R. Marques, S. Dulauroy, M. Fedoseeva, M. Busslinger, N. Cerf-Bensussan, I. G. Boneca, D. Voehringer, K. Hase, K. Honda, S. Sakaguchi, and G. Eberl, “The microbiota regulates type 2 immunity through ROR γ t T cells,” *Science*, vol. 349, pp. 989–993, 2015.
- [21] R. M. Steinman and Z. A. Cohn, “Identification of a novel cell type in peripheral lymphoid organs of mice,” *The Journal of experimental medicine*, vol. 137, pp. 1142–1162, 1973.
- [22] A. W. Purcell and T. Elliott, “Molecular machinations of the MHC-I peptide loading complex,” *Current Opinion in Immunology*, vol. 20, no. 1, pp. 75–81, 2008.
- [23] E. S. Trombetta, M. Ebersold, W. Garrett, M. Pypaert, and I. Mellman, “Activation of lysosomal function during dendritic cell maturation,” *Science*, vol. 299, no. 2003, pp. 1400–1404, 2003.

-
- [24] M. J. Bevan, "Cross-priming for a secondary cytotoxic response to minor H antigens with H-2 congenic cells which do not cross-react in the cytotoxic assay," *The Journal of experimental medicine*, vol. 143, 1976.
- [25] C. Kurts, W. R. Heath, F. R. Carbone, J. Allison, J. F. Miller, and H. Kosaka, "Constitutive class I-restricted exogenous presentation of self antigens in vivo," *Journal of Experimental Medicine*, vol. 184, no. 3, pp. 923–930, 1996.
- [26] W. R. Heath and F. R. Carbone, "Cross-presentation in viral immunity and self-tolerance," *Nature Reviews Immunology*, vol. 1, no. 2, pp. 126–135, 2001.
- [27] M. Colonna, G. Trinchieri, and Y. J. Liu, "Plasmacytoid dendritic cells in immunity," *Nature Immunology*, vol. 5, no. 12, pp. 1219–1226, 2004.
- [28] F. Geissmann, M. G. Manz, S. Jung, M. H. Sieweke, and K. Ley, "Development of monocytes, macrophages and dendritic cells," *Science*, vol. 327, no. 5966, pp. 656–661, 2010.
- [29] A. Mildner and S. Jung, "Development and function of dendritic cell subsets," *Immunity*, vol. 40, no. 5, pp. 642–656, 2014.
- [30] J. M. den Haan, S. M. Lehar, and M. J. Bevan, "CD8⁺ but Not CD8⁻ Dendritic Cells Cross-Prime Cytotoxic T Cells in Vivo," *The Journal of Experimental Medicine*, vol. 192, no. 12, pp. 1685–1696, 2000.
- [31] S. Bedoui, P. G. Whitney, J. Waithman, L. Eidsmo, L. Wakim, I. Caminschi, R. S. Allan, M. Wojtasiak, K. Shortman, F. R. Carbone, A. G. Brooks, and W. R. Heath, "Cross-presentation of viral and self antigens by skin-derived CD103⁺ dendritic cells," *Nature Immunology*, vol. 10, no. 5, pp. 488–495, 2009.
- [32] C. Reis e Sousa, S. Hieny, T. Schariton-kersten, D. Jankovic, H. Charest, R. N. Germain, and A. Sher, "In Vivo Microbial Stimulation Induces Rapid CD40Ligand-independent

- Production of Interleukin 12 by Dendritic Cells and their Redistribution to T Cell Areas,” *The Journal of experimental medicine*, vol. 186, no. 11, pp. 1819–1829, 1997.
- [33] D. Dudziak, A. O. Kamphorst, G. F. Heidkamp, V. R. Buchholz, C. Trumpheller, S. Yamazaki, C. Cheong, K. Liu, H.-W. Lee, C. Gyu Park, R. M. Steinman, and M. C. Nussenzweig, “Differential Antigen Processing by Dendritic Cell Subsets in Vivo,” *Science*, no. January, pp. 107–111, 2007.
- [34] E. Persson, H. Uronen-Hansson, M. Semmrich, A. Rivollier, K. Hägerbrand, J. Marsal, S. Gudjonsson, U. Håkansson, B. Reizis, K. Kotarsky, and W. W. Agace, “IRF4 Transcription-Factor-Dependent CD103⁺CD11b⁺ Dendritic Cells Drive Mucosal T Helper 17 Cell Differentiation,” *Immunity*, vol. 38, no. 5, pp. 958–969, 2013.
- [35] A. Schlitzer, N. McGovern, P. Teo, T. Zelante, K. Atarashi, D. Low, A. W. Ho, P. See, A. Shin, P. S. Wasan, G. Hoeffel, B. Malleret, A. Heiseke, S. Chew, L. Jardine, H. A. Purvis, C. M. Hilkens, J. Tam, M. Poidinger, E. R. Stanley, A. B. Krug, L. Renia, B. Sivasankar, L. G. Ng, M. Collin, P. Ricciardi-Castagnoli, K. Honda, M. Haniffa, and F. Ginhoux, “IRF4 Transcription Factor-Dependent CD11b⁺ Dendritic Cells in Human and Mouse Control Mucosal IL-17 Cytokine Responses,” *Immunity*, vol. 38, no. 5, pp. 970–983, 2013.
- [36] C. Abraham and R. Medzhitov, “Interactions between the host innate immune system and microbes in inflammatory bowel disease,” *Gastroenterology*, vol. 140, no. 6, pp. 1729–37, 2011.
- [37] V. Bekiaris, E. K. Persson, and W. W. Agace, “Intestinal dendritic cells in the regulation of mucosal immunity,” *Immunological reviews*, vol. 260, pp. 86–101, 2014.
- [38] S. Tamoutounour, S. Henri, H. Lelouard, B. de Bovis, C. de Haar, C. J. van der Woude, A. M. Woltman, Y. Reyat, D. Bonnet, D. Sichien, C. C. Bain, A. M. Mowat, C. Reis e Sousa, L. F. Poulin, B. Malissen, and M. Guillems, “CD64 distinguishes macrophages

- from dendritic cells in the gut and reveals the Th1-inducing role of mesenteric lymph node macrophages during colitis,” *European Journal of Immunology*, vol. 42, no. 12, pp. 3150–3166, 2012.
- [39] M. Rescigno, M. Urbano, B. Valzasina, M. Francolini, G. Rotta, R. Bonasio, F. Granucci, J. Kraehenbuhl, and P. Ricciardi-Castagnoli, “Dendritic cells express tight junction proteins and penetrate gut epithelial monolayers to sample bacteria,” *Nature Immunology*, vol. 2, no. 4, pp. 361–7, 2001.
- [40] J. H. Niess, S. Brand, X. Gu, L. Landsman, S. Jung, B. A. McCormick, J. M. Vyas, M. Boes, H. L. Ploegh, J. G. Fox, D. R. Littman, and H. C. Reinecker, “CX3CR1-mediated dendritic cell access to the intestinal lumen and bacterial clearance,” *Science*, vol. 307, no. 5707, pp. 254–258, 2005.
- [41] O. Schulz, E. Jaensson, E. K. Persson, X. Liu, T. Worbs, W. W. Agace, and O. Pabst, “Intestinal CD103⁺, but not CX3CR1⁺, antigen sampling cells migrate in lymph and serve classical dendritic cell functions,” *The Journal of Experimental Medicine*, vol. 206, no. 13, pp. 3101–3114, 2009.
- [42] A. Vallon-Eberhard, L. Landsman, N. Yogev, B. Verrier, and S. Jung, “Transepithelial Pathogen Uptake into the Small Intestinal Lamina Propria,” *The Journal of Immunology*, vol. 176, no. 4, pp. 2465–2469, 2006.
- [43] E. Mazzini, L. Massimiliano, G. Penna, and M. Rescigno, “Oral Tolerance Can Be Established via Gap Junction Transfer of Fed Antigens from CX3CR1⁺ Macrophages to CD103⁺ Dendritic Cells,” *Immunity*, vol. 40, no. 2, pp. 248–261, 2014.
- [44] J. Farache, I. Koren, I. Milo, I. Gurevich, K. W. Kim, E. Zigmond, G. C. Furtado, S. A. Lira, and G. Shakhar, “Luminal Bacteria Recruit CD103⁺ Dendritic Cells into the Intestinal Epithelium to Sample Bacterial Antigens for Presentation,” *Immunity*, vol. 38, no. 3, pp. 581–595, 2013.

- [45] M. H. Jang, N. Sougawa, T. Tanaka, T. Hirata, T. Hiroi, K. Tohya, Z. Guo, E. Umemoto, Y. Ebisuno, B.-G. Yang, J.-Y. Seoh, M. Lipp, H. Kiyono, and M. Miyasaka, "Response to Comment on "CCR7 Is Critically Important for Migration of Dendritic Cells in Intestinal Lamina Propria to Mesenteric Lymph Nodes"," *The Journal of Immunology*, vol. 176, no. 4, pp. 803–810, 2006.
- [46] V. Cerovic, S. A. Houston, C. L. Scott, A. Aumeunier, U. Yrlid, A. M. Mowat, and S. W. F. Milling, "Intestinal CD103- dendritic cells migrate in lymph and prime effector T cells," *Mucosal Immunology*, vol. 6, no. 1, pp. 104–113, 2013.
- [47] J. L. Coombes, K. R. R. Siddiqui, C. V. Arancibia-Cárcamo, J. Hall, C.-M. Sun, Y. Belkaid, and F. Powrie, "A functionally specialized population of mucosal CD103+ DCs induces Foxp3+ regulatory T cells via a TGF-beta and retinoic acid-dependent mechanism.," *The Journal of experimental medicine*, vol. 204, no. 8, pp. 1757–64, 2007.
- [48] J. J. Worthington, B. I. Czajkowska, A. C. Melton, and M. A. Travis, "Intestinal dendritic cells specialize to activate transforming growth factor- β and induce Foxp3+ regulatory T cells via integrin $\alpha\upsilon\beta$ 8," *Gastroenterology*, vol. 141, no. 5, pp. 1802–1812, 2011.
- [49] M. Iwata, A. Hirakiyama, Y. Eshima, H. Kagechika, C. Kato, and S. Y. Song, "Retinoic acid imprints gut-homing specificity on T cells," *Immunity*, vol. 21, no. 4, pp. 527–538, 2004.
- [50] B. Johansson-Lindbom, M. Svensson, O. Pabst, C. Palmqvist, G. Marquez, R. Förster, and W. W. Agace, "Functional specialization of gut CD103+ dendritic cells in the regulation of tissue-selective T cell homing," *The Journal of Experimental Medicine*, vol. 202, no. 8, pp. 1063–1073, 2005.
- [51] D. Esterházy, J. Loschko, M. London, V. Jove, T. Y. Oliveira, and D. Mucida, "Classical dendritic cells are required for dietary antigen-mediated induction of peripheral Treg cells and tolerance," *Nature Immunology*, vol. 20, no. August 2015, 2016.

- [52] I. I. Ivanov, R. d. L. Frutos, N. Manel, K. Yoshinaga, D. B. Rifkin, R. B. Sartor, B. B. Finlay, and D. R. Littman, “Specific Microbiota Direct the Differentiation of IL-17-Producing T-Helper Cells in the Mucosa of the Small Intestine,” *Cell Host and Microbe*, vol. 4, no. 4, pp. 337–349, 2008.
- [53] A. N. Hegazy, N. R. West, M. J. Stubbington, E. Wendt, K. I. Suijker, A. Datsi, S. This, C. Danne, S. Campion, S. H. Duncan, B. M. Owens, H. H. Uhlig, A. McMichael, A. Bergthaler, S. A. Teichmann, S. Keshav, and F. Powrie, “Circulating and Tissue-Resident CD4⁺ T Cells With Reactivity to Intestinal Microbiota Are Abundant in Healthy Individuals and Function Is Altered During Inflammation,” *Gastroenterology*, vol. 153, no. 5, pp. 1320–1337.e16, 2017.
- [54] K. L. Edelblum, G. Sharon, G. Singh, M. A. Odenwald, A. Sailer, S. Cao, S. Ravens, I. Thomsen, K. El Bissati, R. McLeod, C. Dong, S. Gurbuxani, I. Prinz, S. K. Mazmanian, and J. R. Turner, “The Microbiome Activates CD4 T-cell-mediated Immunity to Compensate for Increased Intestinal Permeability,” *Cmgh*, vol. 4, no. 2, pp. 285–297, 2017.
- [55] H. Kayama, Y. Ueda, Y. Sawa, S. G. Jeon, J. S. Ma, R. Okumura, A. Kubo, M. Ishii, T. Okazaki, M. Murakami, M. Yamamoto, H. Yagita, and K. Takeda, “Intestinal CX3C chemokine receptor 1^{high} (CX3CR1^{high}) myeloid cells prevent T-cell-dependent colitis,” *Proceedings of the National Academy of Sciences*, vol. 109, no. 13, pp. 5010–5015, 2012.
- [56] G. Monteleone, A. Kumberova, N. M. Croft, C. Mckenzie, H. W. Steer, and T. T. Macdonald, “Blocking Smad7 restores TGF- β 1 signaling in chronic inflammatory bowel disease,” *Journal of Clinical Investigation*, vol. 108, no. 4, pp. 601–609, 2001.
- [57] I. S. Hansen, L. Krabbendam, J. H. Bernink, F. Loayza-Puch, W. Hoepel, J. A. Van Burgsteden, E. C. Kuijper, C. J. Buskens, W. A. Bemelman, S. A. Zaat, R. Agami, G. Vidarsson, G. R. Van Den Brink, E. C. De Jong, M. E. Wildenberg, D. L. Baeten,

- B. Everts, and J. Den Dunnen, “Fc α RI co-stimulation converts human intestinal CD103+ dendritic cells into pro-inflammatory cells through glycolytic reprogramming,” *Nature Communications*, vol. 9, no. 1, 2018.
- [58] C. van Kooten and J. Banchereaut, “Functions of CD40 on B cells , dendritic cells and other cells,” *Current opinion in immunology*, vol. 9, pp. 330–337, 1997.
- [59] J. Banchereau, F. Bazan, D. Blanchard, F. Briè, J. P. Galizzi, C. van Kooten, Y. J. Liu, F. Rousset, and S. Saeland, “The CD40 Antigen and its Ligand,” *Annual Review of Immunology*, vol. 12, no. 1, pp. 881–926, 1994.
- [60] I. S. Grewal and R. A. Flavell, “CD40 and CD154 in Cell-Mediated Immunity,” *Annual Review of Immunology*, vol. 16, no. 1, pp. 111–135, 1998.
- [61] V. Henn, J. R. Slupsky, M. Gräfe, I. Anagnostopoulos, R. Förster, G. Müller-Berghaus, and R. A. Kroczeck, “CD40 ligand on activated platelets triggers an inflammatory reaction of endothelial cells,” *Nature*, vol. 391, pp. 591–594, 1998.
- [62] Z. Liu, S. Colpaert, D. H. GR, A. Kasran, M. Boer, P. Rutgeerts, K. Geboes, and J. L. Ceuppens, “Hyperexpression of CD40 ligand (CD154) in inflammatory bowel disease and its contribution to pathogenic cytokine production,” *J Immunol*, vol. 163, no. 7, pp. 4049–4057, 1999.
- [63] S. Danese, J. A. Katz, S. Saibeni, A. Papa, G. A, M. Vecchi, and C. Fiocchi, “Activated platelets are the source of elevated levels of soluble CD40 ligand in the circulation of inflammatory bowel disease patients,” *Gut*, vol. 52, pp. 1435–1441, 2003.
- [64] O. Ludwiczek, A. Kaser, and H. Tilg, “Plasma levels of soluble CD40 ligand are elevated in inflammatory bowel diseases,” *International journal of colorectal disease*, vol. 18, no. 2, pp. 142–7, 2003.
- [65] S. Danese, M. Sans, and C. Fiocchi, “The CD40/CD40L costimulatory pathway in inflammatory bowel disease,” *Gut*, vol. 53, no. 7, pp. 1035–1043, 2004.

- [66] A. L. Hart, H. O. Al-Hassi, R. J. Rigby, S. J. Bell, A. V. Emmanuel, S. C. Knight, M. A. Kamm, and A. J. Stagg, "Characteristics of intestinal dendritic cells in inflammatory bowel diseases," *Gastroenterology*, vol. 129, no. 1, pp. 50–65, 2005.
- [67] A. Kasran, L. Boon, C. H. Wortel, R. A. Van Hogezaand, S. Schreiber, E. Goldin, M. D. Boer, K. Geboes, P. Rutgeerts, and J. L. Ceuppens, "Safety and tolerability of antagonist anti-human CD40 Mab ch5D12 in patients with moderate to severe Crohn 's disease," *Aliment Pharmacol Ther*, vol. 22, pp. 111–122, 2005.
- [68] C. Caux, C. Massacrier, B. Vanbervliet, B. Dubois, C. Van Kooten, I. Durand, and J. Banchereau, "Activation of human dendritic cells through CD40 cross-linking," *Journal of Experimental Medicine*, vol. 180, no. 4, pp. 1263–1272, 1994.
- [69] L. M. Pinchuk, P. S. Polacino, M. B. Agy, S. J. Klaus, and E. A. Clark, "The role of CD40 and CD80 accessory cell molecules in dendritic cell-dependent HIV-1 infection," *Immunity*, vol. 1, no. 4, pp. 317–325, 1994.
- [70] B. F. Sallusto and A. Lanzavecchia, "Efficient Presentation of Soluble Antigen by Cultured Human Dendritic Cells Is Maintained by Granulocyte/Macrophage Colony-stimulating Factor Plus Interleukin 4 and Downregulated by Tumor Necrosis Factor alpha," *Journal of Experimental Medicine*, vol. 179, no. April, pp. 1109–1118, 1994.
- [71] M. Cella, D. Scheidegger, K. Palmer-lehmann, P. Lane, A. Lanzavecchia, and G. Alber, "Ligation of CD40 on Dendritic Cells Triggers Production of High Levels of Interleukin-12 and Enhances T Cell Stimulatory Capacity: T-T Help via APC Activation," *Journal of Experimental Medicine*, vol. 184, no. August, pp. 747–752, 1996.
- [72] L. Bonifaz, D. Bonnyay, K. Mahnke, M. Rivera, M. C. Nussenzweig, and R. M. Steinman, "Efficient targeting of protein antigen to the dendritic cell receptor DEC-205 in the steady state leads to antigen presentation on major histocompatibility complex class I products and peripheral CD8+ T cell tolerance.," *The Journal of experimental medicine*, vol. 196, no. 12, pp. 1627–38, 2002.

- [73] O. Schulz, A. D. Edwards, M. Schito, J. Aliberti, S. Manickasingham, A. Sher, and C. Reis e Sousa, "CD40 triggering of heterodimeric IL-12 p70 production by dendritic cells in vivo requires a microbial priming signal," *Immunity*, vol. 13, no. 4, pp. 453–462, 2000.
- [74] P. J. Sanchez, J. A. McWilliams, C. Haluszczak, H. Yagita, and R. M. Kedl, "Combined TLR/CD40 Stimulation Mediates Potent Cellular Immunity by Regulating Dendritic Cell Expression of CD70 In Vivo," *The Journal of Immunology*, vol. 178, no. 3, pp. 1564–1572, 2007.
- [75] O. Annacker, J. L. Coombes, V. Malmstrom, H. H. Uhlig, T. Bourne, B. Johansson-Lindbom, W. W. Agace, C. M. Parker, and F. Powrie, "Essential role for CD103 in the T cell-mediated regulation of experimental colitis," *The Journal of Experimental Medicine*, vol. 202, no. 8, pp. 1051–1061, 2005.
- [76] K. Kimura, H. Moriwaki, M. Nagaki, M. Saio, Y. Nakamoto, M. Naito, K. Kuwata, and F. V. Chisari, "Pathogenic role of B cells in anti-CD40-induced necroinflammatory liver disease," *American Journal of Pathology*, vol. 168, no. 3, pp. 786–795, 2006.
- [77] C. Barthels, A. Ogrinc, V. Steyer, S. Meier, F. Simon, M. Wimmer, A. Blutke, T. Straub, U. Zimmer-Strobl, E. Lutgens, P. Marconi, C. Ohnmacht, D. Garzetti, B. Stecher, and T. Brocker, "CD40-signalling abrogates induction of ROR γ t⁺ Treg cells by intestinal CD103⁺ DCs and causes fatal colitis," *Nature Communications*, vol. 8, p. 14715, 2017.
- [78] B. R. Pires, R. C. Silva, G. M. Ferreira, and E. Abdelhay, "NF-kappaB: Two sides of the same coin," *Genes*, vol. 9, no. 1, 2018.
- [79] C. Hömig-Hölzel, C. Hojer, J. Rastelli, S. Casola, L. J. Strobl, M. Werner, L. Quintanilla-Martinez, A. Gewies, J. Ruland, K. Rajewsky, and U. Zimmer-strobl, "Constitutive CD40 signaling in B cells selectively activates the noncanonical NF-

- kB pathway and promotes lymphomagenesis,” *The Journal of experimental medicine*, vol. 205, no. 6, pp. 1317–1329, 2008.
- [80] S. C. Sun, “The non-canonical NF- κ B pathway in immunity and inflammation,” *Nature Reviews Immunology*, vol. 17, no. 9, pp. 545–558, 2017.
- [81] H. J. Coope, P. G. Atkinson, B. Huhse, M. Belich, J. Janzen, M. J. Holman, G. G. Klaus, L. H. Johnston, and S. C. Ley, “CD40 regulates the processing of NF- κ B2 p100 to p52,” *EMBO Journal*, vol. 21, no. 20, pp. 5375–5385, 2002.
- [82] E. F. Lind, C. L. Ahonen, A. Wasiuk, Y. Kosaka, B. Becher, K. A. Bennett, and R. J. Noelle, “Dendritic Cells Require the NF- κ B2 Pathway for Cross-Presentation of Soluble Antigens,” *The Journal of Immunology*, vol. 181, no. 1, pp. 354–363, 2014.
- [83] A. K. Katakam, H. Brightbill, C. Franci, C. Kung, V. Nunez, C. Jones, I. Peng, S. Jeet, L. C. Wu, I. Mellman, L. Delamarre, and C. D. Austin, “Dendritic cells require NIK for CD40-dependent cross-priming of CD8+ T cells,” *Proceedings of the National Academy of Sciences*, vol. 112, no. 47, pp. 14664–14669, 2015.
- [84] S. W. Tas, M. J. Vervoordeldonk, N. Hajji, J. H. N. Schuitemaker, K. F. V. D. Sluijs, M. J. May, S. Ghosh, M. L. Kapsenberg, P. P. Tak, and E. C. de Jong, “Noncanonical NF- κ B signaling in dendritic cells is required for indoleamine 2,3-dioxygenase (IDO) induction and immune regulation,” *Blood*, vol. 110, no. 5, pp. 1540–1549, 2007.
- [85] S. Gill, M. Pop, R. T. DeBoy, P. B. Eckburg, P. J. Turnbaugh, B. S. Samuel, J. I. Gordon, D. A. Relman, C. M. Fraser-Liggett, and K. E. Nelson, “Metagenomic analysis of the human distal gut microbiome,” *Science*, vol. 312, no. 5778, pp. 1355–1359, 2006.
- [86] T. Yatsunenko, F. E. Rey, M. J. Manary, I. Trehan, M. G. Dominguez-Bello, M. Contreras, M. Magris, G. Hidalgo, R. N. Baldassano, A. P. Anokhin, A. C. Heath, B. Warner, J. Reeder, J. Kuczynski, J. G. Caporaso, C. A. Lozupone, C. Lauber, J. C. Clemente,

- D. Knights, R. Knight, and J. I. Gordon, "Human gut microbiome viewed across age and geography," *Nature*, vol. 486, no. 7402, pp. 222–228, 2012.
- [87] The Human Microbiome Project Consortium, "Structure, function and diversity of the healthy human microbiome," *Nature*, vol. 486, no. 7402, pp. 207–214, 2012.
- [88] The Human Microbiome Project Consortium, "A framework for human microbiome research," *Nature*, vol. 486, no. 7402, pp. 215–221, 2012.
- [89] I. Sekirov, S. L. Russell, L. C. M. Antunes, and B. B. Finlay, "Gut Microbiota in Health and Disease," *Physiol Rev*, vol. 90, pp. 859–904, 2010.
- [90] W. Dieterich, M. Schink, and Y. Zopf, "Microbiota in the Gastrointestinal Tract," *Medical Sciences*, vol. 6, no. 4, p. 116, 2018.
- [91] R. E. Ley, D. A. Peterson, and J. I. Gordon, "Ecological and evolutionary forces shaping microbial diversity in the human intestine," *Cell*, vol. 124, no. 4, pp. 837–848, 2006.
- [92] F. Backhed, R. Ley, J. Sonnenburg, D. Peterson, and J. Gordon, "Host-Bacterial Mutualism in the Human Intestine - supplemental materials," *Science*, vol. 307, no. 5717, pp. 1915–1920, 2005.
- [93] A. J. Macpherson and N. L. Harris, "Interactions between commensal bacteria and the chicken immune system," *Nature Reviews Immunology*, vol. 4, no. 6, pp. 478–85, 2004.
- [94] J. G. LeBlanc, F. Chain, R. Martín, L. G. Bermúdez-Humarán, S. Courau, and P. Langel, "Beneficial effects on host energy metabolism of short-chain fatty acids and vitamins produced by commensal and probiotic bacteria," *Microbial Cell Factories*, vol. 16, no. 1, pp. 1–10, 2017.
- [95] M. A. Garcia, W. J. Nelson, and N. Chavez, "Cell-Cell Junctions Organize Structural and Signaling Networks To Regulate Epithelial Tissue Homeostasis," *Cold Spring Harbor Perspect Biol.*, vol. 10, no. 4, 2018.

-
- [96] T. Pelaseyed, J. H. Bergström, J. K. Gustafsson, A. Ermund, G. M. H. Birchenough, A. Schütte, S. van der Post, F. Svensson, A. M. Rodríguez-Piñeiro, E. E. L. Nyström, C. Wising, M. E. V. Johansson, and G. C. Hansson, “The mucus and mucins of the goblet cells and enterocytes provide the first defense line of the gastrointestinal tract and interact with the immune system,” *Immunological Reviews*, vol. 260, no. 1, pp. 8–20, 2014.
- [97] J. D. Forbes, G. Van Domselaar, and C. N. Bernstein, “The gut microbiota in immune-mediated inflammatory diseases,” *Frontiers in Microbiology*, vol. 7, no. JUL, pp. 1–18, 2016.
- [98] K. A. Knoop and R. D. Newberry, “Goblet cells: multifaceted players in immunity at mucosal surfaces,” *Mucosal Immunology*, vol. 11, no. 6, pp. 1551–1557, 2018.
- [99] J. R. McDole, L. W. Wheeler, K. G. McDonald, B. Wang, V. Konjufca, K. A. Knoop, R. D. Newberry, and M. J. Miller, “Goblet cells deliver luminal antigen to CD103+ DCs in the small intestine,” *Nature*, vol. 483, no. 7389, pp. 345–349, 2012.
- [100] R. N. Cunliffe and Y. R. Mahida, “Expression and regulation of antimicrobial peptides in the gastrointestinal tract,” *Journal of Leukocyte Biology*, vol. 75, no. 1, pp. 49–58, 2004.
- [101] H. Seno, H. Miyoshi, S. L. Brown, M. J. Geske, M. Colonna, and T. S. Stappenbeck, “Efficient colonic mucosal wound repair requires Trem2 signaling,” *PNAS*, vol. 106, no. 1, pp. 256–261, 2009.
- [102] F. Heller, P. Florian, C. Bojarski, J. Richter, M. Christ, B. Hillenbrand, J. Mankertz, A. H. Gitter, N. Bürgel, M. Fromm, M. Zeitz, I. Fuss, W. Strober, and J. D. Schulzke, “Interleukin-13 is the key effector Th2 cytokine in ulcerative colitis that affects epithelial tight junctions, apoptosis, and cell restitution,” *Gastroenterology*, vol. 129, no. 2, pp. 550–64, 2005.

-
- [103] C. Papista, L. Berthelot, and R. C. Monteiro, “Dysfunctions of the Iga system: A common link between intestinal and renal diseases,” *Cellular and Molecular Immunology*, vol. 8, no. 2, pp. 126–134, 2011.
- [104] P. N. Boyaka, “Inducing mucosal IgA: A challenge for vaccine adjuvants and delivery systems,” *J Immunol.*, vol. 199, no. 1, pp. 9–16, 2017.
- [105] C. Gutzeit, G. Magri, and A. Cerutti, “Intestinal IgA production and its role in host-microbe interactions,” *Immunological Reviews*, vol. 260, no. 1, pp. 76–85, 2014.
- [106] S. Fagarasan and M. Muramatsu, “Critical Roles of Activation-Induced Cytidine Deaminase in the Homeostasis of Gut Flora | Science,” *Science*, vol. 298, pp. 1424–1428, 2002.
- [107] M. Wei, R. Shinkura, Y. Doi, M. Maruya, S. Fagarasan, and T. Honjo, “Mice carrying a knock-in mutation of Aicda resulting in a defect in somatic hypermutation have impaired gut homeostasis and compromised mucosal defense,” *Nature Immunology*, vol. 12, no. 3, pp. 264–270, 2011.
- [108] M. C. Moreau, R. Ducluzeau, D. Guy-Grand, and M. C. Muller, “Increase in the population of duodenal immunoglobulin A plasmocytes in axenic mice associated with different living or dead bacterial strains of intestinal origin,” *Infection and Immunity*, vol. 21, no. 2, pp. 532–539, 1978.
- [109] D. A. Peterson, N. P. McNulty, J. L. Guruge, and J. I. Gordon, “IgA Response to Symbiotic Bacteria as a Mediator of Gut Homeostasis,” *Cell Host and Microbe*, vol. 2, no. 5, pp. 328–339, 2007.
- [110] S. Boullier, M. Tanguy, K. A. Kadaoui, C. Caubet, P. Sansonetti, B. Corthesy, and A. Phalipon, “Secretory IgA-Mediated Neutralization of *Shigella flexneri* Prevents Intestinal Tissue Destruction by Down-Regulating Inflammatory Circuits,” *J Immunol*, vol. 183, no. 9, pp. 5879–5885, 2009.

- [111] J. J. Bunker and A. Bendelac, "IgA Responses to Microbiota," *Immunity*, vol. 49, no. 2, pp. 211–224, 2018.
- [112] A. Cerutti, "The regulation of IgA class switching.," *Nature reviews. Immunology*, vol. 8, pp. 421–34, jun 2008.
- [113] S. Hapfelmeier, M. a. E. Lawson, E. Slack, J. K. Kirundi, M. Stoel, M. Heikenwalder, J. Cahenzli, Y. Velykoredko, M. L. Balmer, K. Endt, M. B. Geuking, R. Curtiss, K. D. McCoy, and A. J. Macpherson, "Reversible Microbial Colonization of Germ-Free Mice Reveals the Dynamics of IgA Immune Responses," *Science*, vol. 328, pp. 1705–09, 2010.
- [114] O. L. Wijburg, T. K. Uren, K. Simpfendorfer, F.-E. Johansen, P. Brandtzaeg, and R. A. Strugnell, "Innate secretory antibodies protect against natural *Salmonella typhimurium* infection," *The Journal of Experimental Medicine*, vol. 203, no. 1, pp. 21–26, 2006.
- [115] N. W. Palm, M. R. D. Zoete, T. W. Cullen, N. A. Barry, J. Stefanowski, L. Hao, P. H. Degnan, J. Hu, I. Peter, W. Zhang, E. Ruggiero, J. H. Cho, A. L. Goodman, and R. A. Flavell, "Immunoglobulin A Coating Identifies Colitogenic Bacteria in Inflammatory Bowel Disease," *Cell*, 2014.
- [116] L. A. Van Der Waaij, F. G. Kroese, A. Visser, G. F. Nelis, B. D. Westerveld, P. L. Jansen, and J. O. Hunter, "Immunoglobulin coating of faecal bacteria in inflammatory," *European Journal of Gastroenterology and Hepatology*, vol. 16, no. 7, pp. 669–674, 2004.
- [117] M. Viladomiu, C. Kivolowitz, A. Abdulhamid, B. Dogan, D. Victorio, J. Castellanos, V. Woo, F. Teng, N. Tran, A. Szczesnak, C. Chai, M. Kim, G. Diehl, N. Ajami, J. Petrosino, X. Zhou, S. Schwartzman, L. Mandl, M. Abramowitz, V. Jacob, B. Bosworth, A. Steinlauf, E. Scherl, H.-J. Wu, and K. Simpson, "IgA-coated *E. Coli* enriched in Crohn's disease spondyloarthritis promote TH17-dependent inflammation," *Science Translational Medicine*, vol. 9, no. 376, p. eaaf9655, 2017.
- [118] M. A. Koch, G. L. Reiner, K. A. Lugo, L. S. Kreuk, A. G. Stanbery, E. Ansaldo, T. D.

- Seher, W. B. Ludington, and G. M. Barton, “Maternal IgG and IgA Antibodies Dampen Mucosal T Helper Cell Responses in Early Life,” *Cell*, vol. 165, no. 4, pp. 827–841, 2016.
- [119] M. Y. Zeng, D. Cisalpino, S. Varadarajan, J. Hellman, H. S. Warren, M. Cascalho, N. Inohara, and G. Núñez, “Gut Microbiota-Induced Immunoglobulin G Controls Systemic Infection by Symbiotic Bacteria and Pathogens,” *Immunity*, vol. 44, no. 3, pp. 647–658, 2016.
- [120] J. R. Wilmore, B. T. Gaudette, D. Gomez Atria, T. Hashemi, D. D. Jones, C. A. Gardner, S. D. Cole, A. M. Misic, D. P. Beiting, and D. Allman, “Commensal Microbes Induce Serum IgA Responses that Protect against Polymicrobial Sepsis,” *Cell Host and Microbe*, vol. 23, no. 3, pp. 302–311.e3, 2018.
- [121] K. Mitsuyama, M. Niwa, H. Takedatsu, H. Yamasaki, K. Kuwaki, S. Yoshioka, R. Yamauchi, S. Fukunaga, and T. Torimura, “Antibody markers in the diagnosis of inflammatory bowel disease,” *World Journal of Gastroenterology*, vol. 22, no. 3, pp. 1304–1310, 2016.
- [122] C. J. Landers, O. Cohavy, R. Misra, H. Yang, Y. C. Lin, J. Braun, and S. R. Targan, “Selected loss of tolerance evidenced by Crohn’s disease-associated immune responses to auto- and microbial antigens,” *Gastroenterology*, vol. 123, no. 3, pp. 689–699, 2002.
- [123] M. J. Lodes, Y. Cong, C. O. Elson, R. Mohamath, C. J. Landers, S. R. Targan, M. Fort, and R. M. Hershberg, “Bacterial flagellin is a dominant antigen in Crohn disease,” *Journal of Clinical Investigation*, vol. 113, no. 9, pp. 1296–1306, 2004.
- [124] S. V. Sitaraman, J.-M. Klapproth, D. A. Moore, C. Landers, S. Targan, I. R. Williams, and A. T. Gewirtz, “Elevated flagellin-specific immunoglobulins in Crohn’s disease,” *American Journal of Physiology-Gastrointestinal and Liver Physiology*, vol. 288, no. 2, pp. G403–G406, 2005.
- [125] R. Iversen, O. Snir, M. Stensland, J. E. Kroll, Ø. Steinsbø, I. R. Korponay-Szabó,

- K. E. Lundin, G. A. de Souza, and L. M. Sollid, "Strong Clonal Relatedness between Serum and Gut IgA despite Different Plasma Cell Origins," *Cell Reports*, vol. 20, no. 10, pp. 2357–2367, 2017.
- [126] J. Zhu, H. Yamane, and W. E. Paul, "NIH Public Access: Differentiation of Effector CD4 T Cell Populations*," *Annu Rev Immunol*, vol. 28, no. 1, pp. 445–489, 2010.
- [127] S. J. Szabo, S. T. Kim, G. L. Costa, X. Zhang, C. G. Fathman, and L. H. Glimcher, "A novel transcription factor, T-bet, directs Th1 lineage commitment," *Cell*, vol. 100, no. 6, pp. 655–669, 2000.
- [128] V. K. Kuchroo, A. C. Anderson, H. Waldner, M. Munder, E. Bettelli, and L. B. Nicholson, "T Cell response in Experimental Autoimmune Encephalomyelitis (EAE): Role of Self and Cross-Reactive Antigens in Shaping, Tuning, and Regulating the Autopathogenic T Cell Repertoire," *Annual Review of Immunology*, vol. 20, no. 1, pp. 101–123, 2002.
- [129] S. J. Simpson, S. Shah, M. Comiskey, Y. P. de Jong, B. Wang, E. Mizoguchi, A. K. Bhan, and C. Terhorst, "T Cell-mediated Pathology in Two Models of Experimental Colitis Depends Predominantly on the Interleukin 12/Signal Transducer and Activator of Transcription (Stat)-4 Pathway, but Is Not Conditional on Interferon γ Expression by T Cells," *The Journal of Experimental Medicine*, vol. 187, no. 8, pp. 1225–1234, 1998.
- [130] M. F. Neurath, B. Weigmann, S. Finotto, J. Glickman, E. Nieuwenhuis, H. Iijima, A. Mizoguchi, E. Mizoguchi, J. Mudter, P. R. Galle, A. Bhan, F. Autschbach, B. M. Sullivan, S. J. Szabo, L. H. Glimcher, and R. S. Blumberg, "The transcription factor T-bet regulates mucosal T cell activation in experimental colitis and Crohn's disease," *The Journal of experimental medicine*, vol. 195, no. 9, pp. 1129–43, 2002.
- [131] M. Veldhoen, R. J. Hocking, C. J. Atkins, R. M. Locksley, and B. Stockinger, "TGF β

- in the context of an inflammatory cytokine milieu supports de novo differentiation of IL-17-producing T cells,” *Immunity*, vol. 24, no. 2, pp. 179–189, 2006.
- [132] P. R. Burkett, G. Meyer, K. Vijay, J. C. Invest, P. R. Burkett, G. Meyer, and V. K. Kuchroo, “Pouring fuel on the fire: Th17 cells , the environment , and autoimmunity,” vol. 125, no. 6, pp. 2211–2219, 2015.
- [133] Y. Lee, A. Awasthi, N. Yosef, F. J. Quintana, S. Xiao, A. Peters, C. Wu, M. Kleinewitfeld, S. Kunder, D. A. Hafler, R. A. Sobel, A. Regev, and V. K. Kuchroo, “Induction and molecular signature of pathogenic Th17 cells,” *Nature Immunology*, vol. 13, no. 10, pp. 991–999, 2012.
- [134] C. L. Langrish, Y. Chen, W. M. Blumenschein, J. Mattson, B. Basham, J. D. Sedgwick, T. McClanahan, R. A. Kastelein, and D. J. Cua, “IL-23 drives a pathogenic T cell population that induces autoimmune inflammation,” *The Journal of Experimental Medicine*, vol. 201, no. 2, pp. 233–240, 2005.
- [135] K. Ghoreschi, A. Laurence, X. P. Yang, C. M. Tato, M. J. McGeachy, J. E. Konkel, H. L. Ramos, L. Wei, T. S. Davidson, N. Bouladoux, J. R. Grainger, Q. Chen, Y. Kanno, W. T. Watford, H. W. Sun, G. Eberl, E. M. Shevach, Y. Belkaid, D. J. Cua, W. Chen, and J. J. O’Shea, “Generation of pathogenic Th17 cells in the absence of TGF- β 2 signalling,” *Nature*, vol. 467, no. 7318, pp. 967–971, 2010.
- [136] K. Hirota, J. H. Duarte, M. Veldhoen, E. Hornsby, Y. Li, D. J. Cua, H. Ahlfors, C. Wilhelm, M. Tolaini, U. Menzel, A. Garefalaki, A. J. Potocnik, and B. Stockinger, “Fate mapping of IL-17-producing T cells in inflammatory responses,” *Nature Immunology*, vol. 12, no. 3, pp. 255–263, 2011.
- [137] T. Korn, E. Bettelli, M. Oukka, and V. K. Kuchroo, “IL-17 and Th17 Cells.,” *Annual review of immunology*, vol. 27, pp. 485–517, 2009.

- [138] C. M. Wilke, K. Bishop, D. Fox, and W. Zou, “Deciphering the role of Th17 cells in human disease,” *Trends in Immunology*, vol. 32, no. 12, pp. 603–611, 2011.
- [139] I. I. Ivanov, K. Atarashi, N. Manel, E. L. Brodie, T. Shima, U. Karaoz, D. Wei, K. C. Goldfarb, C. A. Santee, S. V. Lynch, T. Tanoue, A. Imaoka, K. Itoh, K. Takeda, Y. Umesaki, K. Honda, and D. R. Littman, “Induction of intestinal Th17 cells by segmented filamentous bacteria,” *Cell*, vol. 139, no. 3, pp. 485–98, 2009.
- [140] C. E. Zielinski, F. Mele, D. Aschenbrenner, D. Jarrossay, F. Ronchi, M. Gattorno, S. Monticelli, A. Lanzavecchia, and F. Sallusto, “Pathogen-induced human TH17 cells produce IFN- γ or IL-10 and are regulated by IL-1 β ,” *Nature*, vol. 484, no. 7395, pp. 514–518, 2012.
- [141] P. M. Smith, M. R. Howitt, N. Panikov, M. Michaud, C. A. Gallini, M. Bohlooly-y, J. N. Glickman, and W. S. Garrett, “The Microbial Metabolites, Short-Chain Fatty Acids, Regulate Colonic Treg Cell Homeostasis,” *Science*, vol. 341, pp. 569–574, 2013.
- [142] K. Atarashi, T. Tanoue, T. Shima, A. Imaoka, T. Kuwahara, Y. Momose, G. Cheng, S. Yamasaki, T. Saito, Y. Ohba, T. Taniguchi, K. Takeda, S. Hori, I. I. Ivanov, Y. Umesaki, K. Itoh, and K. Honda, “Induction of colonic regulatory T cells by indigenous *Clostridium* species,” *Science*, vol. 331, pp. 337–341, 2011.
- [143] J. L. Round and S. K. Mazmanian, “Inducible Foxp3+regulatory T-cell development by a commensal bacterium of the intestinal microbiota: Commentary,” *PNAS*, vol. 107, no. 27, pp. 12204–12209, 2010.
- [144] R. B. Sartor, “Mechanisms of disease: Pathogenesis of Crohn’s disease and ulcerative colitis,” *Nature Clinical Practice Gastroenterology and Hepatology*, vol. 3, no. 7, pp. 390–407, 2006.
- [145] M. Zeng, N. Inohara, and G. Nuñez, “Mechanisms of inflammation-driven bacterial dysbiosis in the gut,” *Mucosal immunology*, vol. 10, no. 1, pp. 18–26, 2017.

- [146] J. Qin, R. Li, J. Raes, M. Arumugam, S. Burgdorf, C. Manichanh, T. Nielsen, N. Pons, T. Yamada, D. R. Mende, J. Li, J. Xu, S. Li, D. Li, J. Cao, B. Wang, H. Liang, H. Zheng, Y. Xie, J. Tap, P. Lepage, M. Bertalan, J.-m. Batto, T. Hansen, D. L. Paslier, A. Linneberg, H. B. Nielsen, E. Pelletier, P. Renault, Y. Zhou, Y. Li, X. Zhang, S. Li, N. Qin, H. Yang, J. Wang, S. Brunak, J. Doré, F. Guarner, K. Kristiansen, O. Pedersen, J. Parkhill, J. Weissenbach, M. Consortium, P. Bork, S. D. Ehrlich, and J. Wang, “A human gut microbial gene catalog established by metagenomic sequencing,” *Nature*, vol. 464, no. 7285, pp. 59–65, 2010.
- [147] D. Gevers, S. Kugathasan, L. A. Denson, Y. Vázquez-Baeza, W. Van Treuren, B. Ren, E. Schwager, D. Knights, S. J. Song, M. Yassour, X. C. Morgan, A. D. Kostic, C. Luo, A. González, D. McDonald, Y. Haberman, T. Walters, S. Baker, J. Rosh, M. Stephens, M. Heyman, J. Markowitz, R. Baldassano, A. Griffiths, F. Sylvester, D. Mack, S. Kim, W. Crandall, J. Hyams, C. Huttenhower, R. Knight, and R. J. Xavier, “The treatment-naive microbiome in new-onset Crohn’s disease,” *Cell Host and Microbe*, vol. 15, no. 3, pp. 382–392, 2014.
- [148] H. M. Wexler, “Bacteroides: The good, the bad, and the nitty-gritty,” *Clinical Microbiology Reviews*, vol. 20, no. 4, pp. 593–621, 2007.
- [149] M. T. Whary and J. G. Fox, “Natural and Experimental Helicobacter Infections,” *Comparative Medicine*, vol. 54, no. 2, pp. 128–158, 2004.
- [150] B. J. Marshall and J. R. Warren, “Unidentified Curved Bacilli in the Stomach of Patients With Gastritis and Peptic Ulceration,” *The Lancet*, vol. 323, no. 8390, pp. 1311–1315, 1984.
- [151] J. G. Fox, F. E. Dewehirst, J. G. Tully, B. J. Paster, L. Yan, N. S. Taylor, M. J. Collins, P. L. Gorelick, and J. M. Ward, “*Helicobacter hepaticus* sp. nov., a Microaerophilic Bacterium Isolated from Livers and Intestinal Mucosal Scrapings from Mice,” *Journal of Clinical Microbiology*, vol. 32, no. 5, pp. 1238–1245, 1994.

- [152] B. Shames, J. G. Fox, F. Dewhirst, L. Yan, Z. Shen, and N. S. Taylor, "Identification of widespread *Helicobacter hepaticus* infection in feces in commercial mouse colonies by culture and PCR assay," *Journal of Clinical Microbiology*, vol. 33, no. 11, pp. 2968–2972, 1995.
- [153] N. S. Taylor, S. Xu, P. Nambiar, F. E. Dewhirst, and J. G. Fox, "Enterohepatic *Helicobacter* Species Are Prevalent in Mice from Commercial and Academic Institutions in Asia, Europe, and North America," *Journal of Clinical Microbiology*, vol. 45, no. 7, pp. 2166–2172, 2007.
- [154] J. G. Fox, X. Li, L. Yan, R. J. Cahill, R. Hurley, R. Lewis, and J. C. Murphy, "Chronic proliferative hepatitis in A/JCr mice associated with persistent *Helicobacter hepaticus* infection: A model of helicobacter-induced carcinogenesis," *Infection and Immunity*, vol. 64, no. 5, pp. 1548–1558, 1996.
- [155] M. Ihrig, M. D. Schrenzel, and J. G. Fox, "Differential susceptibility to hepatic inflammation and proliferation in AXB recombinant inbred mice chronically infected with *Helicobacter hepaticus*," *American Journal of Pathology*, vol. 155, no. 2, pp. 571–582, 1999.
- [156] R. J. Cahill, C. J. Foltz, J. G. Fox, C. A. Dangler, F. Powrie, and D. B. Schauer, "Inflammatory bowel disease: An immunity-mediated condition triggered by bacterial infection with *Helicobacter hepaticus*," *Infection and Immunity*, vol. 65, no. 8, pp. 3126–3131, 1997.
- [157] S. E. Erdman, T. Poutahidis, M. Tomczak, A. B. Rogers, K. Cormier, B. Plank, B. H. Horwitz, and J. G. Fox, "CD4⁺ CD25⁺ Regulatory T Lymphocytes Inhibit Microbially Induced Colon Cancer in Rag2-Deficient Mice," *American Journal Of Pathology*, vol. 162, no. 2, pp. 2079–2090, 2003.
- [158] A. Burich, R. Hershberg, K. Waggie, W. Zeng, T. Brabb, G. Westrich, J. L. Viney, and L. Maggio-Price, "Helicobacter-induced inflammatory bowel disease in IL-10- and T cell-

- deficient mice,” *American Journal of Physiology-Gastrointestinal and Liver Physiology*, vol. 281, no. 3, pp. G764–G778, 2001.
- [159] M. C. Kullberg, J. M. Ward, P. L. Gorelick, P. Caspar, S. Hieny, A. Cheever, D. Jankovic, and A. Sher, “*Helicobacter hepaticus* triggers colitis in specific-pathogen-free interleukin-10 (IL-10)-deficient mice through an IL-12-and gamma interferon-dependent mechanism,” *Infection and Immunity*, vol. 66, no. 11, pp. 5157–5166, 1998.
- [160] E. Y. Chin, C. A. Dangler, J. G. Fox, and D. B. Schauer, “*Helicobacter hepaticus* infection triggers inflammatory bowel disease in T cell receptor alphabeta mutant mice,” *Comp Med*, vol. 50, no. 6, pp. 586–594, 2000.
- [161] M. C. Kullberg, D. Jankovic, C. G. Feng, S. Hue, P. L. Gorelick, B. S. McKenzie, D. J. Cua, F. Powrie, A. W. Cheever, K. J. Maloy, and A. Sher, “IL-23 plays a key role in *Helicobacter hepaticus*-induced T cell-dependent colitis,” *The Journal of Experimental Medicine*, vol. 203, no. 11, pp. 2485–2494, 2006.
- [162] M. Xu, M. Pokrovskii, Y. Ding, R. Yi, C. Au, O. J. Harrison, C. Galan, Y. Belkaid, R. Bonneau, and D. R. Littman, “C-MAF-dependent regulatory T cells mediate immunological tolerance to a gut pathobiont,” *Nature*, vol. 554, no. 7692, pp. 373–377, 2018.
- [163] N. S. Taylor, J. G. Fox, and L. Yan, “In-vitro hepatotoxic factor in *Helicobacter hepaticus*, *H. Pylori* and other *Helicobacter* species,” *Journal of Medical Microbiology*, vol. 42, no. 1, pp. 48–52, 1995.
- [164] J. C. Ranford, A. R. Coates, and B. Henderson, “Chaperonins are cell-signalling proteins: the unfolding biology of molecular chaperones,” *Expert reviews in molecular medicine*, vol. 2, no. 8, pp. 1–17, 2000.
- [165] N. A. Ranson, H. E. White, and H. R. Saibil, “Chaperonins,” *Biochemical Journal*, vol. 333, pp. 233–242, 1998.

-
- [166] J. L. Feltham and L. M. Gierasch, “GroEL-Substrate Interactions: Minireview Molding the Fold, or Folding the Mold?,” *Cell*, vol. 100, pp. 193–196, 2000.
- [167] S. H. Kaufmann, U. Vath, J. E. Thole, J. D. Van Embden, and F. Emmrich, “Enumeration of T cells reactive with Mycobacterium tuberculosis organisms and specific for the recombinant mycobacterial 64-kDa protein,” *European Journal of Immunology*, vol. 17, no. 3, pp. 351–357, 1987.
- [168] J. M. Ward, R. E. Benveniste, C. H. Fox, J. K. Battles, M. A. Gonda, and J. G. Tully, “Autoimmunity in chronic active Helicobacter hepatitis of mice: Serum antibodies and expression of heat shock protein 70 in liver,” *American Journal of Pathology*, vol. 148, no. 2, pp. 509–517, 1996.
- [169] N. A. Nagalingam, C. J. Robinson, I. L. Bergin, K. A. Eaton, G. B. Huffnagle, and V. B. Young, “The effects of intestinal microbial community structure on disease manifestation in IL-10-/- mice infected with Helicobacter hepaticus,” *Microbiome*, pp. 1–15, 2013.
- [170] C. S. Beckwith, C. L. Franklin, R. R. Hook, C. L. Besch-williford, and L. K. Riley, “Fecal PCR Assay for Diagnosis of Helicobacter Infection in Laboratory Rodents,” *Microbiology*, vol. 35, no. 6, pp. 1620–1623, 1997.
- [171] C. L. Franklin, P. L. Gorelick, L. K. Riley, F. E. Dewhirst, R. S. Livingston, J. M. Ward, C. S. Beckwith, and J. G. Fox, “Helicobacter typhlonius sp. nov., a novel murine urease-negative Helicobacter species,” *Journal of Clinical Microbiology*, vol. 39, no. 11, pp. 3920–3926, 2001.
- [172] Z. Shen, J. G. Fox, F. E. Dewhirst, B. J. Paster, C. J. Foltz, L. Yan, B. Shames, and L. Perry, “Helicobacter rodentium sp. nov., a Urease-Negative Helicobacter Species Isolated from Laboratory Mice,” *International Journal of Systematic Bacteriology*, vol. 47, no. 3, pp. 627–634, 1997.
- [173] J. G. Fox, L. L. Yan, F. E. Dewhirst, B. J. Paster, B. Shames, J. C. Murphy, A. Hayward,

- J. C. Belcher, and E. N. Mendes, “*Helicobacter bilis* sp. nov., a novel *Helicobacter* species isolated from bile, livers, and intestines of aged, inbred mice,” *Journal of Clinical Microbiology*, vol. 33, no. 2, pp. 445–454, 1995.
- [174] M. L. Caton, M. R. Smith-Raska, and B. Reizis, “Notch-RBP-J signaling controls the homeostasis of CD8⁺ dendritic cells in the spleen,” *The Journal of Experimental Medicine*, vol. 204, no. 7, pp. 1653–1664, 2007.
- [175] P. Kusters, T. Seijkens, C. Bürger, B. Legein, H. Winkels, M. Gijbels, C. Barthels, R. Bennett, L. Beckers, D. Atzler, E. Biessen, T. Brocker, C. Weber, N. Gerdes, and E. Lutgens, “Constitutive CD40 Signaling in Dendritic Cells Limits Atherosclerosis by Provoking Inflammatory Bowel Disease and Ensuing Cholesterol Malabsorption,” *The American Journal of Pathology*, vol. 187, no. 12, pp. 2912–2919, 2017.
- [176] S. Rakoff-Nahoum, J. Paglino, F. Eslami-varzaneh, S. Edberg, and R. Medzhitov, “Recognition of Commensal Microflora by Toll-Like Receptors Is Required for Intestinal Homeostasis,” *Cell*, vol. 118, pp. 229–241, 2004.
- [177] I. R. Peters, E. L. Calvert, E. J. Hall, and M. J. Day, “Measurement of Immunoglobulin Concentrations in the Feces of Healthy Dogs,” *Clinical and Vaccine Immunology*, vol. 11, no. 5, pp. 841–848, 2004.
- [178] J. J. Kozich, S. L. Westcott, N. T. Baxter, S. K. Highlander, and P. D. Schloss, “Development of a dual-index sequencing strategy and curation pipeline for analyzing amplicon sequence data on the miseq illumina sequencing platform,” *Applied and Environmental Microbiology*, vol. 79, no. 17, pp. 5112–5120, 2013.
- [179] C. Ubeda, L. Lipuma, A. Gobourne, A. Viale, I. Leiner, M. Equinda, R. Khanin, and E. G. Pamer, “Familial transmission rather than defective innate immunity shapes the distinct intestinal microbiota of TLR-deficient mice,” *The Journal of Experimental Medicine*, vol. 209, no. 8, pp. 1445–1456, 2012.

-
- [180] S. Takahashi, J. Tomita, K. Nishioka, T. Hisada, and M. Nishijima, “Development of a prokaryotic universal primer for simultaneous analysis of Bacteria and Archaea using next-generation sequencing,” *PLoS ONE*, vol. 9, no. 8, 2014.
- [181] J. Caporaso, J. Kuczynski, J. Stombaugh, K. Bittinger, F. Bushman, E. Costello, F. N. A. Gonzalez-Peña, J. Goodrich, J. Gordon, G. Huttley, S. T. Kelley, D. Knights, J. E. Koenig, C. A. Lozupone, D. McDonald, B. D. Muegge, M. Pirrung, J. Reeder, J. R. Sevinsky, P. J. Turnbaugh, W. A. Walters, J. Widmann, T. Yatsunenko, J. Zaneveld, and R. Knight, “QIIME allows analysis of high-throughput community sequencing data,” *Nat Methods*, vol. 7, no. 5, pp. 335–336, 2010.
- [182] R. C. Edgar, “Search and clustering orders of magnitude faster than BLAST,” *Bioinformatics*, vol. 26, no. 19, pp. 2460–2461, 2010.
- [183] C. Quast, E. Pruesse, P. Yilmaz, J. Gerken, T. Schweer, P. Yarza, J. Peplies, and F. O. Glöckner, “The SILVA ribosomal RNA gene database project: Improved data processing and web-based tools,” *Nucleic Acids Research*, vol. 41, no. D1, pp. 590–596, 2013.
- [184] B. Chassaing, G. Srinivasan, M. A. Delgado, A. N. Young, A. T. Gewirtz, and M. Vijay-Kumar, “Fecal Lipocalin 2, a Sensitive and Broadly Dynamic Non-Invasive Biomarker for Intestinal Inflammation,” *PLoS ONE*, vol. 7, no. 9, pp. 3–10, 2012.
- [185] S. L. Brandwein, R. P. McCabe, Y. Cong, K. B. Waites, B. U. Ridwan, P. A. Dean, T. Ohkusa, E. H. Birkenmeier, J. P. Sundberg, and C. O. Elson, “Spontaneously colitic C3H/HeJBir mice demonstrate selective antibody reactivity to antigens of the enteric bacterial flora,” *Journal of immunology (Baltimore, Md. : 1950)*, 1997.
- [186] C. J. Boog, E. R. de Graeff-Meeder, M. A. Lucassen, R. van der Zee, M. M. Voorhorst-Ogink, P. J. S. van Kooten, H. J. Geuze, and W. van Eden, “Two monoclonal antibodies generated against human hsp60 show reactivity with synovial membranes of patients

- with juvenile chronic arthritis,” *Journal of Experimental Medicine*, vol. 175, no. 6, pp. 1805–1810, 1992.
- [187] A. Ogrinc Wagner, V. Friedrich, C. Barthels, P. Marconi, A. Blutke, F. Brombacher, and T. Brocker, “Strain specific maturation of Dendritic cells and production of IL-1 β controls CD40-driven colitis,” *PloS one*, pp. 1–20, 2019.
- [188] E. Furrie, S. Macfarlane, J. H. Cummings, and G. T. Macfarlane, “Systemic antibodies towards mucosal bacteria in ulcerative colitis and Crohn’s disease differentially activate the innate immune response,” *Gut*, vol. 53, no. 1, pp. 91–98, 2004.
- [189] I. Dotan, “New serologic markers for inflammatory bowel disease diagnosis,” *Digestive Diseases*, vol. 28, no. 3, pp. 418–423, 2010.
- [190] A. Konrad, Y. Cong, W. Duck, R. Borlaza, and C. O. Elson, “Tight Mucosal Compartmentation of the Murine Immune Response to Antigens of the Enteric Microbiota,” *Gastroenterology*, vol. 130, no. 7, pp. 2050–2059, 2006.
- [191] K. Zimmermann, A. Haas, and A. Oxenius, “Systemic antibody responses to gut microbes in health and disease,” *Gut Microbes*, vol. 3, no. 1, 2012.
- [192] S. Suerbaum, C. Josenhans, T. Sterzenbach, B. Drescher, P. Brandt, M. Bell, M. Droge, B. Fartmann, H.-P. Fischer, Z. Ge, A. Horster, R. Holland, K. Klein, J. Konig, L. Macko, G. L. Mendz, G. Nyakatura, D. B. Schauer, Z. Shen, J. Weber, M. Frosch, and J. G. Fox, “The complete genome sequence of the carcinogenic bacterium *Helicobacter hepaticus*,” *PNAS*, vol. 100, no. 13, pp. 7901–7906, 2003.
- [193] A. Noll and I. B. Autenrieth, “Immunity against *Yersinia enterocolitica* by vaccination with *Yersinia* HSP60 immunostimulating complexes or *Yersinia* HSP60 plus interleukin-12,” *Infection and Immunity*, vol. 64, no. 8, pp. 2955–2961, 1996.
- [194] D. Young, R. Lathigra, R. Hendrix, D. Sweetser, and R. A. Young, “Stress proteins are

- immune targets in leprosy and tuberculosis,” *Proceedings of the National Academy of Sciences*, vol. 85, pp. 4267–4270, 1988.
- [195] Y. Bulut, K. S. Michelsen, L. Hayrapetian, Y. Naiki, R. Spallek, M. Singh, and M. Arditi, “Mycobacterium tuberculosis heat shock proteins use diverse toll-like receptor pathways to activate pro-inflammatory signals,” *Journal of Biological Chemistry*, vol. 280, no. 22, pp. 20961–20967, 2005.
- [196] A. Tanaka, T. Kamada, K. Yokota, A. Shiotani, J. Hata, K. Oguma, and K. Haruma, “Helicobacter pylori heat shock protein 60 antibodies are associated with gastric cancer,” *Pathology Research and Practice*, vol. 205, no. 10, pp. 690–694, 2009.

Acknowledgements

Herrn Prof. Dr. Thomas Brocker danke ich insbesondere für seine Unterstützung und seinen Input, den großen wissenschaftlichen Freiraum, mit dem ich dieses Projekt gestalten durfte und die vielen Möglichkeiten, das Projekt auf nationalen und internationalen Konferenzen vorstellen zu können.

Vielen Dank an Prof. Dr. Bärbel Stecher und Dr. Debora Garzetti, die mich bei der Analyse der Microbiota unterstützten. Herzlichsten Dank vor allem an Diana, die Heli-Expertin, die ich ein paar Nerven gekostet habe...

Prof. Dr. Axel Imhof und Dr. Ignasi Forne danke ich für die Proteinanalytik.

Ein großes Dankeschön geht an Christian, der mir den Einstieg in dieses Projekt sehr erleichtert hat und mich mit Tipps und Tricks für die Zeit als Doktorandin ausgestattet hat.

Vielen Dank auch all unseren Tierpflegern und insbesondere Dana für die Unterstützung im finalen Experiment.

Ein riesiges Dankeschön an Frau Eisen, die sich "the" Mühe der Vorkorrektur machen musste und immer ein offenes Ohr für mich hatte.

Ganz besonders danke ich der lieben Cri...ich wusste es sehr zu schätzen, dass sie mir immer zu Hilfe geeilt kam, wenn ich sie brauchte. Sie stand mir "nichtsdestowenigertrotz" einfach immer mit Rat und Tat (nicht nur als TA) zur Seite.

Von ganzem Herzen bedanke ich mich bei meinen lieben Eltern und Mikosch, die mich sowieso immer unterstützen und mir auch während der Zeit der Doktorarbeit im Hintergrund den Rücken gestärkt haben.

Meinem Mann danke ich vor allem für all unsere Gespräche und Diskussionen, die mich immer antreiben. Danke, dass du mich auch in diesem Abschnitt begleitet hast und ich immer auf dich zählen kann.